AFRL-RH-WP-TR-2013-0002

Bioeffects of Gold Nanorods as a Function of Aspect Ratio and Surface Chemistry

Beth Maurer
Henry M. Jackson Foundation
For the Advancement of Military Medicine
Wright-Patterson AFB OH 45433

Emily Untener
Christin Grabinski
ORISE

Saber Hussain
Bioeffects Division
Molecular Bioeffects Branch

November 2012

Interim Report

Air Force Research Laboratory
711th Human Performance Wing
Human Effectiveness Directorate
Bioeffects Division
Molecular Bioeffects Branch
Wright-Patterson AFB OH 45433

NOTICE AND SIGNATURE PAGE

REPORT DOCUMENTATION PAGE

Form Approved
OMB No. 0704-0188

1. REPORT DATE *(DD-MM-YYYY)*	2. REPORT TYPE	3. DATES COVERED *(From - To)*
06-11-2012	Interim	May 2011- November 2012

4. TITLE AND SUBTITLE

Bioeffects of Gold Nanorods as a Function of Aspect Ratio

and Surface Chemistry

5a. CONTRACT NUMBER

5b. GRANT NUMBER
NA

5c. PROGRAM ELEMENT NUMBER
62202F

6. AUTHOR(S)
*Emily Untener, **Beth Maurer, *Christin Grabinski, ***Saber Hussain

5d. PROJECT NUMBER
OAFW

5e. TASK NUMBER
PO

5f. WORK UNIT NUMBER
OAFWP000

7. PERFORMING ORGANIZATION NAME(S) AND ADDRESS(ES) AND ADDRESS(ES)
*ORISE, Wright-Patterson AFB OH 45433-5707 **Henry M. Jackson Foundation, Wright-Patterson AFB OH 45433-5707 ***711 HPW/RHDJ, Wright-Patterson AFB OH 45433-5707

8. PERFORMING ORGANIZATION REPORT NUMBER
PA #88ABW-2013-0724

9. SPONSORING / MONITORING AGENCY NAME(S) AND ADDRESS(ES)
Air Force Materiel Command
Air Force Research Laboratory
Human Effectiveness Directorate
Bioeffects Division
Molecular Bioeffects Branch
Wright-Patterson AFB OH 45433-5707

10. SPONSOR/MONITOR'S ACRONYM(S)
711 HPW/RHDJ

11. SPONSOR/MONITOR'S REPORT
AFRL-RH-WP-TR-2013-0002

12. DISTRIBUTION / AVAILABILITY STATEMENT
Distribution A: Approved for public release, distribution unlimited

13. SUPPLEMENTARY NOTES
NA

14. ABSTRACT

One of the major challenges to the use of nanoparticles as drug delivery agents is that nanoparticles often become trapped in endosomes; unable to reach their desired target. Functionalization of gold nanorods (GNRs) was used in this study to attempt delivery outside of endosomes as well as study the role of surface chemistry and aspect ratio (AR) on bio-effects relevant to delivery applications. GNRs were used in this study due to their unique optical properties and enhanced delivery abilities. GNRs were synthesized with ARs 3 and 6 and functionalized with negatively charged tannic acid (TA) and carboxylic acid (COOH) as well as positively charged TAT (transactivator of transcription peptide with the sequence: GRKKRRQRRRPQ) and TAT HA2 (hemaglutanin peptide with the sequence: RRRQRRKKRGGDIMGEWGNEIFGAIAGFLG). After functionalization all the GNRs used in the study were biocompatible, making them applicable for biological applications. The cellular uptake of GNRs into keratinocytes was dependent on both AR and surface charge. AR 6 GNRs showed quantitatively higher uptake than AR 3 GNRs. Additionally, positively charged GNRs had higher uptake than negatively charged GNRs. Further studies showed that surface chemistry played a role in the uptake pathway used. TAT, TAT HA2, and COOH GNRs were uptaken by a variety of mechanisms of endocytosis. TA GNRs, however, were uptaken independently of endocytosis resulting in a unique orientation of TA GNRs within cells. This result makes TA GNRs extremely useful for the development of delivery, bio-imaging, and therapeutic applications.

15. SUBJECT TERMS
Gold nanorods, cellular uptake, delivery, endocytosis

16. SECURITY CLASSIFICATION OF:			17. LIMITATION OF ABSTRACT	18. NUMBER OF PAGES	19a. NAME OF RESPONSIBLE PERSON S. Hussain
a. REPORT	**b. ABSTRACT**	**c. THIS PAGE**			19b. TELEPHONE NUMBER *(include area code)*
U	U	U	SAR	75	NA

Standard Form 298 (Rev. 8-98)
Prescribed by ANSI Std. 239.18

THIS PAGE INTENTIONALLY LEFT BLANK.

TABLE OF CONTENTS

LIST OF FIGURES

LIST OF TABLES

PREFACE

The work was completed by Emily Untener as a master's thesis in Chemical Engineering from the University of Dayton. The work was performed within the Biological Interaction of Nanomaterials Group under Saber M. Hussain, PhD.

1.0 SUMMARY

The study of gold nanoparticles (NPs) is a high-impact research topic due to the many applications being discovered for these materials. Biological applications are especially relevant as NPs are typically the same size as biological molecules. Gold is a common material for biological applications due to its perceived inertness, ease of synthesis and functionalization, and unique optical properties which allow for these materials to aid in cell imaging or delivery of biomolecules. Many additional applications could be developed upon achieving subcellular delivery of the NPs to a biological target with high efficiency and specificity.

However, typically NPs taken up into cells remain trapped in the endo-lysosomal pathway. Endocytosis transports the NPs into the cell within vesicles, and these vesicles are either trafficked to the lysosome for degradation or exocytosed out of the cell. Thus it is a desirable goal to either avoid the endo-cytic pathways, or to provide a mechanism to release the NPs from the endosomes after entry into the cell. There are several physical methods which have been developed to actively deliver the NPs into the cell while avoiding endocytosis. However, these methods are very invasive, technically challenging, and costly. There have also been several studies on promoting endosomal release of NPs through functionalization of the NPs with some type of reagent. Some of the reagents used include viruses, fusogen peptides, cationic lipids, and cationic polymers. Typically these surface coatings take advantage of the pH change from 6 to 4 that accompanies the maturation of intracellular vesicles to late endosomes and lysosomes. This pH change could introduce some change in the reagent which could destabilize the membrane of the vesicle.

Functionalization of gold nanorods (GNRs) was used in this study to attempt delivery outside of endosomes as well as study the role of surface chemistry and aspect ratio (AR) on bio-effects relevant to delivery applications. GNRs were used in this study due to their unique optical properties and enhanced delivery abilities. GNRs were synthesized with ARs 3 and 6 and functionalized with negatively charged tannic acid (TA) and carboxylic acid (COOH) as well as positively charged TAT (transactivator of transcription peptide with the sequence: GRKKRRQRRRPQ) and TAT HA2 (transactivator of transcription peptide and hemagglutanin with the sequence: RRRQRRKKRGGDIMGEWGNEIFGAIAGFLG). After functionalization all the GNRs used in the study were biocompatible, making them applicable for biological applications. The cellular uptake of GNRs into keratinocytes was dependent on both AR and surface charge. AR 6 GNRs showed quantitatively higher uptake than AR 3 GNRs. Additionally, positively charged GNRs had higher uptake than negatively charged GNRs. Further studies showed that surface chemistry played a role in the uptake pathway used. TAT, TAT HA2, and COOH GNRs were uptaken by a variety of mechanisms of endocytosis. TA GNRs, however, were uptaken independently of endocytosis resulting in a unique orientation of TA GNRs within cells. This result makes TA GNRs extremely useful for the development of delivery, bio-imaging, and therapeutic applications.

2.0 NANOPARTICLES AS DELIVERY AGENTS: LITERATURE REVIEW

2.1   Nanomaterials and Nanotechnology

Nanotechnology is the study and use of materials on the atomic, molecular or supramolecular scale (1-100 nm). Due to their "nano" size, these materials have different properties than their bulk counterparts such as unique optical, mechanical, and conductive properties. Nanotechnology has been increasing in recent years due to the number of promising applications in electronics, fuel cells, catalysis, consumer products, and medicine (1). In 2000, the U.S. Government took a strong interest in the research of these materials with its formation of the National Nanotechnology Initiative (NNI). The NNI is a massive government effort currently involving thirteen federal agencies and spending $1.8 billion in 2010 alone, one of the largest government investments in technology since the Apollo program (http://www.nano.gov/node/748). The large interest in nanotechnology is understandable as it covers many different disciplines such as physics, engineering, materials science, biology and computer science. Many exciting discoveries have been made such as carbon nanotubes, a composite material which is much stronger than steel while only a fraction of the weight, as well as nanoparticles used in the detection of cancer (2). While there are exciting possibilities that come with a young field such as nanotechnology there are also uncertainties and chances of negative effects. Some nanomaterials have been shown to be harmful to skin, brain and lung tissue, be persistent in the environment, or kill microorganisms (3). Thus it is important to examine health and environmental effects of these materials as well as their positive applications.

The use of nanoparticles for biomedical applications is an especially promising subset of nanotechnology. Nanoparticles are particularly relevant to biological systems since they are typically the same size as biological molecules and smaller than the cells. Gold is an optimal material for biomedical applications due to its unique optical properties, perceived inertness, and ease of synthesis and functionalization which allow for these materials to aid in cell imaging, cancer treatment, and gene and drug delivery (4-6).

2.2   Optical Properties of Nanoparticles

Optical properties can be described as the way an object or material interacts with electromagnetic radiation (EMR). EMR includes not only visible light but also x-rays, gamma rays, microwaves and radio waves. The entire range of electromagnetic wavelengths is called the electromagnetic spectrum. The spectrum is broken down into named regions as shown in Figure 1. Visible light is only a small portion extending from 400nm to 700 nm.
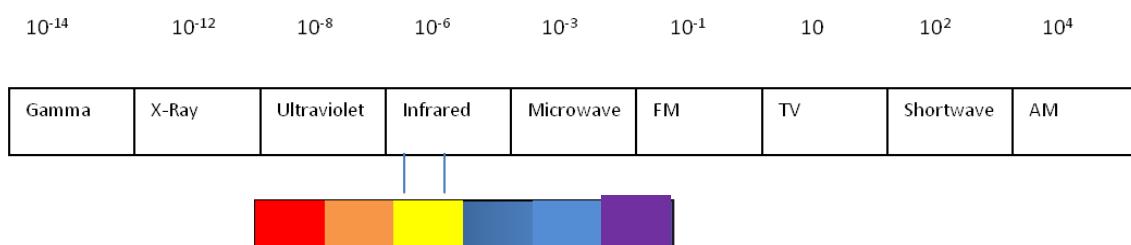
Figure 1: Electromagnetic Spectrum, Showing the Visible Region in Detail

Bulk materials can interact with EMR in three different ways. They can reflect, absorb, or transmit the EMR through the substance. Noble metal nanoparticles, such as gold, have a unique optical property called Surface Plasmon Resonance (SPR). Because of delocalized electrons on the surface of these metals, when incident light hits the surface these electrons begin to oscillate. Although other metals also have these delocalized electrons, an oxidation layer forms on these metals which inhibit SPR.

Nanoparticles differ in their optical properties from bulk in that they are able to confine resonant photons within their small particle size which induces localized surface plasmon oscillations of conduction band electrons. This is called localized surface plasmon resonance (LSPR). This confinement of photons increases the amplitude of the light wave by orders of magnitude, which therefore increases the light intensity. Because of this, all radiative properties such as light absorption, fluorescence, and scattering are enhanced by orders of magnitude in nanoparticles compared to the bulk (7). In fact, light absorption is 5-6 orders of magnitude larger than that of dye molecules (8). This, along with the fact that fluorescent dyes photobleach over time, makes nanoparticles a much better choice for biological imaging applications. Size, shape structure, dielectric properties of the metal, and the surrounding medium all affect the SPR since they all affect the electron charge density on the particle surface (9-11). Gold nanospheres, for example, have a strong SPR absorption in the visible region of the electromagnetic spectrum. Silver nanoparticles have shorter SPR wavelengths than gold, and nanospheres have shorter SPR wavelengths than nanoshells, nanocages, or nanorods (12, 13).

2.2.1 Gold Nanorod Optical Properties. Gold nanorods (GNRs) can have electron oscillation occurring either on the short axis or the long axis. When incident light hits the short axis and induces SPR, this results in an absorption band in the visible region, similar to gold nanospheres. This is referred to as the transverse band. Excitation of SPR along the long axis produces a stronger absorption band in a region of higher wavelengths on the spectrum. This is called the longitudinal band, and the wavelength of this band is dependent on the aspect ratio (AR) (length/width) of the nanorod (7). Figure 2 is GNR and gold nanosphere UV-Vis data, representing the absorption bands that occur and illustrating the difference in peak absorbance for different ARs.
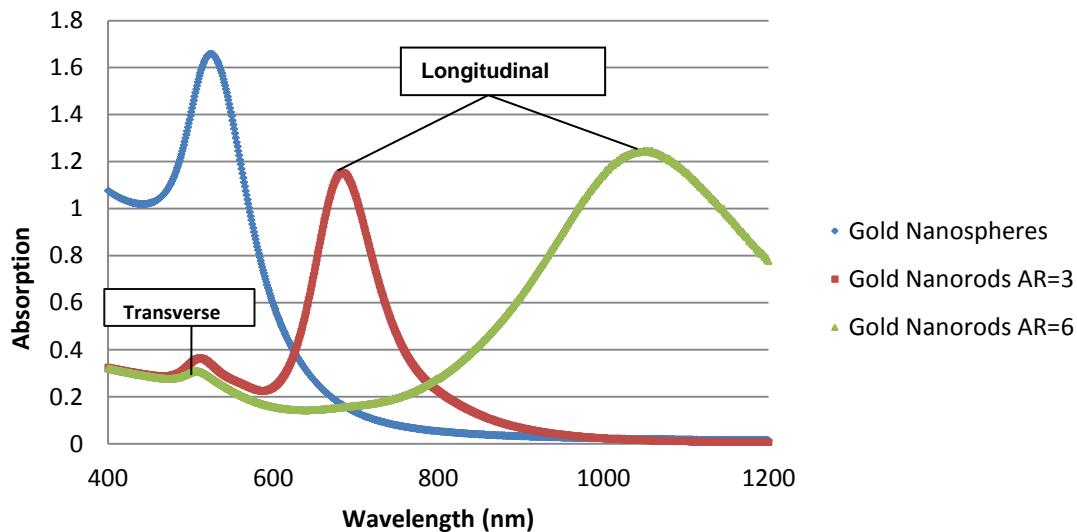
Figure 2: Gold Nanoparticle Absorption Bands

The dependence of longitudinal band wavelength on aspect ratio can be explained by Gans theory and Discrete Dipole Approximation (14). Gans theory was developed to explain the optical properties of ellipsoid particles, but can also be applied to nanorods. Discrete Dipole Approximation is a method in which a larger object is approximated by an array of discrete dipoles (15). Both Equations 1 and 2 show that GNRs can be optically tuned by varying the size. As AR increases, the longitudinal wave is red-shifted.

$$\text{Gans Theory Equation:} \quad \lambda_{max} = 97.65(AR) + 381.49 \quad \text{(1)}$$
$$\text{Discrete Dipole Approximation Equation:} \quad \lambda_{max} = 96(AR) + 418 \quad \text{(2)}$$

The tuning of GNRs can also have use in biomedical applications. For example, tissue absorption is minimal in a window of light around the Near Infrared Region (NIR) (800-1100 nm). Having minimal tissue absorption would improve the quality of imaging *in vivo* since light would penetrate through the tissue. GNRs can be tuned to the near infrared region by changing the AR, whereas many other particles including gold nanospheres cannot. Thus, GNRs have an advantage over other particles for biological imaging.

2.2.2 Light Absorption and Scattering. Nanoparticles do not reflect light, instead they induce light scattering. When light hits a plasmonic nanoparticle light is absorbed and LSPR is induced releasing photons. This release of light is referred to as light scattering. Thus the total light extinction consists of only light absorption and light scattering. Gans theory shows that the quantitative scattering and absorption are dependent on the surrounding medium, the metal, and the AR. This can be seen looking at the following equations for the cross sections of absorption and scattering in Equations 3 and 4 (7).

$$C_{abs} = \frac{2\pi}{3\lambda} \varepsilon_m^{\frac{3}{2}} V \sum_i \frac{\varepsilon_2/(n^i)^2}{(\varepsilon_1 + \left[\frac{1-n^i}{n^i}\right]\varepsilon_m)^2 + \varepsilon_2^2} \quad \text{(3)}$$

$$C_{sca} = \frac{8\pi^3}{9\lambda^4} \varepsilon_m^2 V^2 \sum_i \frac{(\varepsilon_1 - \varepsilon_m)^2 + \varepsilon_2^2/(n^i)^2}{(\varepsilon_1 + \left[\frac{1-n^i}{n^i}\right]\varepsilon_m)^2 + \varepsilon_2^2} \quad \text{(4)}$$

Where λ is the wavelength of light, V is the volume of the nanoparticle, ε_m is the dielectric constant of the surrounding medium, ε is the dielectric constant of the metal ($\varepsilon = \varepsilon_1 + i\varepsilon_2$), and n^i is the depolarization factor defined in Equation 5 and 6 as:

$$n^a = \frac{2}{R^2-1} \left(\frac{2}{2\sqrt{R^2-1}} ln \frac{R+\sqrt{R^2-1}}{R-\sqrt{R^2-1}} - 1 \right) \quad \text{(5)}$$

$$n^b = n^c = \frac{1-n^a}{2} \quad \text{(6)}$$

Where *a*, *b*, and *c* are the three axes of the nanoparticle, *a>b=c*, and the Aspect Ratio, *R*, is equal to *a/b* (7). With this quantification of absorbance, scattering, and total extinction of nanoparticles, one can look at whether scattering or absorption is more dominant in varying types of particles. This was studied with different aspect ratios and sizes of gold nanoparticles by Lee and El-Sayed (16). They used Gans theory and Discrete Dipole Approximation to look at nanorods that can have their plasmon resonance shifted into the near infrared region which is in

the window of transparency of biological tissue (800-1100 nm). The absorption and scattering peak wavelengths can also be tuned by manipulating the aspect ratio of the nanorod scattering quantum yield, the ratio of scattering efficiency to total extinction efficiency. They found that the scattering quantum yield was 0.326 for spheres and 0.603 for a rod and, at a fixed aspect ratio, the yield was higher for larger rods. Thus these studies show that larger nanorods tend to scatter more light whereas smaller particles tend to absorb more light (16).

This is useful information when looking at appropriate gold nanoparticles for biomedical applications. Larger nanorods that scatter more light would be ideal for biological imaging applications. Additionally the ability of a nanoparticle to absorb light strongly has various biomedical applications. When plasmonic nanoparticles are exposed to light resonant with their SPR they can convert it into heat through various photophysical processes (17). If a nanoparticle is selectively attached to a cancer cell this heating can kill the cancer cells while not affecting normal cells. This method of selective photothermal therapy has been shown to work in both *in vitro* and *in vivo* studies (18). Stronger laser heating of nanoparticles can also cause nanorod to melt into spheres. This could be used for a drug release mechanism if a drug or biomolecule was attached to the surface of the nanorod.

2.2.3 Gold Nanoparticles as Sensors. Another optical property of gold nanoparticles that is promising for biological applications is the longitudinal band's sensitivity to its surroundings. The refractive index of the solvent affects the peak absorption. GNRs are the most sensitive to this due to the greater polarizability compared to spheres (19). This SPR shift due to the dielectric properties of the solvent could be used for biological sensing. Additionally, gold nanoparticles can sense other plasmonic particles. When LSPR is excited, this creates surface electromagnetic fields which propagate around the particle and experience a size dependent exponential decay (20). This is referred to as a "near-field" and it can have an effect on nearby particles. When plasmonic nanoparticles are near each other, the longitudinal band will shift towards higher wavelengths. There is even a distinct color change that occurs. As two particles become closer together the red-shift increases. There has been a lot of data collected on this coupling of nanoparticles which paved the way for Su et al. (21) to develop a relationship for the shift in SPR based on physical properties of the nanoparticle. Equation 7 was developed where $\Delta\lambda$ is the shift in SPR wavelength, λ_o is the SPR wavelength, D is the particle size, κ is proportionality constant, s is the distance between nanoparticles, and τ is a decay length around 0.2:

$$\frac{\Delta\lambda}{\Delta\lambda_o} = \kappa \, exp^{\frac{-s}{\tau D}} \qquad (7)$$

This relationship has been shown to be independent of surrounding medium and holds for all plasmonic nanostructures (20). This is referred to as the "Universal Scaling Law" and there are many potential applications for this phenomenon. For example, Sonnichesen et al. (22) used coupling gold nanospheres to monitor a biomolecule. When the biological species was trapped between two nanospheres they were able to monitor this coupled pair for up to 3000 seconds. They also determined the size of the trapped particles by looking at the interparticle distance using the Universal Scaling Law. While this coupling has been performed for several different nanoparticles, it has yet to be demonstrated for nanorods. Nanorods would be better for this application than nanospheres or nanodisks because they have stronger oscillator strength and their SPR can be more easily tuned (20, 23).

2.3   Gold Nanorod Synthesis

2.3.1   Methods. GNRs are also seen as promising for many potential applications because of their ease of synthesis. There are many different techniques to create nanorods of varying ARs. One of the first synthesis methods developed was referred to as the template method. This procedure, described by Martin et al. (24,25) uses electrochemical deposition of gold onto a polycarbonate or aluminum template with nano-sized pores First, silver or copper is sputtered onto the membrane to provide a conductive layer for electrodeposition. Next, gold is electrodeposited into the nanopores. The alumina membrane and copper or silver film is then selectively dissolved using a polymeric stabilizer such as Polyvinylpyrrolidone. Finally, the GNRs are dispersed in solvent through some form of agitation. In this method, any shape of nanopore can be used to control the size and shape of the resulting nanoparticle. Additionally the nanorods are not coated with any surfactants. The downside to this method is that it produces a very low yield of GNRs.

In an attempt to create a higher yield, Wang et al. (26,27) developed an electrochemical method. The synthesis takes place in an electrochemical cell with a gold sacrificial anode and a platinum cathode of similar sizes. The electrodes are immersed in an electrolytic solution containing two cationic surfactants, different forms of cetyltrimethylammonium bromide (CTAB): $C_{16}TAB$ and $TC_{12}AB$. $C_{16}TAB$ stabilizes the nanoparticles and prevents aggregation while $TC_{12}AB$ induces rod formation. A silver plate is also immersed behind the platinum cathode during synthesis and small amounts of acetone and cyclohexane are added. Acetone and cyclohexane facilitate the mixing of the different types of CTAB which allow CTAB to form rod-like micelles. During synthesis, the gold anode is consumed forming $AuBr_4^-$ which groups to cationic surfactants and travels to the platinum cathode. Nucleation occurs and sonication is used to remove rods from the cathode. The redox reaction between the gold ions and the silver plate create silver ions. It was found that the rate of release of these silver ions relates to the length of the nanorods, although a complete mechanism is not known (19).

The most popular method of synthesis is probably the seed-mediated growth due to the simple procedure and high yield of nanorods. This type of synthesis was first reported in 1989 by Wiesner and Wokaun (28). When gold nuclei were added to $HAuCl_4$ growth solutions, gold colloids were formed. $HAuCl_4$ was reduced with phosphorus and the growth of nanorods was initiated by adding H_2O_2.(7)

A more updated method was introduced by Jana et al. (29) in 2001 in which citrate-capped small gold nanospheres were added to $HAuCl_2$ growth solution. This $HAuCl_2$ was obtained by reducing $HAuCl_4$ with ascorbic acid in the presence of CTAB surfactant and silver ions. In this method gold nanorods produced from the previous stage are used for seeds for the next stage. The downside to this protocol is that there is a large fraction of nanospheres produced along with the nanorods.

In 2003, Nikoobakht and El-Sayed (30) improved upon this method by replacing sodium citrate with CTAB to stabilize seed formation and using silver ions to control the AR of the GNRs. There are two steps in this synthesis method. First, a seed solution is made by reducing auric acid with ice cold sodium borohydride in the presence of CTAB. Second, that seed solution is added to a growth solution made up of Au^+ formed from the reduction of $HAuCl_4$ in the presence of CTAB. Silver nitrate is added to the gold growth solution before seed addition to promote rod formation and tune the aspect ratio. This method creates GNRs with ARs from 1.5

to 4.5. Unlike the previous method which produced a high concentration of spheres, this protocol produces 99% nanorods. In order to produce higher ARs from 4.6-10, a co-surfactant, benzyldimethylhexadecylammonium chloride (BDAC) was added to the growth solution. It was shown that molar ratios of BDAC:CTAB from 0-6 decrease the width from 12 nm to 6 nm, therefore increasing the AR. This is in agreement with Li et al. (31) who looked at the effect of adding molar ratios of BDAC:CTAB and found that molar ratios from 0.5 to 2 produced increasingly higher aspect ratios.

There have been other unique methods for synthesizing GNRs although they have not had as high yield or reproducibility as the seed mediated synthesis. For example, Yang et al. (32) developed a photochemical method of synthesis. It is similar to the electrochemical method but nanorod formation is induced by UV light irradiation. El-Sayed et al. (33,34) developed a method in which silver ions are used to control the aspect ratio. Other methods include synthesizing GNRs directly on glass surfaces, the use of bioreduction, x-ray irradiation, proton beam irradiation, microwave reduction, sodium borate reduction, and solvothermal reduction (7).

2.3.2 Sensitivity to Variables. One of the biggest challenges to synthesis of GNRs is that the process is sensitive to many other variables which are complex and often interrelated. For example factors that affect ARs include the temperature, pH, nature of the surfactant, ratio of gold to surfactant, and presence of ions (1). However, these sensitive variables can also provide ways to tune the AR even further.

GNR synthesis has been shown to be very temperature sensitive. Becker et al. (1) found that at higher temperatures, GNRs had more impurities present. Additionally they studied how temperature affects AR and found that the lowest synthesis temperature tested, 25°C, produced the highest AR and then a decrease in AR occurred until 55°C. Then from 55°C to 80°C AR increased, and then decreased again after 80°C. The total range of ARs was 3.25 to 2.52. They proposed this was due to two competing temperature dependencies existing during synthesis. The first is that entropy increases with increasing temperature, which tends to decrease AR. The second is that as temperature increases, there is more CTAB available for crystal formation which increases AR. When CTAB is in solution, it creates double layered structures called micelles, in which the nanorods grow. At lower temperatures, CTAB is thought to exist only as single layer which would impede the growth of the nanorods. Therefore, at temperatures above 55°C there are more micelles available for crystal growth causing AR to increase. At temperatures as high as 80°C the increasing disorder becomes too much and AR begins to decrease again.

Park et. al (35) looked at effect of temperatures from 42°C to 3°C on AR. It was found that ARs increased with decreasing temperature. At temperatures of 3°C they achieved ARs of 60 while at 42°C they had ARs of only 1. They looked at the shape of the micelles using a cryogenic transmission electron microscope (TEM) and found that the micelles changed from a spherical to a more cylindrical shape with decreasing temperature.

Studies on effect of temperature are not all in agreement, probably due to other variations in the synthesis procedure. For example, Li et al. (31) also found a decrease in AR with increasing temperature from 25°C to 90°C when the surfactant CTAB was used. However when a dual surfactant CTAB/BDAC was used increasing temperature resulted in increasing AR.

pH has also been shown to affect AR during synthesis. Wang et al. (36) used a seed mediated synthesis for GNRs and varied the pH from 3.6 to 9.6. This variation changed the shape of GNRs into different shapes such as rectangular, 'dogbone', and peanut-like

7

nanoparticles. Park et. al (37) also found that change in pH influenced the formation of triangular nanoplates amongst GNR formation. They found additionally that increasing pH from 1.29 to 7.06 decreased AR of GNRs from 25.6 to 20.0. Busbee et al. (38) found that by increasing pH from 2.8 to 3.5, the yield of nanorods increased from ~4% to ~ 90%. They also found that increasing pH from 2.8 to 5.6 increased AR from approximately 18 to 25. They postulated that the basis for change in AR with change in pH is that pH affects the activity of ascorbic acid. The pK_a of ascorbic acid is 4.1 so increasing pH from 2.8 to 5.6 increases the fraction of ascorbate present as the monoanion compared to the acid. Although results are conflicting, it seems there is a definite shape dependence on pH for GNR synthesis.

The nature of the surfactant used also affects the AR. Gao et. al (39) tested different surfactants including C_nTAB where n= 10, 12, 14, and 16. They found that the longer the surfactant chain, the higher the AR. The AR increased from 1 for $C_{10}TAB$ to 23 for $C_{16}TAB$. The authors propose this is because the longer hydrocarbon tails stabilize the formation of micelles. The GNRs have been said to grow into rods within these micelles. Smith et. al (40) also found that nanorod formation was sensitive to CTAB used. They obtained CTAB from ten different suppliers and found that this varied the yield of GNRs when using the same seed-mediated synthesis procedure. Three of the CTABs only yielded spherical gold particles while others yielded 100% GNRs. Additionally, using other surfactants such as $C_{16}P$ or BDAC at varying molar ratios also will change the synthesis of nanorods (41).

2.3.3 Post-Synthesis. After nanorods have been synthesized using the seed mediated synthesis, they are coated with a bilayer of CTAB. CTAB has an ammonium head group with a long hydrocarbon tail as shown in Figure 3.

Figure 3: Cetyl Trimethylammonium Bromide Structure

The CTAB is present on the gold surface as a bilayer. One layer of CTAB has the ammonium head group associated with the GNR surface, while in the other layer the head group is facing the surroundings. This is energetically favorable because there are hydrophobic interactions at the gold surface and hydrophilic interactions at the CTAB-solvent interface. The CTAB is thought to bind to the gold surface through electrostatic interactions between the positive ammonium head groups and anionic sites on the nanorod surface (42), as shown in Figure 4.
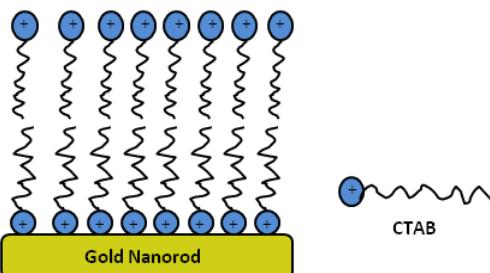
Figure 4: CTAB Bilayer on GNR Surface

It is not fully known what these anionic sites are. It has been hypothesized to be bromide ions, or silver ions. Murphy et al. (42) looked at inductively coupled emission atomic spectroscopy on the surface of the gold nanorods and found about four monolayers of silver. This CTAB bilayer provides stability to the synthesized GNRs (1).

After synthesis of GNRs, 100% yield of nanorods is not obtained. Therefore, purification steps are needed to remove spheres or other unwanted shapes. It is important to remove impurities to give validity to experiments looking at effects of size or shape. The most common method for purification is successive centrifugation steps. If GNRs are centrifuged at around 3,000 xg then nanorods will collect on the sides of the centrifugation tube while spheres around 60 nm will deposit at the bottom of the tube (43). In order to remove smaller spheres, repeated centrifugation at 6000-14500 xg can remove spheres less than 5 nm (44). Typically centrifugation for 30 minutes is sufficient for separation. This separation is due to different mass-dependent sedimentation coefficients of the nanoparticles (45). Sharma et al. (46) added that there is also a shape-dependent sedimentation behavior in addition to mass dependent sedimentation. Separation can be monitored by a color change. Impurities should be a different color than GNRs making them easier to separate.

A negative side to this method is that centrifugation removes CTAB which can make the GNR solution unstable. For example Becker et al. (1) found that centrifugation could only be performed twice before aggregation started to occur. This is because if concentration of CTAB becomes too low, multiple GNRs will have to share the same CTAB resulting in aggregation. It has been suggested to use an appropriate concentration of CTAB, 1 mM, during centrifugation steps to avoid this instability. It is important to use an appropriate concentration because too much CTAB results in more impurities while not enough results in aggregation (1). Other methods explored for purification include capillary electrophoresis and column chromatography (47,48).

An improved purification method for GNRs, called depletion induced separation, has been demonstrated by Park et al. (49) which separates nanoparticles as a function of not only size, but also shape. This method is based on adding a second surfactant, BDAC for example, to a concentration higher than a critical micelle concentration. The critical micelle concentration differs for varying shapes and sizes of nanoparticles, so separation can be tuned to a species of interest. When the separation between two colloids is the same order as the size of the second surfactant, the surfactant will be excluded from the space between the colloids (Figure 5), resulting in a concentration gradient that produces an attractive osmotic pressure. This will cause the colloids of interest to form flocculates. Then the remaining impurities can be removed by sedimentation or low centrifugation leaving only the desired gold nanoparticles.
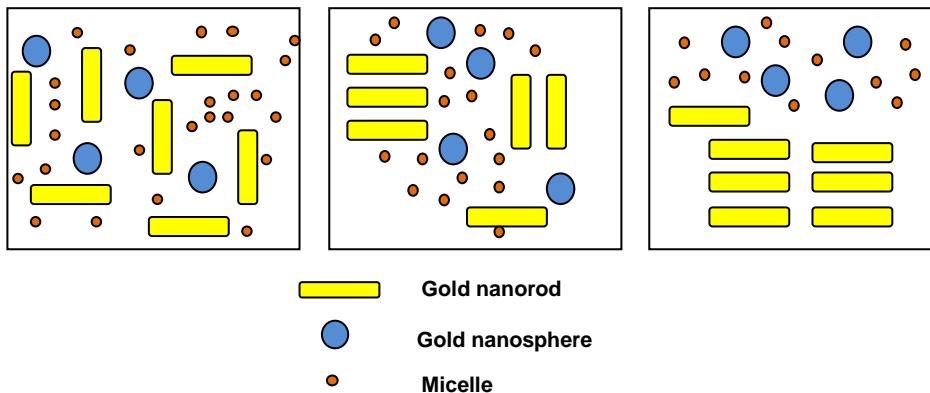
Figure 5: Depletion Induced Separation Technique

Another benefit of this process is that it is reversible. By simply adding water to the colloids the micelle molar concentration of the surfactant will decrease from its critical level and the nanoparticles will redisperse.

2.4 Gold Nanorod Functionalization

Although as-synthesized GNRs contain a CTAB bilayer on the surface, it is possible to functionalize GNRs with different surface chemistries or other biologically relevant cargo. Functionalization can be achieved through direct ligand exchange, the use of a biofunctional linker, surface coating, and electrostatic adsorption (7). For biological applications it is often desirable to replace or overcoat this CTAB layer as it has been shown to be toxic to cells (50,51).

2.4.1 Ligands. There have been several attempts to replace CTAB though the use of other gold binding ligands such as alkane thiols (50,52) or phospholipids. When functionalizing using the method, the CTAB electrostatic interaction must be displaced by a gold-sulfur bond. Challenges to this approach are that the CTAB interaction is not that weak, thiols or lipids could just accumulate within the CTAB bilayer, or they could replace only the outer layer of the CTAB bilayer since this outer leaflet is more weakly bound than the layer attached to the gold surface. However, successful studies have been demonstrated in which thiolated compounds functionalize gold nanoparticles (42).

One of the most popular surface chemistries for eliminating the cytotoxicity of GNRs is thiolated polyethylene glycol (PEG). When CTAB GNRs are functionalized with PEG their zeta potential changes from a positive value to a neutral charge (50,53). It has been shown that CTAB GNRs have strong cytotoxicity at 0.5 mM whereas PEGylated GNRs have 90% cell viability (50). Modification with PEG has not been shown to cause aggregation of the nanoparticles (50). Liu et al. (53) used PEG of molar weights 900 g/mol, 1500 g/mol and 5000 g/mol and looked at the nanoparticle stability. They found that high molecular weights of PEG provided the most stability. Additionally, modification with PEG has been shown to circulate in the blood longer *in vivo* than CTAB GNRs which tend to quickly accumulate in the liver. This stealth character makes PEGylated GNRs useful for biomedical applications such as targeted delivery systems (50). Since PEGylation is a method of direct ligand exchange, it is assumed that CTAB is completely replaced by PEG and that CTAB in solution could be easily removed through

centrifugation and replacement of the supernatant with water. The process of PEGylation is shown in Figure 6.
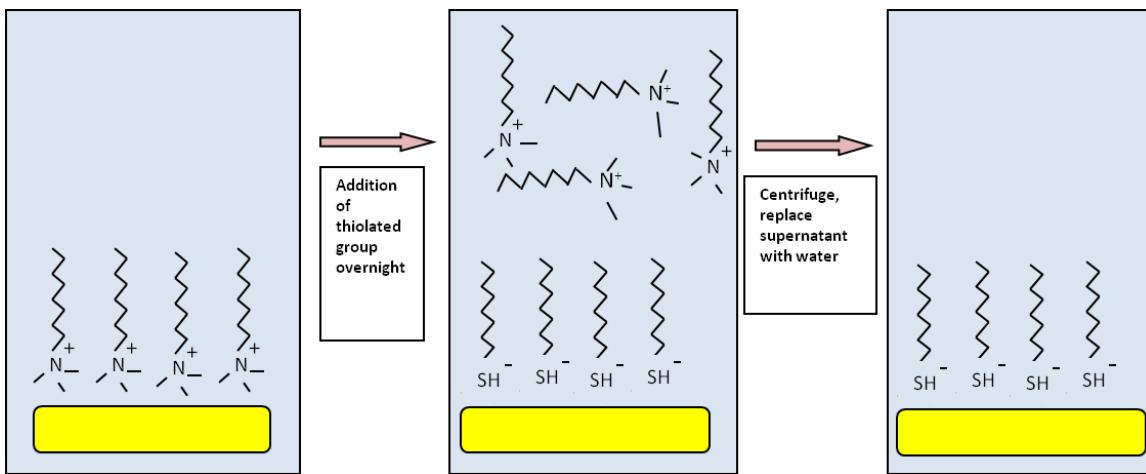
Figure 6: PEG Functionalization Technique
A: GNRs coated with CTAB, B: GNRs coated with a thiolated group prior to centrifugation, C: GNRs coated with a thiolated group after centrifugation and removal of CTAB

2.4.2 Ion Exchange Approach. In addition to using thiolated groups, another approach to replace CTAB is referred to as an ion exchange approach. In this method, CTAB is replaced by another molecule with a similar cationic head group (54,55). For example Orendorff et al. (54) used a phospholipid with a quaternary ammonium head group to replace CTAB, making the GNRs more biocompatible. Murphy et al. (42) also replaced CTAB with a tail-modified CTAB to add a polymerizable surfactant.

2.4.3 Layer by Layer Approach. There are also other methods of functionalizing GNRs which do not replace CTAB, but rather overcoat it. A layer-by-layer approach of functionalizing nanoparticles, as illustrated in Figure 7, was first introduced in 1998 and has since been applied to many colloidal nanoparticles (56). Alkilany et al. (51) used a layer by layer coating of gold nanorods with positively charged poly(allylamine) hydrochloride (PAH) and negatively charged polyacrylic acid (PAA). Since CTAB GNRs have a net positive charge, nanorods were functionalized first with PAA and then with PAH. It was found that even though CTAB was not replaced, by overcoating the CTAB, toxicity was eliminated (90% viability). It was also found that the toxicity of the CTAB GNRs was equal to the toxicity of the supernatant of the CTAB GNRs solution. This shows that the toxicity of CTAB GNRs is due to the free CTAB not the bound CTAB. Liu et al. (57) also demonstrated layer-by-layer functionalization using negatively charged polystyrene sulfonate (PSS) and positively charged poly(diallyldimethyl ammonium chloride) (PDDAC).

DISTRIBUTION A. Approved for public release; distribution unlimited, AFRL-RH-WP-TR-2013-0002, PA #88ABW-2013-0724
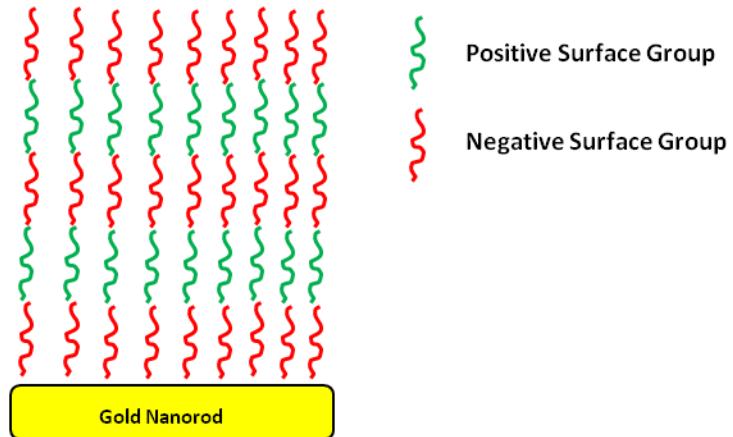
Figure 7: Layer-by-Layer Functionalization

There are a few limitations to the layer-by-layer technique. For example, there is a limit to the number of layers that can be deposited. For GNRs with AR 1-5 aggregation occurs if more than about 6 layers are overcoated. For longer GNRs with AR 18-20, it is possible to deposit 8-10 layers (42). Another difficulty with layer-by-layer functionalization is that a salt must be added to optimize electrostatic screening of the polyelectrolyte, but too much salt will cause the nanorods to aggregate (56). Typically, layers of surface groups that are added would be on the scale of Angstroms, which is one tenth of a nanometer. However larger surface groups with long chains could also be used. Therefore, while the core size of the GNR will not change, it is possible that many layers would slightly change the observed AR. Overall, however, this technique has a lot of potential for future engineering of complex overcoated particles for biological targeting or delivery. After coating with polyelectrolytes these terminal functional groups can react further with other groups such as proteins or inorganics. Future studies need to be done, however, to examine the long term stability of these layer-by-layer coated particles to see if they are applicable to biomedical uses.

2.4.4 Bilayer Functionalization. Another method of functionalization does not result in an outer layer of a chemical, but rather involves sequestering species within the CTAB bilayer. The CTAB bilayer on GNRs is an approximately 2-3 nm hydrophobic region. This region has the ability to concentrate hydrophobic molecules from the aqueous bulk solution. For example, napthol, styrene, and metal thiobenzoate have been shown to sequester in this CTAB bilayer. Napthol has shown to reach a maximum concentration of 15,000 molecules per 15nm x 60 nm GNR (58). Exposing the GNRs to styrene monomers followed by addition of an initiator to polymerize the monomers resulted in polystyrene-coated GNRs (59). Sun et al. (60) showed that metal thiobenzoate could be concentrated in the bilayer and then reduced to form a gold-metal sulfide core-shell structure. This type of functionalization is shown in Figure 8.
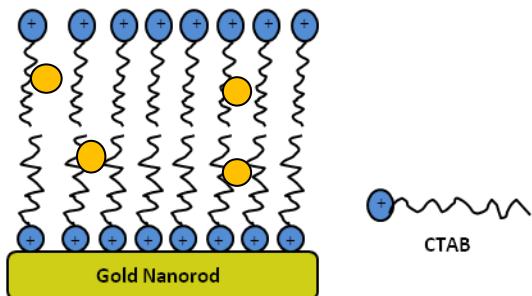
Figure 8: Bilayer Functionalization

An advantage to this form of functionalization is that, due to the unique optical properties of GNRs, NIR laser irradiation can trigger controlled release of the molecules from the CTAB bilayer. This has been demonstrated with the release of octadecylrhodamine B chloride through pulsed laser irradiation (61). Additionally, this allows for the potential of sequestering and controlled release of hydrophobic drugs for drug delivery applications.

2.4.5 Adsorption of Proteins. A functionalization that takes place automatically if GNRs are exposed to media with serum is adsorption of serum proteins. When looking at bio-effects of GNRs they are usually dispersed in media before exposure to cells. Therefore, this change in surface chemistry is something that should be considered. Alkilany et. al (51) demonstrated the adsorption of serum proteins, in particular bovine serum albumin (BSA), which is the main protein component of the serum. Within 5 minutes of exposure to media the nanorods changed zeta potentials to meet the charge of BSA. Adsorption was also confirmed by Fourier transform infrared (FTIR) measurements of the particles. PEGylated nanorods, however, tend to not adsorb as many of these proteins because PEG repels the proteins from approaching the particle core (42,62).

2.5 Bio-effects of Size, Shape, and Surface Chemistry

It has been previously discussed how it is possible to synthesize a wide variety of ARs of GNRs with a large variety of surface functionalizations. When considering nanoparticles for biomedical applications it is worthwhile to examine the bio-effects of size, shape, and surface chemistry. There have been several studies performed on this; however, many results are conflicting (57, 62-64).

2.5.1 Effect on Cellular Uptake. There has been much interest in how size, shape and surface chemistry affect the cellular uptake of the gold nanoparticles. Malgin et. al found that nanorods had more cellular uptake than nanospheres. They found that the smaller the core size, the greater the uptake (62). Qui et al. (57) showed that the longer GNRs were less internalized than shorter GNRs. Arnida et. al also found that uptake was dependent on core size, not hydrodynamic diameter. Hydrodynamic diameter increases as layers of functionalization are added, but the core size of the metal remains the same. Their group looked at PEGylated GNRs and gold nanospheres. They found that smaller nanospheres had greater uptake, whereas, longer nanorods had slightly more uptake than shorter nanorods in their study (63). Chithrani et. al (65) found that uptake of gold nanospheres increased from sizes 10-50 nm and then decreased for particles

larger than 50 nm. Overall, it seems there is a definite effect of size and shape of gold nanoparticles on uptake. However, there have been some conflicting reports probably largely due to other variables in the process such as surface coating, colloidal stability and cell line used. Additionally, the evaluation of uptake can be based on particles per cell or by mass of materials which can cause results to vary as well (64).

Cellular uptake is also affected by surface chemistry. It has been shown many times, for example, that functionalization with PEG decreases cellular uptake (57, 62, 66). It has been hypothesized that the reduced interaction of the nanoparticles with cells is due to the hydrophilic stealth coating around the particles (67). It has been further hypothesized that since PEGylated particles do not adsorb proteins from serum, that this inhibits uptake. This is due to the method of uptake being receptor mediated endocytosis using the protein coating. It has also been shown that in general, positive surface functionalizations have higher uptake than negative surface chemistries. This may be due to the fact that negatively charged GNRs have poor interactions with the negatively charged cell membrane (68). For example, positively charged GNRs coated with PAH had uptake of 2,320 nanorods per cell while negatively charged PAA particles only had 270 nanorods per cell (58). Additionally positively charged GNRs coated with PDDAC had greater cellular uptake than negatively charged GNRs coated with PSS (57). In this study, SDS Page was used to look at protein adsorption from the serum. The positively charged GNRs had greater protein loading capacity than negatively charged. This again suggests that adsorption of protein from the serum aids in the uptake, supporting the mechanism for why PEGylation reduces uptake. However, there have been some conflicting studies on the effect of serum in media. For example, it has also been reported that serum media hinders cellular uptake (62).

2.5.2 Effect on Toxicity. The effects of size, shape, and surface chemistry on toxicity have also been studied. Toxicity refers to the death of cells due to exposure to the nanoparticles. It has been reported that toxicity of gold nanoparticles is largely independent of size and shape (57). Toxicity is, however, very dependent on surface chemistry. For example, the cationic surfactant used in the synthesis of GNRs, CTAB, is highly toxic to cells. Surface modifications with other chemistries can also affect toxicity and have biological effects once internalized (69). There is not a distinct trend between negative or positive charged gold nanoparticles on toxicity, however. Rather surface chemistries should be tested for toxicity on a case by case basis.

2.6 Targeting of Nanoparticles

There have been many biomedical applications for gold nanoparticles discussed such as gene or drug delivery, photothermal cancer treatment, or biological imaging. These applications hinge on the achievement of a targeted intracellular delivery to specific types of cells or specific subcellular compartments. There are three main barriers to overcome for intracellular targeting. Firstly, the nanoparticles need to be taken up into the cell. Secondly, if the nanoparticles are within an endosome or lysosome they need to escape from that compartment. Thirdly, the nanoparticles need to reach their desired intracellular target.

2.6.1 Uptake into the Cell. Uptake of nutrients and much communication between cells takes place through the plasma membrane. Oxygen, carbon dioxide, water, and small hydrophobic molecules can diffuse through the membrane through concentration gradients. Nanoscale macromolecules have been shown to be taken into the cell via active or passive mechanisms.

Passive mechanisms take advantage of the enhanced permeability and retention (EPR) effect of tumor tissues. This EPR effect is explained by the fact that since cancer cells are growing so fast they need to create more vessels near the tumor mass to supply them with oxygen and nutrients (70). The resulting imbalance of angiogenic regulators such as growth factors and matrix metalloproteinases makes tumor vessels very disorganized. They contain many pores which cause enlarged gap junctions between endothelial cells and poorer lymphatic drainage (70). Therefore, nanoparticles that can fit into these gaps can selectively accumulate in the cell. The structure and surface properties of the nanoparticles may affect the EPR effect.

Nanoparticles can also be uptaken into the cell through active mechanisms. Endocytosis is an energy dependent process in which the cell ingests materials from outside the cell by enclosing them in vesicles pinched off from the plasma membrane. There are several different methods of endocytosis that nanoparticles can use depending on their size, surface coating, and other factors. A summary of the endocytosis methods and subdivisions are shown in Figure 9.
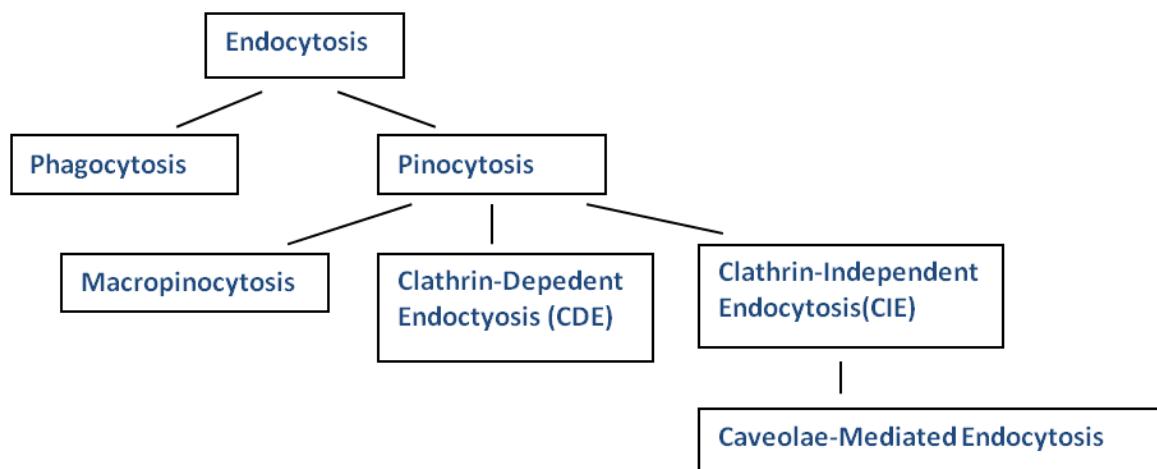
Figure 9: Methods of Endocytosis

There are two broad types of endocytosis: phagocytosis which is used for specialized cells, and pinocytosis which takes place in all cell types. Pinocytosis can be further divided into macropinocytosis, clathirin-dependent (CDE), and clathrin-independent (CIE) endocytosis. Macropinocytosis is a non-selective method which internalizes macromolecules. During macropinocytosis the membrane forms protrusions or "ruffles" which fuse with each other and with the plasma membrane to enclose large volumes. These vesicles which become internalized can have sizes up to 5 μm (71). CDE is the best characterized pathway and has been said to be the most used endocytosis method for nanospheres up to 200 nm (72). Certain macromolecules are known to preferentially use CDE. For example, transferrin which is one of the main proteins in the serum contained in growth media uses CDE preferentially. CIE endocytosis is still being studied, and has not been characterized as well as CDE. Although the detailed mechanism is not known, the method is based on the role of dynamin and small GTPases (73). CIE could also involve the use of uptake from lipid rafts or the use of flotillin. Lipid rafts are ordered liquid environments within biological membranes that contain unsaturated phospholipids, cholesterol, glycosphinglolipids and proteins (73). The best characterized form of CIE is probably caveolae-

mediated endocytosis. Caveolae are flask shaped invaginations of the plasma membrane, 50-80 nm, which are characterized by the presence of caveoline-1 (73).

When nanoparticles are taken up into the cell by endocytosis, they are localized within endosomes inside the cell. These endosomes are then typically transferred to lysosomes where the contents are rapidly degraded by hydrolases (74,75). For targeting applications, it would often be desirable to avoid endocytosis so that the nanoparticles can enter into the cytoplasm and reach their desired target before being degraded or exocytosed out of the cell. There are several physical methods which have been used to uptake nanoparticles into cells without the use of endocytosis.

There have been several physical methods to bypass endocytosis. One of these methods is called microinjection. During microinjection, samples are delivered directly into the cytoplasm or nucleus using a fine tipped glass microcapillary while using an optical microscope to monitor the injection into the cell. Advantages to this technique are that there is a high cell survival rate, and an exact volume can be inserted so that the toxicity of a specific dose can be easily examined. Disadvantages are that it is technically demanding and very expensive, costing about $40,000 per device (76). Another physical technique is electroporation. In this technique, a rapid high voltage electric field impulse is applied to the cell, which temporarily causes hydrophilic pores in the plasma membrane of the cell. These pores allow nanoparticles to passively enter into the cell without endocytosis. This method is high throughput, but requires specialized equipment, only works when the cells are in suspension, and could lead to cell death due to the electrical impulses (76). A technique similar to this is sonoporation, which uses ultrasound to generate temporary non-selective pores on the cell membrane. It is typically used in conjunction with microbubbles which cause bubble cavitation resulting in pore formation. Sonoporation and microbubbles have been used to delivery chemotherapeutic drugs, siRNA, DNA, and peptides (77-79). Genegun is another physical approach. Genegun uses a high pressure helium gas burst to accelerate the cargo and deliver it into the cells. This has been used *in vivo* for gene delivery, and has been recently used to delivery nanosensors. A disadvantage to this technique is that the viability of the cells after using Genegun is questionable. While the physical delivery methods have their advantages, they tend to be costly and very invasive.

In addition to physical delivery, another method to aid in the uptake of nanoparticles into the cell is functionalization with different surface chemistries. Viruses are an archetypal biological nanoparticle which exploit cell uptake and transport mechanisms to deliver their cargo into the cytoplasm or nucleus of the cell (80). Similarly, engineered nanoparticles can use biochemical approaches to pass through the cell. This can be achieved by coating with different chemical functional groups and targeting molecules or by enclosing nanoparticles in a carrier matrix (76). These surface chemistries can either aid in an endocytosis uptake mechanism or in a direct entry mechanism in which the nanoparticles avoid the endo-lysosomal pathway.

One of these facilitated delivery mechanisms commonly used is cationic molecules. Since the plasma membrane is negatively charged, cationic molecules can often interact with it and cause nanoscale holes on the membrane. The higher the cationic charge, the greater permeability induced on the plasma membrane. There have been various types of cationic functionalizations used including liposomes (81), polypeptides (82), and polymers (83). One example is the use of cationic liposomes with DNA coated gold nanoparticles. The cationic liposomes were shown to improve the cell uptake of the DNA-gold nanoparticles, most likely because it neutralized the negative charge of the DNA-gold nanoparticles causing better association with the plasma membrane (84). Additionally, certain amine-containing cationic

polymers such as polyethyleneimine (PEI) can be conjugated to gold nanoparticles. These cationic polymers induce membrane permeability, allowing nanoparticles to passively enter into cells. PEI has been shown to transfect a broad range of cell lines with high efficiency. Other cationic polymers have been produced commercially for transfection including Fugene-6, Effectene, GeneSHUTTLE, and lipofectamine (64). However, there has been some concern about the cytotoxicity of cationic polymers and their poor stability in biological media. To alleviate this, Zhang et. al used PEI with PEG and a polysaccharide chitoson which increased uptake, but was also stable and non-toxic. Duan and Nie also used PEI with PEG in order to deliver quantum dots while not inducing toxicity to the cell (76).

Another surface chemistry used to increase transfection across the plasma membrane includes cell penetrating peptides (CPPs). CPPs are often derived from nature, for example from parts of viruses. One example is the transactivator of transcription (TAT) peptide. This peptide is derived from the protein transduction domain of the HIV-1 virus. TAT conjugated nanoparticles have been found to be taken up by macropinocytosis and localized in endosomes, to localize in cytoplasm, and to localize in the nucleus depending on the attached cargo. These conflicting results could be due to the different size, shape, and material of particles being delivered as well as varying cell lines. In addition to peptides derived from protein transduction domains, CPPs also include amphipathic peptides and cationic peptides. Some examples of specific CPPs include penetratin, transportan, Pep-1, MPG, polyarginine, and Pvec to name a few (76).

Liposomes can also be used as carriers for nanoparticles across the cell membrane. A liposome is a vesicle composed of a bilayer of phospholipids with an inner aqueous compartment. They have been used for drug delivery because they can carry either hydrophilic or hydrophobic molecules. Typically, liposomes have been shown to enter into the cell through endocytosis. When liposomes were used to deliver small gold nanoparticles into the cell gold nanoparticle delivery efficiency was increased 1,000 fold (85).

Another method to increase uptake is the use of bacterial toxins. Toxins of microbial origin cause transient pores in the cell membrane, so that nanoparticles can passively enter. One example is Streptolysin-O which increased delivery of oligodeoxynucleotides, proteins, peptide-nucleic acid, and functionalized gold nanoparticles (86).

2.6.2 Targeting to Specific Cells. In addition to engineering nanoparticles to have increased cellular uptake, it also would be useful to target nanoparticles to specific cells. For example, for photothermal therapy to be effective, the nanoparticles must selectively bind to cancer cells only. Targeting of specific cell types can be achieved by attaching targeting ligands to the nanoparticles which will associate with cell surface antigens or membrane receptors overexpressed in the desired cells. For example, the transferrin protein has been shown to provide enhanced internalization for 20 nm gold nanoparticles (64). It is known to deliver nanoparticles into a variety of cell types via clathrin-dependent endocytosis. Additionally, transferrin receptors are overexpressed in a variety of cancers making transferrin useful as a cancer targeting ligand. Folate receptors are also overexpressed in ovarian and breast cancer cells (87). Therefore folic acid can be used as a cancer targeting molecule for the delivery of nanoparticles. Additionally, folic acid is inexpensive, binds strongly to the folate receptor, and has been shown to delivery many types of nanoparticles such as polymer, gold, magnetic, and semiconductor nanocrystals selectively into cancer cells. ErbB2/EGFR are receptors that are over expressed in breast cancer cells. Thus, nanoparticles functionalized with anti-EGFR antibodies such as Herceptin can be used for targeting. Finally, short single-stranded DNA or RNA

oligonucleotides can also be used for targeting cells both *in vivo* and *in vitro.* Specific targets can be selected from a large number of random sequences using a technique called Systematic Evolution of Ligands by Exponential Enrichment (SELEX) (66).

2.6.3 Subcellular Endosomal Release. It has been discussed how to improve the cellular uptake of gold nanoparticles either through physical methods or through functionalization with different surface chemistries. Some of these techniques, such as the physical delivery and a few transfection reagents, enable nanoparticles to enter cells independent of the endo-lysosomal pathway. However, most of the time nanoparticles are entering the cell through endocytosis and thus become trapped in the endo-lysosomal pathway. The maturation of vesicles into late endosomes and lysosomes is characterized by a rapid acidification from pH 6 to 4 within the vesicles and recruitment of degradative enzymes which digest the content of the vesicles (76). Thus, there have been methods studied to release the nanoparticles from the endosomes so that they can enter the cytoplasm and eventually reach a potential intracellular target.

One way to release the nanoparticles from the endosomes is to functionalize the particles with a lysosomotropic agent, such as chloroquine or sucrose. Chloroquine induces vesicular disruption by elevating the pH within endosomes and lysosomes (64). This prevents endosomal acidification and degradation by the lysosomal enzymes, however, toxicity has been a problem when using chloroquine.

Cationic polymers, lipids containing PEI and imidazoles have also been used to disrupt endosomes using the "proton sponge effect" (88). Cationic particles bind to lipid groups on the plasma membrane and are endocytosed into the cell in small vesicles. Once the cationic nanoparticles enter an acidifying lysosome, the unsaturated amino groups can sequester protons that are supplied by the proton pump. This causes the pump to keep creating more protons and leads to retention of one chloride ion and one water molecule per proton. Thus, the lysosomes swell and eventually rupture, releasing their contents into the cytoplasm (89). However, similar to the chloroquine, the cationic charges may have a toxic effect.

Another method is to functionalize the nanoparticles with endosome disruptive peptides. These peptides might take advantage of the strategies used by viruses to enter into cells, and release their DNA into the cytoplasm. For example, for the influenza virus to enter the cell, its hemaglutinin (HA) protein binds to sialic acids on the plasma membrane and its uptaken by receptor mediated endocytosis (90). The HA protein has two subunits, HA1 and HA2. HA1 is responsible for the recognition with sialic acids and the N-terminus of the HA2 subunit is a hydrophobic domain which undergoes a pH-induced conformation change in membranes (91). Plank et. al modified the HA2 peptide and improved upon it to create the INF7 peptide. This peptide has the ability to induce more potent pH-dependent perturbations than HA2 (92).

Similar to the influenza virus, the bacterial toxin diphtheria also can induce pH dependent membrane fusion. Diphtheria is a protein secreted from *Corynebacterium diphtheria.* It has also has two fragments A and B. Fragment B has a region called the R domain which is responsible for receptor binding, and aids in cellular uptake. Fragment B also has a region called the T domain which changes conformation as pH is lowered in the endosomes, allowing endosomal release. Fragment A is responsible for entering the cytosol and stopping protein synthesis and exerting toxicity to the cells. Therefore, Fragment B is the only part of interest for nanoparticle delivery applications using the diphtheria protein. Because of this, the toxic part of Fragment A could be replaced by a different nontoxic sequence which could be released into the cytosol. For

example, the toxic section has been replaced by different genes so that the diphtheria could act as a gene carrier (93).

A peptide called GALA was created in an attempt to mimic the function of the viral fusion protein segments to mediate escape of the virus genes from acidic endosomes into the cytosol. The peptide is made from a repeated sequence of Glu-Ala-Leu-Ala. The GALA peptide changes in conformation from random to helical when the pH changes from 7.0 to 5.0 which leads to destabilization of the membranes (94). At neutral pH the peptide is water soluble and has a very low affinity for the membranes. Thus, since the cytosol has a pH of 7.2 it will not exhibit toxicity or disrupt the plasma membrane. Unlike HA2 and diphtheria, GALA does not contain a segment which aids in uptake so an additional segment might need to be added to the nanoparticle. For example, efficient delivery of avidin and streptavidin coated quantum dots to the cytosol was achieved when using association with GALA and a cationic liposome, Lipofectamine 2000 (95).

There could be other methods available to release nanoparticles from endosomes. For example, laser illumination of CPPs has been used to redistribute them from endosomes to lysosomes. The lasers are supposed to break open the endosomes without causing cell death. This hasn't been tried with nanoparticles but it could be an interesting study (64).

2.6.4 Reaching Intracellular Target. Once the nanoparticles have either entered directly into the cytosol or have been released from the endosomes into the cytosol the next challenge is to reach the intracellular target. For example, the nucleus may be a desireable target since the genetic information of the cell and transcription machinery is located there. Novel gene and drug therapies would benefit from being able to localize in the nucleus. Additionally, it might be desirable to label specific parts of the cell with nanoparticles for bioimaging purposes.

In order to reach the nucleus, a nuclear localization signal (NLS) derived from the large T antigen of the SV 40 virus has been successfully used to target the nucleus (96). However, if nanoparticles are small enough, they can enter the nucleus without an additional targeting agent such as NLS. Typically nanoparticles must be less than 30 nm to cross nuclear pores. Fuente et al. (97) found that their TAT functionalized 2.8 nm diameter gold nanoparticles crossed the nuclear membrane and accumulated in the nucleus. Additionally, materials might be able to enter during mitosis when the nuclear envelope is temporarily lost (98).

In order to target specific intracellular locations, often antibodies can be used. Monoclonal antibodies have high antigen or target specificity and they bind to a single antigen. For this reason, they can be functionalized to nanoparticles to increase binding specificity to their targets providing active intracellular targeting. For example, Kumar et. al (99) created an intracellular sensor to monitor actin rearrangement in live fibroblasts. 20 nm gold nanoparticles were functionalized with TAT to increase uptake, HA2 to release from endosomes, PEG to increase biocompatibility, and anti-actin and anti-biotin antibodies to target the actin in the cell. Antibodies for other cell components could be used similarly for intracellular targeting.

2.6.5 Successful Targeting and Delivery Studies. Some of the targeting methods discussed above have been successfully used to deliver nanoparticles selectively to tumor cells. Additionally, nanoparticles and any necessary targeting agents have been used successfully to deliver DNA/RNA, proteins, and drugs into cells.

Table 1: Successful Studies Showing Targeting/Delivery with Nanoparticles			
Targeting Agent	*Type of Cell Targeted*	*Delivery Agent*	*Ref*
Anti-EGFR	Cancer cells	Gold Nanoparticles	100
Folate/Folic Acid	Tumor Cells	Gold Nanoparticles	101
		Gold Nanoparticles functionalized with Doxorubicin	102
	Ovarian Cancer Cells	Gold nanorods functionalized with PEG and cis-platin	103
Methotrexate	Lewis Lung Carcinoma Tumors in Mice	Gold Nanoparticles	104
Tumor Necrosis Factor	Colon Carcinoma Tumors in Mice	Gold Nanoparticles	105
	Tumor Cells	Gold Nanoparticles functionalized with Paclitaxel	106

Gold nanoparticles are excellent candidates for gene delivery. Their high surface to volume ratio enables a lot of payload per carrier and also allows for efficient DNA/RNA compaction. In order for successful gene delivery to take place, DNA must functionalize onto the gold nanoparticles, nanoparticles need to be taken up into the cell, released from endosomes, protected from nuclease in the cytoplasm, and eventually delivered into the nucleus. It has been shown that functionalizing gold nanoparticles with cationic quaternary ammonium head groups allows DNA to bind to the nanoparticles through electrostatic interaction and can inhibit the transcription of DNA (107). Positively charged hydrophobic nanoparticles conjugated to DNA can efficiently enter cells. Coating nanoparticles with ligands such as PEI discussed previously can release the DNA-nanoparticle conjugates from endosomes using the "proton sponge effect." Once the DNA/RNA is released from the endosomes it has been shown to be able to localize in the nucleus without an additional targeting agent. (108) Derfus et. al (109) engineered quantum dots for delivery of siRNA. The quantum dot was PEGylated and additionally functionalized with siRNA attached by disulfide cross-linkers as well as a tumor-homing peptide. The tumor homing peptide directed the nanoparticles to EGFP-transfected HeLa cells and after being released from the endosomes, led to significant knockdown of EGFP signal. If this siRNA sequence was designed against a therapeutic agent such as oncogene instead of EGFP, this could be used to both treat and image metastatic cancer.

Delivery of proteins in cells could also be improved with the use of nanoparticles. Typically, delivery of proteins inside living cells is limited due to poor permeability through the cell membrane and the protection of the protein against digestion by enzymes (110). However, by conjugating proteins to nanoparticles these challenges could be largely overcome. The protein can be either covalently or noncovalently attached to the nanoparticle while retaining its activity. Ghosh et al. (111) functionalized cationic gold nanoparticles with short peptides conjugated to tetra(ethylene glycol) units, binding the GNP to anionic β-galactosidase (β-gal) through electrostatic interactions. The β-gal was found to retain its enzymatic activity, escape the endosomes, and localize in the cytosol. Additionally, the particles were nontoxic. Gold nanoparticles have also been modified to bind insulin. These insulin-gold nanoparticles can be delivered for the therapeutic treatment of diabetes mellitus. For example, insulin was functionalized onto aspartic-acid coated gold nanoparticles and delivered orally and through transmucosal pathways in diabetic rats. There was significant reduction in blood glucose level

compared to delivery of insulin only (112). Another study was done where tumor necrosis factor-alpha (TNF-α), a cytokine with anticancer properties, was added to PEG coated gold nanoparticles and delivered into mice. Tumor growth was delayed when treated with the TNF-alpha-PEG-gold nanoparticles (113). In addition to gold nanoparticles, other engineered nanoparticles could be used for protein delivery. Huang et. al modified mesoporous magnetic hollow nanoparticles (MMHs) with amino groups and found them to be efficient in protein loading. The amino modified MMHs transported the protein BSA into cells and released them in the nuclear or cytosolic compartments of the cells. The particles were biocompatible, and the proteins resided in the hollow space of the MMHs where the structure and activity of the proteins remained unaffected. Since the particles are magnetic, they could target specific sites to heal tumors by using a magnetic field (114).

In addition to delivery of nucleic acids and proteins, it is also very desirable to deliver drugs with nanoparticles. The high surface area and tunability of gold nanoparticles make them especially good candidates for controlled or sustained drug release. Drugs can be loaded either covalently or non-covalently. Covalent attachment is more stable, but requires intracellular processing to remove the prodrug. Noncovalent attachment can allow for direct release but there is also the potential problem of early release. Zubarev et. al (115) covalently attached an anticancer drug, paclitaxel, to 2 nm gold nanoparticles through a hexa(ethylene glycol) linker. In this case, the drug does not need to be released for drug efficacy, but rather the entire engineered nanoparticle can remain intact while achieving its desired therapeutic effect. However, it is possible to release drugs from covalently conjugated prodrugs. One advantage to delivering the inactive prodrug and then activating it in the cell, is that delivering inert forms of the drug reduces the side effects One method for release is hydrolysis by phosphodiesterase *in vitro* (116). Another option for intracellular activation of prodrugs is the use of glutathione (117). This strategy is based on the dramatic difference in glutathione (GSH) concentration between the inside of the cell, and the extracellular environment. This GSH mediated release was shown through the release of a hydrophobic dye from gold nanoparticles. This release could be easily monitored by visual conformation in a cuvette. GSH mediated release was further confirmed using glutathione monoester as an external stimulus to release the dye.

Drug delivery has also been demonstrated in three-dimensional *in vitro* models which mimic *in vivo* tumors. GSH release of a fluorescent dye as well as anticancer drug, DOX, was shown in multicellular tumor cylindroids. This study also exhibited the importance of the surface chemistry of the gold nanoparticles. Positive gold nanoparticles have more cellular uptake and can be more effective for drug delivery in proliferating cells, while negatively charged gold nanoparticles have faster diffusion and can delivery nanoparticles deeper into tissues.

There have been other methods studied to release drugs through external stimuli. For example, Agasti et. al developed a strategy to use light to release caged drugs attached to gold nanoparticles through a photocleavable protecting group (118). The drug used was anticancer drug 5-fluorouracil attached to the nanoparticles by an *o*-nitrobenzyl group that could be cleaved using near-UV (365 nm) irradiation. In a similar study, Nakanishi et al. (170) conjugated histamine, a cell signaling agent, to gold nanoparticles using a carbamate linkage that could be dissociated via the photocleavage reaction of the same *o*-nitrobenzyl group with near-UV irradiation. The histamine was inhibited while attached to the gold nanoparticles, and achieved complete recovery after release from the particle.

Non-covalent attachment of drugs allows direct release of unmodified drugs. This is based on a strategy to functionalize the gold nanoparticle with ligands which would create

hydrophobic pockets in the monolayer. Kim et. al (119) used this strategy to deliver hydrophobic drugs/dyes. They developed biocompatible gold nanoparticles functionalized with zwitterionic ligands that encapsulated the hydrophobic payloads (Figure 10) . The zwitterionic headgroup minimized non-specific binding with macromolecules and prevented cellular uptake. The encapsulated hydrophobic groups were then released into MCF-7 cells through membrane-mediated diffusion. These particles had no toxicity indicating their lack of uptake. Thus, these systems have large potential as delivering drugs passively using the EPR effect.
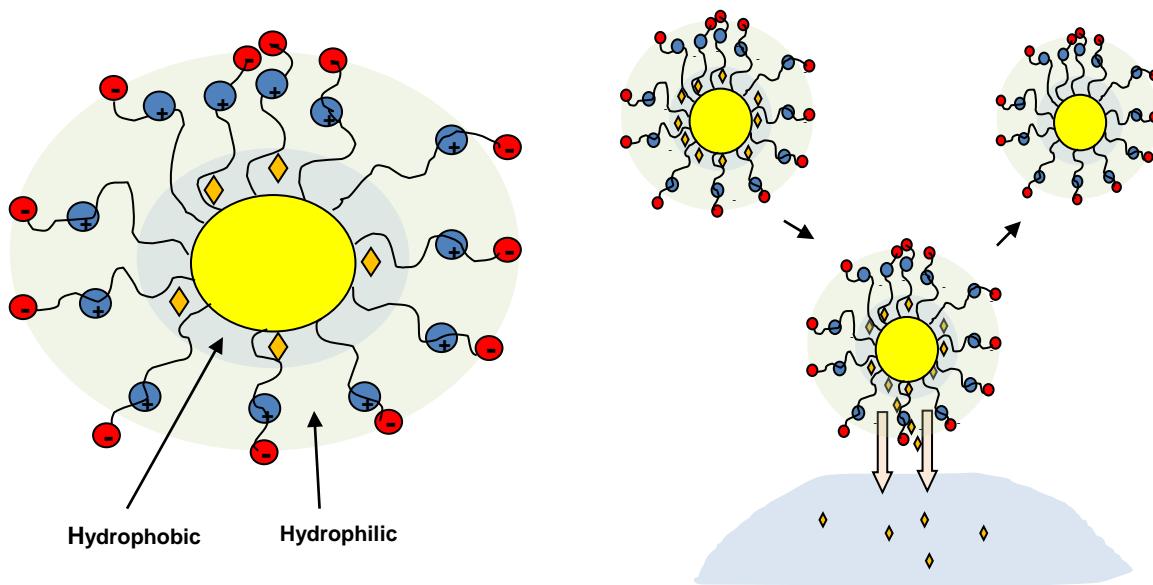
Figure 10: Non-covalent Attachment of Cargo for Cellular Delivery

Other strategies have been developed to load small molecules into the monolayer of gold nanoparticles for delivery purposes. Efficient release of nitrogen oxide from gold nanoparticles was achieved at acidic pH (pH=3) which could be useful for controlling various cellular processes such as angiogenesis, vasodilation, and the immune response. The nitric oxide was attached to the gold nanoparticles through covalent linkage with polyamine ligands (120).

2.7 Conclusions

It can be seen that gold nanoparticles have much potential in biomedical applications. GNRs have the most potential due to their unique optical properties, i.e. visibility in the NIR where there is the window of transparency for biological tissue. Additionally their increased surface area allows more room for functionalization with macromolecules of interest and targeting moieties than gold nanospheres. Also, the ability to synthesize tunable ARs would make it possible to label two different targets in the cell for imaging purposes; something that would be impossible with spheres. However, so far studies which look at gold nanoparticles for delivery or targeted imaging applications have only examined very small spheres or quantum dots. It would be desirable to use gold nanorods for these applications, but several obstacles must be overcome including uptake into the cell, localization outside of endosomes, as well as maintained biocompatibility.

3.0 SYNTHESIS, FUNCTIONALIZATION, AND CHARACTERIZATION OF GOLD NANORODS FOR TARGETED CELL DELIVERY

3.1 Introduction

Due to the exciting potential applications of GNRs it is desirable to develop a technique to produce GNRs in high yield and with few impurities. Additionally, being able to functionalize the GNRs with different surface chemistries is of interest so that GNRs can be engineered for optimal biological applications. It is vital that studies examining the properties and potential applications of gold nanoparticles complete extensive characterization prior to experimentation so that impurities do no alter the results.

As discussed in Ch. 1, there are many different techniques which can be used for the synthesis of GNRs. The synthesis method used in this study was a dual-surfactant seed mediated approach for controlled growth of GNRs with varying ARs. After synthesizing GNRs AR 3 and AR 6, the depletion induced separation procedure developed by Park et. al (49) was used to separate any unwanted shapes or sizes from the GNRs. This separation was vital when studying the bio-effects of different ARs because it ensured that the samples only contained the desired AR. After the GNRs were synthesized and purified they contain a bilayer of CTAB on the surface of the rods (42). There are many methods in which the toxic CTAB layer can be overcoated or removed to provide a different surface chemistry, as discussed in Chapter 1. In this study, it was desired to look at the bio-effects of different surface chemistries of GNRs.

Thus, different options for functionalization were researched to see if they might affect the cellular uptake or intracellular localization of the GNRs. Four different surface chemistries were chosen to study: CTAT, CTAT HA2, tannic acid, and Chariot ^{TM}.

The first functionalization chosen was CTAT. C stands for Cystein which is the amino acid with the chemical structure shown below in Figure 11.The thiol group is available to form a covalent bond with gold (42).
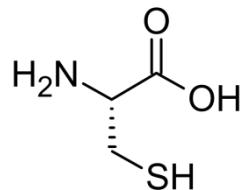
Figure 11: Chemical Structure of L-Cystein

TAT is a peptide derived from the transactivator of transcription protein of the human immunodeficiency virus type 1 (HIV-1). The TAT protein has many roles in HIV such as transcription of HIV genes, infecting cells and inducing apoptosis. The original protein is made up of between 86 and 101 amino acids depending on the subtype. For our functionalization purposes it is desirable only to mimic the cell entry, not the toxicity to the cell. Thus, the peptide used only represents the protein transduction domain of the TAT protein (96, 97). The peptide used has an 11 amino acid sequence of C-RRRQRRKKRG. TAT was chosen because it has been shown to increase uptake of small nanoparticles in other studies, and so it was hypothesized it might do the same for nanorods (121, 99).

CTAT HA2 was also chosen as a surface chemistry to examine uptake and intracellular localization. TAT HA2 contains the TAT amino acid sequence above which has been shown to increase uptake of small nanoparticles. It additionally has a peptide, HA2, derived from a hemaglutinin protein of the influenza virus. The N-terminus of the HA2 subunit is a hydrophobic domain which undergoes a pH-induced conformation change in membranes (122). Therefore, this HA2 subunit is desired because it has been shown to undergo a conformation change in endosomes as they mature and undergo a pH change from 6 to 4 (123). This conformation change would cause the endosomes to burst open, and release the nanoparticle contents into the cytosol. The peptide used has an amino acid sequence of C-RRRQRRKKRGGDIMGEWGNEIFGAIAGFLG.

Another functionalization chosen was Chariot (Active Motif, Carlsbad, California), with a molecular weight of 2,843 grams per mole, often referred to as Pep-1 in literature (124). It has been shown to deliver active proteins and peptides intracellularly and has also been shown to facilitate the cellular uptake of quantum dots (124). Chariot is described as being a novel transfection reagent suitable for delivery of proteins, peptides and antibodies into a variety of cultured mammalian cells (125). Its selling point is that it provides much faster delivery into cells than current transfection techniques. It forms a non-covalent bond with the macromolecule of interest and after delivery, the complex dissociates. Delivery can occur in the presence and absence of serum, is independent of the endosomal pathway, and is non-cytotoxic.

The final functional group chosen was tannic acid, a polyphenol of tannin. There are two forms on tannic acid - quercitannic acid is found in oak bark and leaves and gallotannic acid and is found in oak galls. Tannic acid has many uses including use in wood staining, textiles, wine, pharmaceuticals, and corrosion resistance treatments to name a few. Tannic acid is a weak acid with a pKa around 10 (126) and the protonated structure is shown in Figure 12. In literature, there are not many examples of tannic acid being used to functionalize gold nanorods. However, it has been shown in this lab to successfully functionalize to GNRs resulting in a negative surface charge (127).
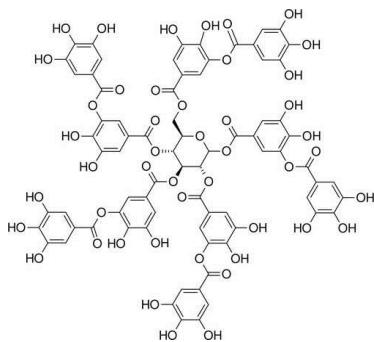
Figure 12: Tannic Acid Chemical Structure

In order to determine if synthesis, purification, and functionalization of the GNRs was successful, many characterization techniques need to be performed before any studies of the bio-effects are started. Otherwise it cannot be stated with certainty that change in the biological properties are due to a specific property or aspect of the nanoparticle being tested. In this study, characterization of synthesized GNRs was by Ultra-visible Spectroscopy (UV-Vis),

Transmission Electron Microscope (TEM) with a software program Image J, and Laser Doppler Electrophoresis (LDE).

Early studies on nanomaterials and their bio-effects tend to not contain much if any characterization of the nanoparticles. A lot of these nanomaterial papers contain conflicting data on bio-effects, and the lack of characterization could be a major reason for this. In 2009 at the Spring Materials Research Society Meeting the importance of characterization of nanoparticles was brought up as a main area for improvement in the study of nanomaterials (128). At a conference on Nanotoxicology: Health and Environmental Impacts held in the UK that same year, a major conclusion of the conference was that more emphasis needed to be given to the importance of characterization of nanomaterials in order to determine safe exposure limits such as in drug delivery (129). This message has continued to be reiterated by other nanomaterial researchers (130,131). Hussain et al. (130) describe the main limitation to assessing toxicity as the characterization of the nanomaterials. They say that state-of-the-art physiochemical characterization methods are needed in order to determine the exact nature of nanomaterials interactions with humans and cells (2).

The reason for this importance is because of how sensitive biological studies are to nanoparticle size, shape, surface chemistry. There are many situations that may be envisioned that would show how a lack of characterization of the nanoparticles being used can skew your experimental results. For example, nanoparticles have been shown to agglomerate in media with serum. Agglomeration changes the size of the particles and thus would skew any size dependent toxicity study. Additionally, purchased nanoparticles can vary from company to company and so this might also skew results if they are not properly characterized beforehand.

Additional characterization methods exist other than the techniques used in this study (UV-Vis, TEM, LDE, ICP-MS). While size was determined in this study using UV-Vis and TEM, it can also be determined by using mass spectrometry, analytical ultracentrifugation, size exclusion chromatography, capillary electrophoresis and gel electrophoresis. Additionally, to assess the surface chemistry of nanoparticles there are other techniques that could have been used instead of or in addition to LDE. These include X-ray photon spectroscopy, Atomic Force Microscopy-based scanning probe techniques and bioRaman. While elemental composition was determined using ICP-MS and UV-Vis, X-ray spectroscopy could have also been used (132). Currently there are more than 400 different characterization techniques that can be used with nanoparticles (130). While it would be very redundant to use all these techniques it is important that the major physiochemical properties of the nanoparticles are fully assessed before any bio-effects experimentation occurs.

3.2 Methods

The specific procedure used for synthesis of the GNRs is a seed mediated synthesis procedure modified from that published by Park et al. (37, 127). It consists of the combination of two solutions, a seed solution and a growth solution. The seed solution is 10 mL and contains 0.1 M CTAB in sterile water to which 25 µL of 0.1 M $HAuCl_4$ is added. The growth solution is 100 mL and contains 0.1 M CTAB, BDAC is varying amount, and deionized water. The concentration of BDAC in the growth solution was increased from 0-0.15 M in order to increase the resulting aspect ratio of the nanorods, with greater concentrations of BDAC resulting in higher aspect ratio GNRs. To the growth solution, 500 µL of 0.1M chlorauric acid, 80 µL 0.1M silver nitrate, and 550 µL 0.1 M ascorbic acid was added to the solution. The ascorbic acids acts

as a weak reducing agent causing the formation of gold ions in the growth solution. Both the seed solution and growth solution were at room temperature (18-24ºC) before proceeding since temperature variation has been shown to affect GNR AR. Upon solution equilibrium to room temperature, 60 µL of ice cold 0.1 M sodium borohydride was added dropwise into the seed solution with mixing. Sodium borohydride is a strong reducing agent causing the formation of gold seeds, resulting in a color change from light yellow to brownish red indicating that the seeds formed. After five minutes, 100 µL of the seed solution is added to the growth solution. The growth solution was stirred overnight during which the solution turned a deep red color as rod formation occurred. Two different ARs were synthesized for this study: AR 3 and AR 6.

After the synthesis procedure, depletion induced separation procedure was used to purify the GNRs (49). In order to separate the impurities, BDAC was added in excess (0.18-0.25 M) to the vials of synthesized GNRs. BDAC was forced into solution as much as possible through sonication, heat, and mixing. The GNRs then sat overnight. After 24 hours, there was a color change between the solution and agglomerates, which settled at the bottom of the vial and contained the longer GNRs. The supernatant solution was removed and replaced with water to resuspend the agglomerates. Once the agglomerates were resuspended, the GNR solution was a slightly different color than the original GNR solution, indicating the removal of impurities.

After synthesis and purification, the nanorods were functionalized with the desired chemical groups. A portion of the GNRs was first functionalized with thiolated PEG to displace CTAB, and resulting in PEG attached covalently to the gold surface (42). The method for functionalization was an addition method using 0.001M PEG solution. The amount of PEG solution to be added to the GNRs was calculated based on the concentration and volume of the GNRs. The number of PEG molecules added per one nanorod was four times the surface area of the nanorod in nm^2. See Appendix for the detailed calculation. Addition took place at room temperature (18-24ºC) and the GNRs were exposed to the PEG for 24 hours.

After adding the appropriate amount of 0.001 M PEG, the solution was mixed and allowed to sit overnight. Then the GNRs/PEG solution was centrifuged and the supernatant was removed and replaced with water. This removed the CTAB which was displaced as well as any PEG which was not attached to the nanoparticles. Then the same amount of PEG was added again to sit overnight, and then centrifuged again to remove any free PEG in the solution. Repeating the process over again ensured that PEG was able to fully attach to the gold surface. This procedure is illustrated in Figure 13.
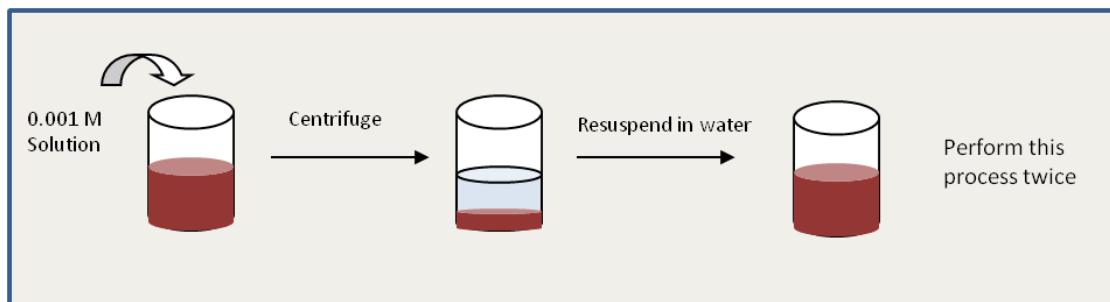
Figure 13: Functionalization Procedure for GNRs

After functionalizing with PEG, the nanorods were further modified with TAT, TAT HA2, or Chariot. The same addition procedure was used as described above except that the process was only performed once. This is because too many centrifugations can result in irreversible agglomeration of the nanorods. Also, in order to make sure that the dominant surface chemistry was one of these functionalizations of interest rather than PEG, three times more of 0.001 M peptide was added than 0.001 M PEG that was added in the previous step. In other words, when functionalizing with PEG the number of molecules added was equal to 4 times the surface area of the nanorod but when functionalizing with TAT, TAT HA2, tannic acid, or Chariot the number of molecules added was 12 times the surface area of the nanorod. This calculation is illustrated in the Appendix.

Tannic acid functionalization was slightly different than that of TAT, TAT HA2, and Chariot. Tannic Acid was functionalized to the plain particles rather than the PEGylated particles. The procedure for functionalizing with tannic acid is the same procedure as for functionalizing with PEG as illustrated in Figure 13.

After synthesis and functionalization, characterization techniques were used to further define the GNRs. Firstly, UV-Vis was used to determine the AR, length, and diameter of the GNRs. As discussed in the section on optical properties, the wavelength of the longitudinal surface Plasmon (LSP band) is dependent on AR. This dependence can be calculated using two major methods: Discrete Dipole Approximation or Gans theory (14, 15).   The equations have been shown previously, but they are shown again below rearranged for convenience.

$$Gans\ Theory\ Equation: \quad AR = \frac{\lambda_{max} - 381.49}{97.65} \tag{8}$$

$$Discrete\ Dipole\ Approximation\ Equation: \quad AR = \frac{\lambda_{max} - 418}{96} \tag{9}$$

In order to calculate the AR for GNRs in this study, an average of the two ARs calculated from each equation was used. The λ_{max} is equivalent to the wavelength of the longitudinal peak. It is also referred to as the LSP band. In order to calculate the diameter of the GNRs, the AR is used in the following equation:

$$D\ (nm) = -2.7(AR) + 26.7 \tag{10}$$

This equation is based on experimental results (127) and is a good approximation of diameter. Diameter can be measured more accurately using Image J and TEM images. Length can then be calculated from the diameter. Length is equal to the diameter times the extinction coefficient. The extinction coefficients are obtained from data published by Nikoobakht (133) and are shown below in Table 2. Data can be interpolated from the data above for ARs not explicitly shown.

Table 2: Extinction Coefficients of GNRs	
Aspect ratio	e (M^{-1})
1	2.400E+08
2.5	8.061E+08
3	1.721E+09
4	3.012E+09
5	4.429E+09
6	5.313E+09
7	6.266E+09
8	7.130E+09

In order to calculate the molar concentration of the solution, Beer's Law can be used.

$$c = \frac{A}{\varepsilon l} \qquad (11)$$

Where *A* is the Absorbance, *l* is the path length, *c* is the molar concentration and ε is the extinction coefficient. When the path length is 1 cm, the molar concentration can be found by dividing the absorption of the longitudinal peak by the extinction coefficient. This molar concentration can be converted to a mass concentration. The amount of functionalizing agent, such as PEG, to be added to a GNR solution can be calculated based on the amount of solution, concentration of GNRs, and surface area of the particle. These calculations can be found in the Appendix.

3.3   Results

UV-Vis was run on the GNR solutions and a graph of absorbance vs. wavelength was produced. Before the GNR solutions were analyzed with UV-Vis, water was run in order to create a baseline. The graph of the baselines is shown in the Appendix. First, a sample of GNRs was run on UV-Vis to confirm the depletion induced separation procedure worked. A graph of UV-Vis plots both before and after the Depletion Induced Separation procedure was performed is shown in Figure 14. A small regularly shaped transverse peak indicates few impurities.
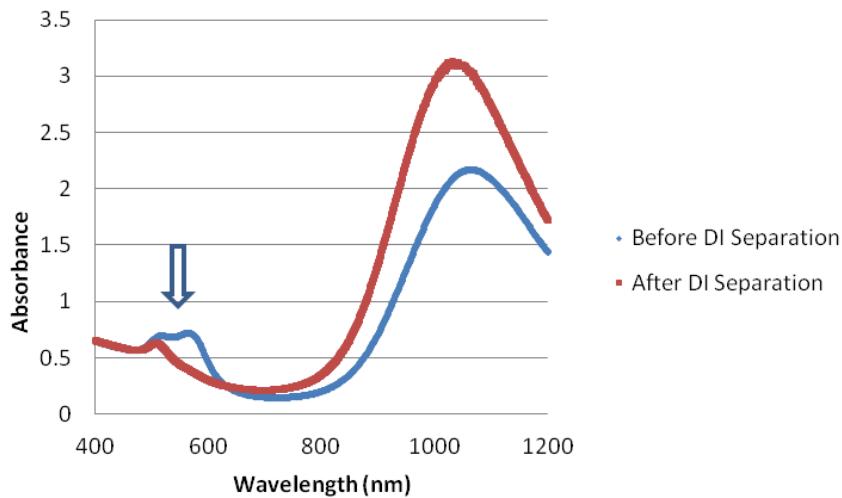
Figure 14: Depletion Induced Separation of AR 6 GNRs

The following UV-Vis plots shown in Figure 15 were obtained for the purified CTAB coated AR 3 and AR 6 GNRs and they were used to calculate the length and diameter of the rods. These plots are obtained after depletion induced separation, as can be seen by the small transverse peak.
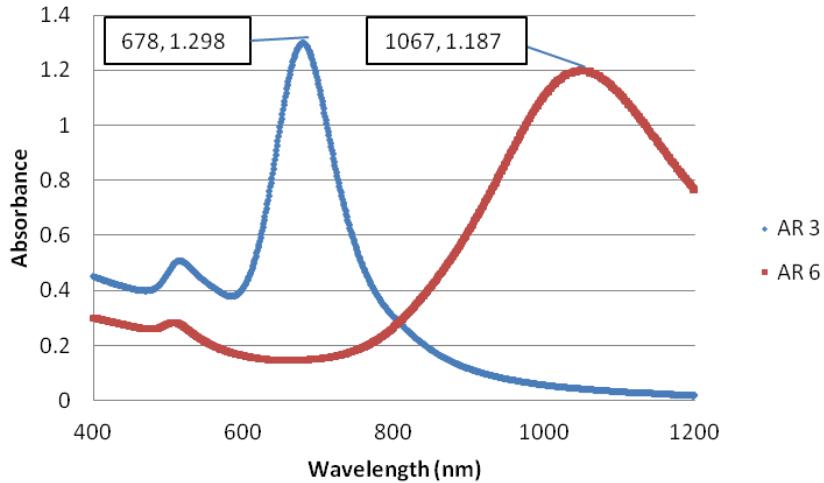
Figure 15: UV-Vis Characterization of Plain GNRs AR 3 and AR 6

The GNRs were also characterized using UV-Vis after functionalization. The plots are shown in Figure 16.
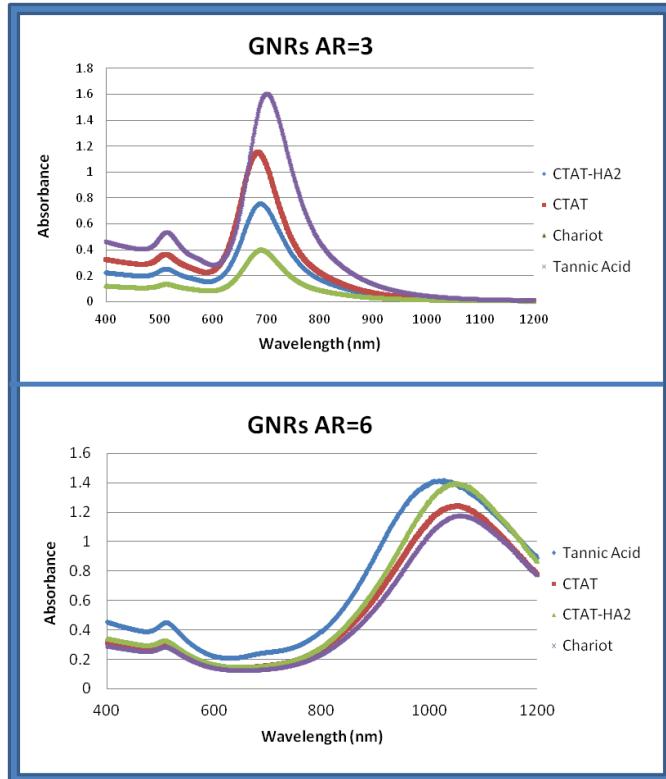
Figure 16: UV-Vis Characterization of Functionalized GNRs AR 3 and AR 6

Calculations described in the Methods section were used to determine the length and diameter of the GNRs from UV-Vis data.

Table 3: UV-Vis Calculated Dimensions of GNRs		
Aspect Ratio	Calculated Length (nm)	Calculated Diameter (nm)
2.85	54.321	19.06
6.85	57.5263	8.398

In addition to calculations based on the UV-Vis results, TEM was also used to determine the size and shape of the GNRs. As shown in Figure 17, the TEM images of the AR 3 GNRs functionalized with CTAT, CTAT HA2, Chariot, and tannic acid were imaged. Over one hundred rods were measured for each of the samples on the computer program Image J to determine average lengths, widths, and aspect ratios. Figure 18 shows the TEM images of AR 6 GNRs and Table 4 is the measured dimensions for these particles.
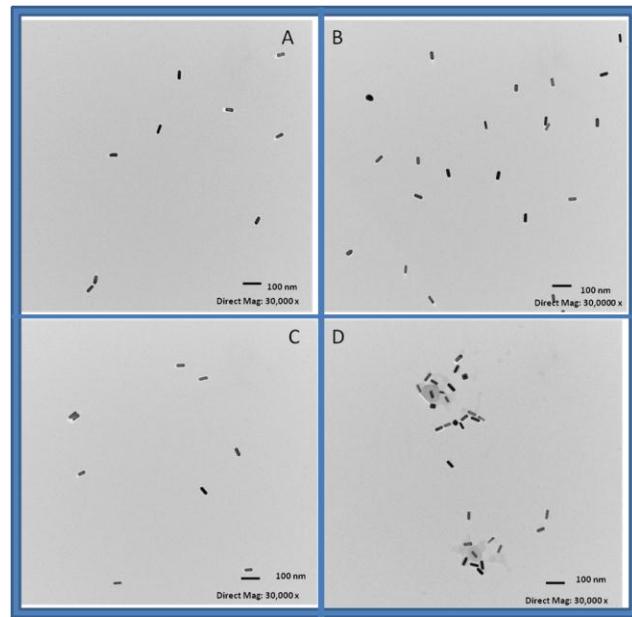
Figure 17: TEM Characterization of Functionalized GNRs AR 3
A: TAT, B: TAT HA2, C: Chariot, D: Tannic Acid
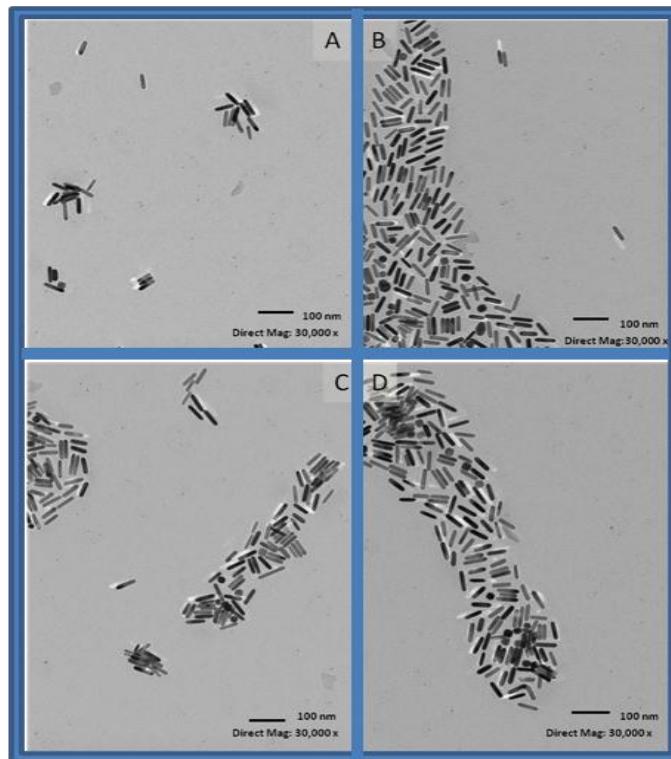
Figure 18: TEM of Functionalized GNRs AR 6
A: TAT, B: TAT HA2, C: Chariot, D: Tannic Acid

Table 4: Calculated Size of Functionalized GNRs Determined by TEM

Aspect Ratio	Functionalization	Average Length	Average Width	Average AR	AR Standard Deviation (n=100)
3	TAT	39.53	13.06	3.11	0.520
	TAT HA2	43.92	14.54	3.06	0.406
	Chariot	43.0	14.51	3.03	0.468
	Tannic Acid	43.2	14.52	3.02	0.468
6	TAT	63.49	10.52	6.04	0.473
	TAT HA2	62.56	10.102	6.19	0.421
	Chariot	65.76	11.07	5.94	0.493
	Tannic Acid	64.12	10.76	5.95	0.473

The zeta potential of the functionalized GNRs was also measured using the LDE as shown below in Table 5. The zeta potentials were measured in GNR solutions diluted in water.

Table 5: Zeta Potentials of Functionalized GNRs

Functionalization	Zeta Potential (mV) AR=3	Zeta Potential (mV) AR=6
PEG	2.6	1.9
TAT	8.4	9.48
TAT HA2	9.2	11.8
Chariot	20.9	22.9
Tannic Acid	-19.7	-25.2

3.4 Discussion

The synthesis of gold nanorods is a result of complex reactions forming rods from gold seeds. The mechanism for the growth of GNRs instead of nanospheres is largely due to the CTAB surfactant. When chlorauric acid is reduced by ascorbic acid, gold ions are formed in the growth solution. In order to keep these ions from simply reducing on the seeds and forming spheres, the gold ions group together with the CTAB and reduce the bromine. The reaction for this is shown below in Equation 1 (7).

$$CTAB + HAuCl_4 \xrightarrow{Ascorbic\ Acid} CTA^+ + Br^- + Au^- \rightarrow CTA - Au \qquad (12)$$
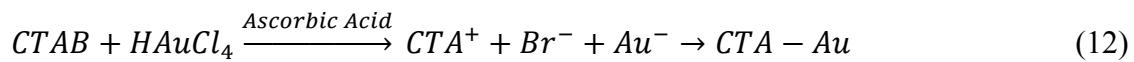
The ammonium head group on the CTAB will bind to the gold surface with the neutral tail pointed outwards. BDAC will also bind its polar head group to the gold surface with the neutral tail pointed outwards (42). The BDAC structure is shown in Figure 19.
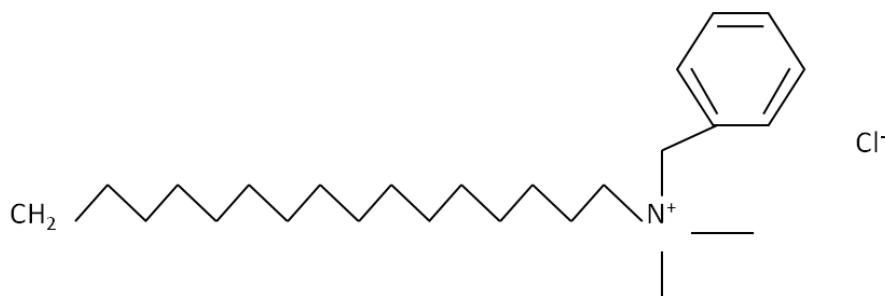
Figure 19: BDAC Chemical Structure

These neutral tails will attract to each other forming metamicelles around the gold ions. The metamicelles are important because they transport the gold ions to the surface of the GNR where they are reduced. The size of the metamicelle controls the speed of the transport to the GNRs. Smaller metamicelles diffuse faster to the surface of the gold and thus react faster onto the surface resulting in smaller ARs. Larger metamicelles take longer to get to the surface and thus it takes longer for the gold ions to reduce, resulting in larger ARs. This is why BDAC is added in order to increase ARs. BDAC is bulkier than CTAB due to its chemical structure, and thus it results in larger metamicelles, slower reaction times, and longer ARs (7, 134).

It has been shown that the structure of GNRs is made up of different lattice planes with different energy levels. The top of the nanorod contains the 001 planes while the sides contain 100,110, and 111 planes. The 100,110 and 111 planes are more energetic and so the CTAB and silver ions attach preferentially to these planes. This allows the gold ions to deposit onto the 001 plane and not onto the other planes, resulting in the formation of a rod shape (7,134).

After the GNRs are synthesized, functionalization can take place as a result of many different methods. By looking at the chemical structure of the surface chemistries chosen it was hypothesized which mechanism of functionalization would be employed. In this case, the TAT and TAT HA2 peptides contain a thiol group to form a covalent bond on the gold whereas Chariot and Tannic acid do not. Thus, it is hypothesized that TAT and TAT HA2 bind semi-covalently to the gold through their cystein group. On the other hand, Chariot is functionalized through hydrostatic attractions with the PEG molecules on the surface of the gold. Tannic Acid is hypothesized to be functionalized through hydrostatic attractions to CTAB, as illustrated in Figure 20.
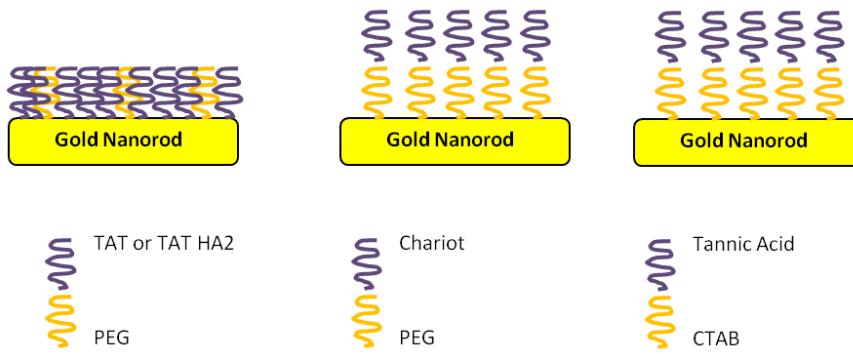
Figure 20: Hypothesized Surface Functionalizations of GNRs
A: TAT or TAT HA2, B: Chariot, C: Tannic Acid

Once the GNRs are synthesized and functionalized, it is important to perform thorough characterization. The UV-Vis results can be used to characterize the GNRs in many different ways. UV-Vis is a spectrophotomer, meaning that it measures light intensity at varying wavelengths in the ultraviolet and visible regions. A light source passes through a sample, and light is diffracted into a spectrum which is detected by a sensor and interpreted into an output. The output is usually a graph of light intensity versus wavelength. The graph of absorbance versus wavelength can be used for many different types of samples to determine many different parameters (135). In this study, UV-Vis was used to characterize samples of GNRs to determine their ARs, concentration, state of agglomerations, and the amount of functionalization groups to be added.

In addition to these calculations, UV-Vis was also used to assess the agglomeration of a sample of GNRs. It is desirable to avoid agglomeration to avoid a variable in the process that is likely to alter the bio-effects. For example it has been shown that particles that are more agglomerated have higher cellular uptake than well dispersed particles (127). Agglomeration can be detected on UV-Vis through peaks shifting or through broadening of peaks. Therefore particles are more stable if the peaks are narrow rather than broad.

UV-Vis can also be used to observe the purity of the GNR solution qualitatively. If the transverse peak seems large or irregular, this represents the presence of impurities (127). After depletion induced separation, the transverse peak should decrease and become less irregular. It can be seen that this is the case for the UV-Vis plots shown, meaning that the GNR solutions are very pure (Figure 15, 16).

Additionally, when looking at the UV-Vis plots for the functionalized GNRs one can see that the LSP peaks have not changed significantly since functionalization, and the peaks have not broadened. Thus, it looks like there hasn't been any significant agglomeration resulting from changing the surface chemistry in these cases. Additionally, no visible agglomeration was observed in the solutions. The only reason for differences in absorbance is that the concentrations are different.

TEM images are another way to examine the size and shape of the nanoparticle samples. In contrast to light microscopes, electron microscopes such as TEM use a beam of electrons in place of a beam of light. When one observes something in a light microscope, it is because light particles, or photons, are reflected off the sample. In order to observe something smaller than photons, a smaller particle needs to be used such as electrons. TEM is a good choice of characterization for GNRs because it can image specimens on the nanometer scale with high

34

resolution (136). In this study, images of the GNRs were taken to verify shape, size, and purity of the samples. In conjunction with the scale bar produced with the TEM image, the length and diameter of the nanorods was determined by ImageJ (NIH, Bethesda Maryland). Looking at the TEM images in Figures 17 and 18 as well as the measurements in Table 4 it can be seen again that the samples were very pure and the functionalization did not have a significant effect on size or shape. The dimensions are similar to those calculated using UV-Vis.

LDE with a Zetasizer (Malvern Instruments, Worcestershire, UK) is also used to assess surface chemistry of the GNRs. When particles are dispersed in an aqueous system they will have a surface charge due to surface groups or adsorption of charged species. This surface charge will modify the distribution of the surrounding ions, which will result in a layer around the particle which is different than the bulk solution. This layer surrounds the particle even as the particle is moving through the bulk fluid. The zeta potential is the potential at the point in this layer where it moves past the bulk solution. For a solution of GNRs, the zeta potential is indicative of the surface charge of the nanorods (137).

The results from LDE confirm successful functionalization as well as insight into the charge of the attached surface group. After functionalizing with PEG the zeta potential of the GNRs was near neutral charge. The change in zeta potential after functionalizing with the additional groups provide insight into what kind of uptake the particles might have and how they might react with other surface chemistries.

3.5 Conclusion

A procedure to synthesize GNRs of varying aspect ratios was successfully employed to produce GNRs in high yield. Additionally, Depletion Induced Separation was a successful technique to produce very pure samples. The addition technique for functionalization was successful for both thiolated chemical groups as well as non-thiolated.

The GNRs to be used in the study have been well characterized. The rods are all of very similar size with few impurities. The size correlates well between UV-Vis calculations and TEM images. Zeta potential shows that functionalization with both PEG and peptide was successful and did not result in any agglomeration of the GNRs.

4.0   FUNCTIONALIZATION OF GOLD NANORODS: STUDIES ON LOCALIZATION, ORIENTATION, AND BIO-EFFECTS

4.1   Introduction

Due to how young the field of nanotechnology is, there are still many questions that need to be answered in order to pave the way for applied nanotechnology. Many potential biological applications were discussed in Chapter 1 such as delivery of biomolecules of interest. In order to aid these applications it would be useful to understand how properties of nanomaterials affect biological responses. Since GNRs have the most potential as new delivery agents due to their strong optical properties and large surface area for functionalization, these are the materials used in this study. The ability to synthesize a variety of aspect ratios and functionalize with various surface chemistries allows these parameters to be examined in a systematic way. In this study, GNRs with ARs 3 and 6 functionalized with TAT, TAT HA2, Chariot, and tannic acid are used to examine the effects of size and surface chemistry on toxicity, cellular uptake, agglomeration,

and intracellular localization. Finally, functionalization with a model biomolecule is used to demonstrate potential applications.

4.1.1   Toxicity. In many applications, such as biological uses, it is necessary for the GNRs to be biocompatible. There are many different tests to assess biocompatibility and to measure the toxicity of GNR on the cell culture. Toxicity is defined as the degree to which a substance can harm humans or animals (138) and can be examined either *in vivo* or *in vitro*. *In vivo* tests are done within a living organism, whereas *in vitro*, which literally means "in glass", is performed in an environment outside of an organism, such as in a plate of cells or cell tissue (139).

In vivo* tests have the advantage of being more realistic in the sense that they can give information about the response of the whole organism. However, these tests are based on the assumption that the adverse effects observed in one animal species would be the same as in another species which is not always the case (140-142). Additionally, there have been recent movements to reduce animal testing due to concerns over animal welfare. Some toxicity test methods consume hundreds of thousands of animals per substance tested (143,144), which has led to several countries prohibiting animal testing if there are other reasonable alternatives available (145). Another disadvantage is that animal testing is extremely expensive and takes much more time than *in vitro* testing.

In vitro* tests are limited in that they can only examine the toxicological process at the cellular and molecular level. In order for these tests to be worthwhile, they need to be related to an *in vivo* situation. Ideally, these tests would be able to determine the mechanism of toxicity so that the events between exposure and the response in the organism would be known. Advantages of *in vitro* tests are that they can be performed in a very controlled environment, and different cell lines can be used to determine which parts of the organism might have a toxic response to the substance *i.e.* skin cells, bone cells, kidney cells etc.

The most common form of *in vitro* testing is using a cell line in a culture plate or dish grown in controlled conditions outside of their natural environment. The cell lines have been immortalized by a mutation or deliberate modification which are then able to proliferate indefinitely. Depending upon the cell type, the cells can be grown in suspension or in adherent cultures on tissue culture treated plates or flasks. The cell line used in this study, HaCaT, is an adherent cell line of epithelial cells cultured in tissue culture treated flasks.

There are several *in vitro* tests which assess the cytotoxicity of a substance. Three common techniques for toxicity are 1) to quantify the number of live/dead cells; 2) to look at the viability of the mitochondria; or 3) to evaluate the oxidative stress of the cells. One example of the live/dead test is the neutral red assay. Cells are seeded in a 96 well plate and exposed to a substance at varying concentrations with positive and negative control chemicals. Then the cells are rinsed and treated with neutral red, a dye that can be taken up only by live cells. The intensity of the color corresponds to the number of live cells and can be quantified in a plate reader at 540 nm wavelength absorbance (146). An example of the mitochondrial activity assay is the MTT (3[4,5-dimethylthiazol-2-yl]-2,5-diphenyltetrazolium bromide) assay. MTT is a tetrazolium dye which is reduced by enzymes in the mitochondria to a blue color. Only viable mitochondria can carry out this reaction, so this tests the mitochondrial integrity of the cells and the intensity of the color is again related to the number of cells with viable mitochondria (147). The MTS (3-(4,5-dimethylthiazol-2-yl)-5-(3-carboxymethoxyphenyl)-2-(4-sulfophenyl)-2H-tetrazolium) assay is very similar, but uses a slightly different tetrazolium dye. Another *in vitro* toxicity test measures the lactate dehydrogenase (LDH) activity. In normal viable cells, the LDH enzyme is present in

the cytoplasm of the cells, however, when cells are dead or dying LDH can escape into the cell culture medium through the cells' leaky vasculature. A small amount of the cell culture medium can be removed and tested for the amount of LDH (147). The third approach of evaluating the reactive oxygen species (ROS), which are chemically reactive molecules containing oxygen. The level of ROS increases dramatically during times of stress and can be quantified through cell staining (148). Figure 21 shows a confocal image of HaCaT cells exposed to 25 µg/mL PEGylated GNRs with blue DAPI stained nucleus and the fluorescent green ROS. In order to assess the toxicity of the GNRs used in this study, the MTS assay was chosen because it has worked well with other nanomaterial toxicity tests in literature and in-house.
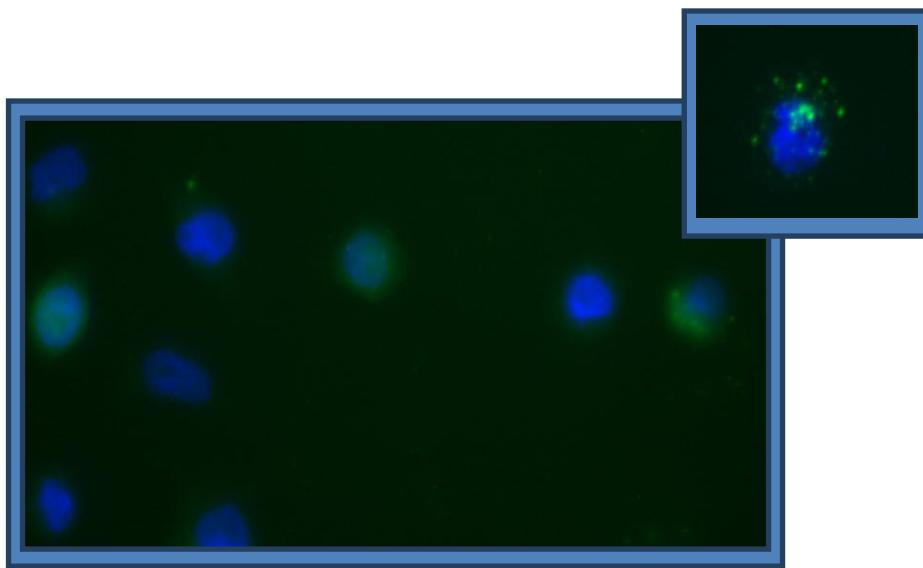
Figure 21: ROS Image of GNRs in HaCaT Cells

4.1.2 Cellular Uptake. Cellular uptake of nanoparticles has been demonstrated to be dependent on many factors such as size, shape, surface chemistry, and agglomeration (40). In this study, we looked at the uptake based on four different surface chemistries and two different ARs. The surface functionalizations used in this study have been looked at with smaller nanoparticles, but they have not been examined for GNRs.

TAT, for example, has been used to functionalize gold nanoparticles in a couple of studies looking at cellular uptake and intracellular localization. Fuente *et al.* (97) exposed human fibroblast cells to 2.8 nm diameter gold nanoparticles (GNP) functionalized with TAT and found that TAT promoted cellular uptake of the GNPs. TAT has also been used to functionalize small nanoparticles of other materials. Zhao *et al.* (149) functionalized superparamagnetic iron oxide nanoparticles with TAT and examined the effect on cellular uptake. They found that increasing the ratio of TAT to nanoparticles resulted in higher uptake in a nonlinear fashion. Similarly, dextran coated 41 nm diameter superparamagentic iron oxide nanoparticles functionalized with TAT were internalized into cells 100 times more efficiently than nonmodified nanoparticles (150). Additionally, TAT was attached to DNA nanocomplexes via PEG spacers and gene transfection efficiency of primary neurons was increased up to 14-fold (151), demonstrating the broad ability of TAT to increase uptake of other species as well.

TAT HA2 has also been conjugated to nanoparticles in literature. Koshman *et al.* (123) conjugated quantum dots with proteins and TAT HA2 and it was thought that the TAT portion of the TAT HA2 was responsible for the cellular internalization of the particles. The HA2 is a hemagglutinin protein which changes conformation at low pH which disrupts the endosomal membrane, releasing the contents into the cytosol (99). Kumar *et al.* (99) conjugated TAT HA2 to 20 nm gold nanoparticles and achieved efficient uptake and localization outside of the endosomes.

The conjugation of Chariot to nanospheres or nanorods has not yet been examined in literature. Chariot has been used in several studies to deliver functionally active proteins and peptides intracellularly without the need for cross-linking or denaturation (152,153). It has also been used to deliver quantum dots independently of endocytosis (124).

Tannic Acid has been conjugated to gold nanoparticles and was shown to prevent aggregation (154). It has also been shown to adsorb to carbon nanotubes (155). The uptake of particles functionalized with tannic acid, however, has not been shown.

In addition to looking at the outcome of surface chemistry on uptake, the effect of AR on cellular uptake was also examined. Thus far, it has not been clearly shown in the literature how the AR of nanorods affects cellular uptake.

4.1.3   Mechanism of Cellular Uptake. In addition to examining the mass of gold uptaken into the cell, it is also worthwhile to understand *how* the gold is entering the cell. Understanding the mechanism of uptake is important to understand the biological fate of the nanoparticles (156). Additionally, by understanding the mechanisms used in the uptake of these particles, more effective delivery complexes could be generated (73). It is thought that engineered nanoparticles enter the cells through endocytosis. More specifically, there are several different methods of endocytosis that were discussed previously. In order to test whether endocytosis is being used and the specific type of endocytosis, chemical inhibitors can be used. An inhibitor blocks the pathway necessary for a particular type of endocytosis. In this study, four different inhibitors were used. These inhibitors are chlorpromazine, 5-(N-Ethyl-N-isopropyl)amiloride (EIPA), genistein, and incubation at 4°C.

Chlorpromazine is used to inhibit clathrin-mediated endocytosis. It is a cationic amphilphilic drug marketed in the United States as an antipsychotic. It is said to inhibit clathrin-coated pit formation by a reversible translocation of clathrin and its adapter proteins from the plasma membrane to intracellular vesicles (157). EIPA has been shown to inhibit Na^+/H^+ exchange which has been documented to inhibit macropinocytosis (158,159). Genistein is a tyrosine-kinase inhibitor used to inhibit caveolae mediated endocytosis. It causes local disruption of the actin network at the site of endocytosis and inhibits the recruitment of dynamin II, both of which are necessary events in the mechanism of caveolae-mediated uptake (73). Incubation at 4°C inhibits any entry into the cell which is energy dependent. Since endocytosis is energy dependent, this can determine if uptake through endocytosis is occurring (156).

There have been several studies in literature using endocytosis inhibitors to look at cellular uptake mechanisms of different particles. These studies found that typically if the particles are in media with serum, the particles adsorb the serum proteins on the surface resulting in uptake by receptor-mediated endocytosis (RME) (160). RME is a form of clathrin dependent endocytosis. If the nanoparticles are coated by organic molecules, the cellular uptake pathway is likely altered. It has been suggested that positively charged particles tend to enter the cell

through macropinocytosis, whereas negatively charged particles tend to rely more on clathrin mediated endocytosis (161). One study found that plain gold nanoparticles, positively charged from CTAB coating, were taken up by macropinocytosis, clathrin mediated endocytosis, and caveolae mediated endocytosis (162). They found that PEG-coated gold nanoparticles with a slightly negative charge entered the cells mostly through caveolin and clathrin mediated endocytosis (163). It has also been suggested that the size of the nanoparticles affects the uptake mechanism and that larger particles or aggregated particles are more likely to use macropinocytosis than smaller particles. Reports on the effect of size on uptake mechanism, however, are often inconsistent (164-166). For example, one study looking at 500 nm nanoparticles found that the primary mechanism of uptake was caveolae mediated endocytosis, whereas another group found that in order for nanoparticles to be taken up by caveolae they must be less than 100 nm. (167).

4.1.4 Nanoparticle Agglomeration. Agglomeration is an issue with nanoparticles that is just recently starting to be addressed. Although nanoparticles may be dispersed in water, when exposed to media with serum, agglomeration will most likely occur. Albanese *et al.* (168) examined the effects of aggregation of gold nanoparticles on cellular uptake and toxicity. They found that aggregation did not affect toxicity and that the aggregated particles decreased uptake in some cell types, but increased uptake in others. All the gold nanoparticles in the study had the same surface chemistry, a transferrin coating. This shows the complexity of the behavior of aggregates and the importance of further studies on aggregation behavior. In order to examine agglomeration as a function of surface chemistry, dynamic light scattering was used to see the size of the GNRs AR 3 in biological media. Additionally, UV-Vis was used to look for peak shifts or broadening of SPR peaks which indicates agglomeration of GNRs. A stability ratio based on this UV-Vis behavior was calculated based on a calculation found in literature (171).

4.1.5 Intracellular Localization. Many applications for GNRs are dependent on the intracellular localization of the particles. It is hypothesized that most nanoparticles enter the cell through varying methods of endocytosis (72). Therefore it is likely that when GNRs first enter the cells, they are localized in endosomes. There are several surface chemistries, however, that have been shown to change configuration in endosomes to promote endosomal release. HA2 for example has been discussed as providing endosomal release when attached to small nanospheres or quantum dots (123). If GNRs are released from endosomes, they would be ideal candidates for delivery or bioimaging agents because they would be free to reach an intracellular target rather than being trafficked to lysosomes and degraded. The only gold nanoparticles shown to be used for delivery and imaging applications to date have been nanospheres or quantum dots. GNRs have much more promise in these applications due to their increased surface area for functionalization and their unique optical effects, however they have not been shown to localize outside of the endosomes in current literature. Besides potential use as delivery agents, information on where GNRs localize intracellularly provides important information about biological effects that might result.

The TEM was first used in Chapter II to characterize the size and shape of the synthesized GNRs. Another use for this instrument is to look at nanoparticles in stained and fixed cells. This is useful because it can provide information on where the nanoparticles have

localized intracellularly. The nucleus, cell wall, and often endosomes can be detected in a TEM image. Therefore, it can be seen whether the GNRs are localized in relation to these.

Another protocol used to look at the intracellular localization of GNRs in the cell is an immunofluorescence staining procedure. In this procedure the endosomes and the nucleic were stained so that it could be examined whether the GNRs were localizing in the endosomes. Cells are first exposed to an antibody for early endosomes which attaches to the endosomes. Next a secondary antibody with TRITC binds to the first antibody, resulting in the endosomes fluorescing under TRITC light. If the particles are fluorescently tagged, these samples can be viewed using a confocal laser scanning microscope (CLSM). The CLSM provides the strongest data of localization in the endosomes because only one z-plane is displayed. If a regular fluorescent microscope was used it would not be clear if the particles were localized in the endosomes or if they were simply directly above the endosome in the cell.

When using CLSM the nanoparticles must be fluorescently tagged. In this study, Doxorubicin (DOX) (Figure 22) was functionalized to the GNRs as the fluorescent tag. This was chosen because in addition to being naturally fluorescent, DOX is also a well known anti-cancer drug. Thus, the ability of GNRs to deliver a model biomolecule can also be assessed through the same study.
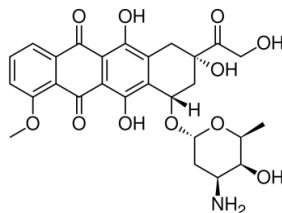
Figure 22: Doxorubicin Chemical Structure

4.2   Methods

4.2.1   MTS Assay. HaCaT cells were plated at 25,000 cells per well in a 96 well plate and grown for 24 hours. The cells were treated with varying concentrations of the GNRs (0 µg/mL, 15µg/mL, 25µg/mL, 50µg/mL) for another 24 hours. Next, the wells were washed with warm PBS and replaced with 100 µL fresh media. 20 µL of the MTS solution was added to each well, and the solution incubated for 2-4 hours. Then the well absorbance at 490 nm was determined in a plate reader (Bio Tek Syngergy HT). By comparing the absorbance of the control to the substance concentration of interest, the percent viability was determined using Equation 1.

$$\% \; Cell \; Viability = \frac{Absorbance \; at \; Concentration \; of \; Interest}{Absorbance \; of \; Blank} * 100\% \qquad (13)$$

4.2.2   Quantification of Cellular Uptake. In order to prepare samples for ICP-MS, cells were exposed to the GNRs for 24 hours before they were digested to release the nanoparticles into solution to be measured by the mass spectrometer. 5 mL of HaCaT cells were seeded in 6-well plates at 200,000 cells/mL and incubated at 37°C in growth media for 24 hours. Following incubation, the media was aspirated and the cells were dosed with 2 mL of 15 µg/mL GNRs in culture media. After 24 hours, the media was aspirated and washed twice with pre-warmed PBS

to remove any nanorods that were not taken up into the cells. 1 mL of 0.25% trypsin-EDTA was added to each well to separate the cells from the bottom of the plate. The cells were incubated with trypsin until the cells detached as observed in a light microscope. Once the cells lifted from the bottom of the plate, 5 mL of culture media was added to neutralize the trypsin. The solution containing the cells and an additional wash with media was centrifuged at 900 g for 5 minutes. Excess supernatant was removed and the cells were re-suspended in water to a final volume of 5 mL. The cells were immediately counted using the Cellometer. The cells were frozen in the -20°C freezer overnight, or until ready for digestion.

The next step of the ICP-MS prep procedure was the cell digestion. The cells were thawed and 500 µL of 1% Triton-X was added to each 5 mL sample to break up the cells. The samples were then vortexed to make sure all cells were lysed. Next, 810 µL of 37% HCl, 144 µL of 69% HNO_3, and 20 µL of internal standard mix were added to each 5.5 mL sample. The samples were vortexed and allowed to sit for 30 minutes at 20-25°C. Finally, H_2O was added until the sample reached a final volume of 10 mL. The samples were vortexed again and then placed in the autosampler for the ICP-MS.

The results of the ICP-MS are produced in units of concentration (µg/mL). To find the mass of gold uptake per cell the Equations 2 and 3 were used.

$$Concentration\left(\frac{ng}{mL}\right) = \frac{ICP\ concentration\left(\frac{\mu g}{mL}\right)*ICP\ Volume\ (10\ mL)}{Sample\ Volume\ (5\ mL)} * \frac{ng}{1000\ \mu g} \quad (14)$$

$$\frac{ng\ gold}{cell} = \frac{Concentration\ (ng/mL)}{Cell\ Concentration\left(\frac{cells}{mL}\right)} \quad (15)$$

4.2.3 Endocytosis Inhibitor Studies. The procedure for looking at uptake with endocytosis inhibitors was similar to the procedure for cellular uptake, however, before exposing the cells to the GNRs they were exposed to 400 µmol/L genistein, 200 µmol/L EIPA, or 31 µmol/L chlorpromazine. These are chemical inhibitors which selectively inhibit one type of endocytosis. Genistein inhibitors caveolae mediated endocytosis, EIPA inhibits macropinocytosis and chlorpromazine inhibits clathrin mediated endocytosis. More details on how the inhibitors work is in Chapter 1 Section 3. Alternatively, for the 4°C incubation, the cells were incubated in the 4°C refrigerator for one hour. 4°C incubation inhibits any energy dependent mechanism of uptake, including all methods of endocytosis. After incubating the cells for one hour with the inhibitor, the GNRs were added to 2 mL of media at the same concentration of inhibitors as what the cells were incubated with. The cells were then exposed to the GNRs and inhibitors for 3 hours. After the 3 hour incubation, the same ICP-MS procedure as described previously was used to look at the effect of the inhibitors on cellular uptake. A 24 hour time point was not chosen because the chemical inhibitors are toxic to the cells if dosed too high or exposed for too long. This procedure was repeated in triplicate for the four peptide coated surface chemistries of the AR 3 GNRs.

The percent inhibited by each inhibitor for each surface chemistry is calculated as per Equation 4. A higher percent inhibited means that method of endocytosis accounts for a higher percent of cellular uptake.

$$\% \ Inhibited = \frac{Uptake \ without \ inhibitor - Uptake \ with \ inhibitor}{Uptake \ without \ inhibitor} \qquad (16)$$

4.2.4 Agglomeration Testing Methods. In order to test the agglomeration patterns based on size and surface chemistry, samples were prepared of GNRs AR 3 and AR 6 functionalized with TAT, TAT HA2, Tannic Acid, and Chariot. Firstly, the zeta potential of the functionalized GNRs was measured in water and then in media to determine if adsorption of serum proteins occurred. Then, dynamic light scattering was used to look at the overall size of the GNRs in media. Since all the GNRs have the same core diameter, this can indicate the thickness of the adsorption layer or if agglomeration is occurring. Both of these experiments were run using a Malvern Instruments' Zetasizer Nano-ZA instrument. GNRs were diluted to 50 µg/mL and transferred to a plastic cuvette where they were analyzed in triplicate.

As a final test of agglomeration, UV-Vis was used to determine a stability ratio. This ratio has been published in literature as a way to examine agglomeration of GNRs in media (171). The area under the SPR peak produced from UV-Vis data is calculated for GNRs in both water and media. Comparing the area under the curve for GNRs in media to GNRs in water will show agglomeration since UV-Vis peaks shift and become more broad with agglomeration. A ratio of 1 indicates no agglomeration whereas a lower ratio indicates more agglomeration. Samples were analyzed using a Varian Cary Bio 300 UV-Vis spectrophotometer which plotted absorbance vs wavelength.

4.2.5 TEM Fixation Studies. This TEM fixation protocol was used to visualize where the GNRs are localized within the cell for cells exposed to GNRs with AR 3 and AR 6 functionalized with tannic acid, TAT, TAT HA2, and Chariot. HaCaT cells were grown to 80-90% confluency in a 6 well plate and treated with GNRs for 24 hours. The cells were trypsinized as per ICP-MS experiments and 5-10 mL of growth media with serum was added to each well. The cells in media were then transferred to a 15 mL conical tube and spun down in a centrifuge for 10 min at a speed of 1,000 g. The supernatant was removed and the cell pellet was transferred to an Eppendorf tube. If the cell pellet was disturbed during this transfer, the Eppendorf tube was centrifuged for 1 min at a speed of 1,000 g. The cell pellets were then fixed in the tube in a mixture of 2% paraformaldehyde and 1% glutaraldehyde diluted in PBS for 2 hours. Then the fixative was removed and washed with PBS 4 times for 15 minutes each to remove residual aldehydes, which interfere with the osmium tetroxide. Next the cells were stained for 1 hr with 1% osmium tetroxide, which enhances the staining due to its high atomic weight, diluted in PBS. Successful staining turned black after 1 hour. The osmium was then removed and neutralized in excess corn oil. The pellet was then washed 3 times for 10 minutes each with PBS. Then the sample was dehydrated with 50% ethanol for ten minutes, 70% ethanol three times for ten minutes each, 80% ethanol for ten minutes, 90% ethanol for ten minutes, and

100% ethanol three times for ten minutes each. After dehydration, the cell pellet was transferred from the Eppendorf tube to a Beem capsule and a 1:1 dilution of 100% ethanol and LR White Resin (Structure Probe, Inc., Westchester, PA) was added to the pellet for 1 hour. After this incubation, the capsule was filled with resin and placed in a vacuum oven at 60°C overnight causing the resin to polymerize and form a solid while the vacuum limits its contact with oxygen.

Next, the samples were sectioned into very thin slices. The solid resin was removed from the Beem capsule and placed in the Leica Ultramicrotome. A microtome is used to section the cells contained in the resin into very thin slices so that electrons from the TEM can pass through the section. The Leica Ultramicrotome uses a glass knife for sectioning and can section slices as thin as 20 nm. For TEM preparation the sample was first sectioned at 1000 nm thick sections. A microscope is attached to the microtome for viewing the sections. At first the sections only contained resin and appeared as uniformly flat sections. Once the sections contained cells they appeared more wrinkled. At that time, the sectioning thicknesses were gradually decreased until sections were 70 nm thick. The section was placed on a copper grid using a Perfect Loop^{TM} shown in Figure 23. A copper grid was used because copper is a good conductor. Once on the grid, the sample was viewed using TEM.
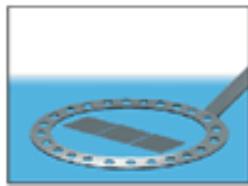
Figure 23: Perfect Loop^{TM} Tool for TEM Preparation Sample Grid

4.2.6   Laser Confocal Microscope Studies. In order to prepare for the confocal studies, HaCaT cells were seeded on glass slides at 400,000 cells per slide overnight and then treated with GNRs for 3 hours. After treatment, the media was aspirated and the slides were washed with PBS. Next the cells were fixed in 4% paraformaldehyde in PBS for 10 minutes. The samples were then washed twice with ice cold (2-8°C) PBS and incubated for 10 minutes with 0.25% Triton X-100 in PBS. Then the cells were washed in PBS three times for 5 minutes each followed by incubation with 1% BSA in PBS for 30 minutes to block unspecific binding of the antibodies. Then the cells were incubated with 1 µg/mL of the primary antibody in 1% BSA in PBS in the incubator for 1 hour. Then the primary antibody solution was aspirated and the cells were washed with PBS three times for 5 minutes each. Next the cells were incubated with 1 µg/mL of the secondary antibody in 1% BSA in PBS for 1 hour at room temperature in the dark. All the following steps were performed in the dark since the secondary antibody is linked to TRITC which is light sensitive. The secondary antibody solution was aspirated and the cells were washed three times with PBS for 5 minutes. The slides then were air dried and a drop of Prolong Gold with DAPI was added to the surface of the slide. A cover slip was placed on the surface of the slide and the slides were placed in the dark overnight. The next day, the coverslip was sealed around the edges using nail polish, and the slides were viewed using the BD Pathway 435 Confocal Microscope (Beckton Dickinson, Franklin Lakes, NJ).

4.2.7 Functionalization with Doxorubicin. DOX was co-functionalized to the GNRs along with the original peptide (i.e. TAT, TAT HA2, Tannic Acid, or Chariot). The DOX GNRs are naturally fluorescent under FITC light. The same addition procedure for functionalization of GNRs shown in Figure 13 was utilized for DOX. The amount of DOX to be added was based off a calculation to functionalize 1,000 molecules of DOX per GNR.

4.3 Results

4.3.1 Cell Viability. Cell viability was determined using MTS assays on HaCaT cells treated with AR 6 GNRs functionalized with TAT, TAT HA2, Chariot, and Tannic Acid, as shown in Figures 24 and 25. The percent viability is shown for corresponding concentrations of GNRs exposed to HaCaT cells and viability is based on a negative control of cells not exposed to any GNRs. None of the functionalizations showed a statistically significant difference in cell viability.
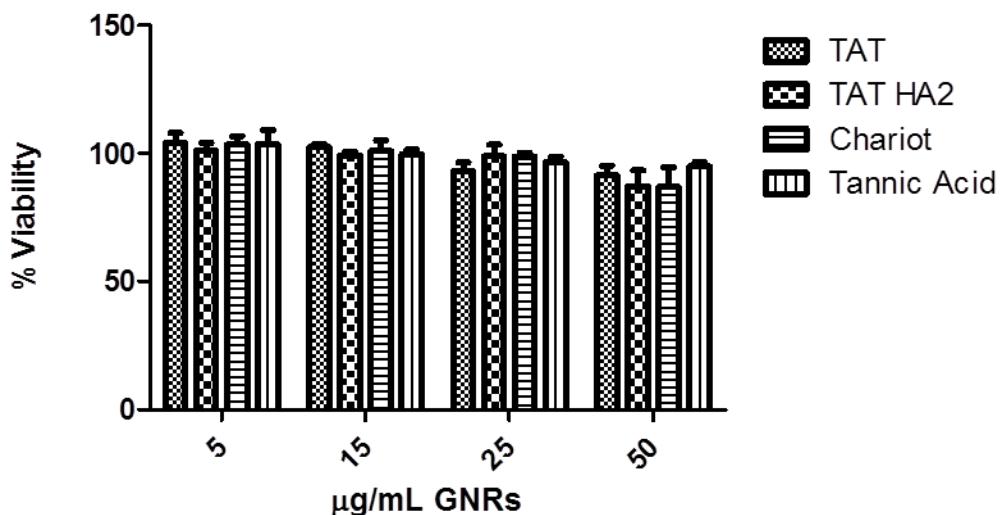
Figure 24: MTS Results for Functionalized GNRs AR 3
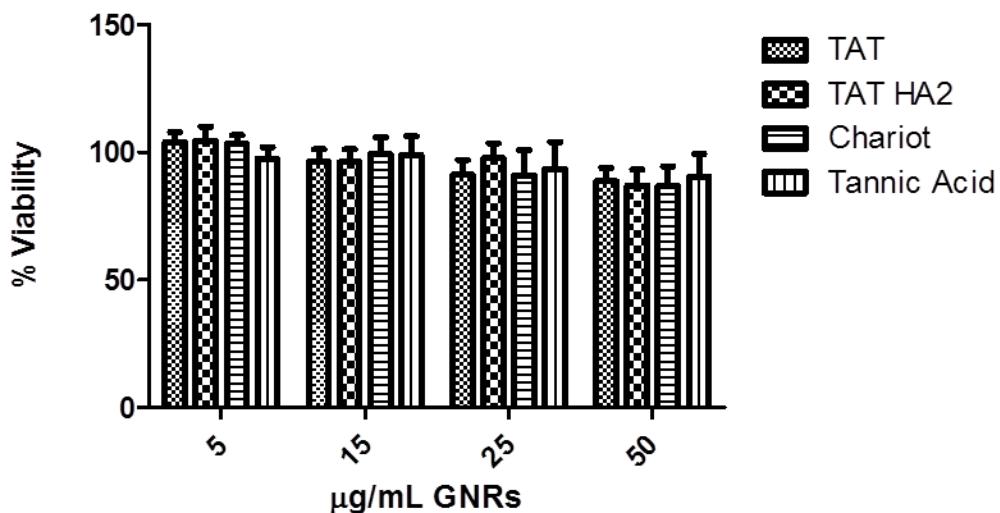
Figure 25: MTS Results for Functionalized GNRs AR 6

The cellular uptake of AR 3 and AR6 GNRs functionalized with TAT HA2, TAT, Tannic Acid, and Chariot was measured using the ICP-MS, as shown in Figure 26. For each functionalization, the AR 6 were taken up by the cells at least twice as readily as the AR 3 GNRs.
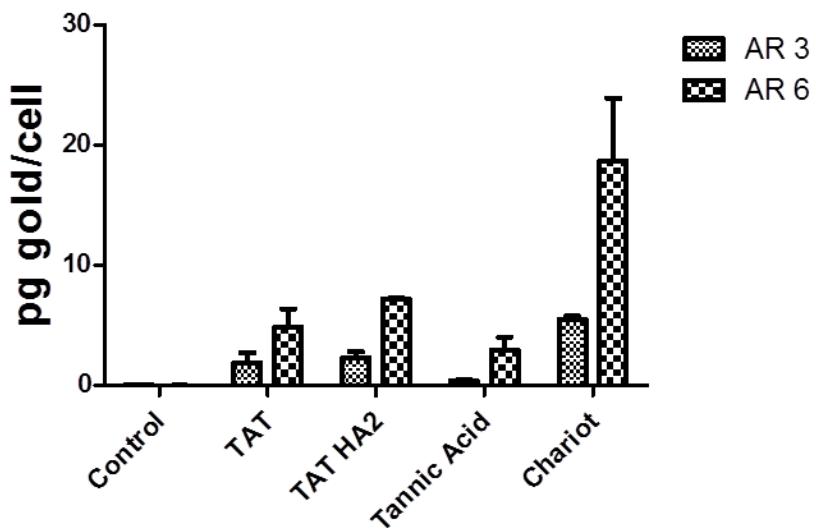
Figure 26: ICP-MS Cellular Uptake Results for GNRs AR 3 and AR 6

4.3.2   Endocytosis Inhibitor Studies. To understand the uptake mechanism, various endocytosis inhibition techniques were investigated. Cells treated with AR 3 GNRs functionalized as described previously were exposed to chlorpromazine, genistein, EIPA and 4°C for 1 hour to inhibit cell uptake of GNRs. These inhibitors inhibited clathrin mediated

endocytosis, caveolae medicated endocytosis, macropinocytosis, and any form of energy dependent uptake respectively. Uptake inhibition success was found to be dependent upon the type of functionalization. ICP-MS was used to quantify the uptake of gold per cell. It was shown that most functionalizations of GNRs were taken up by a variety of methods of endocytosis except for tannic acid which was taken up independently of endocytosis (Figure 27).
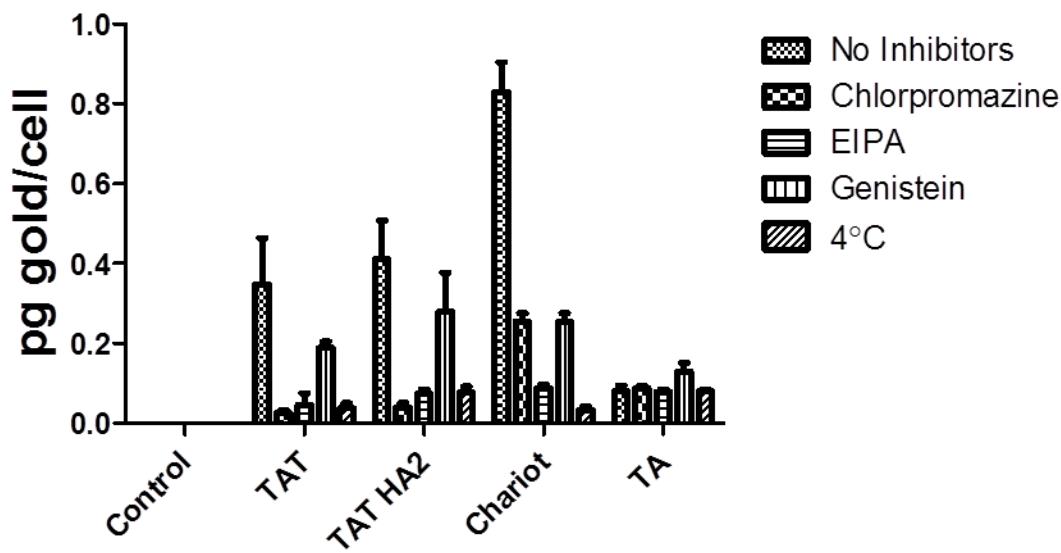
Figure 27: ICP-MS Cellular Uptake of GNRs AR 3 with Endocytosis Inhibitors

4.3.3 Agglomeration Analysis Data. The zeta potential of GNRs AR 3 functionalized with TAT, TAT HA2, Tannic Acid, and Chariot was measured both in water and in media with serum to determine if adsorption of proteins occurred. Since zeta potential is the measure of the charge on the surface, adsorption of proteins would result in the GNRs shifting to the charge of the protein, typically a negative value. Serum adsorption has also been shown to affect agglomeration behavior. Figure 28 shows that all the GNRs adsorbed proteins from the media, changing their surface charge.
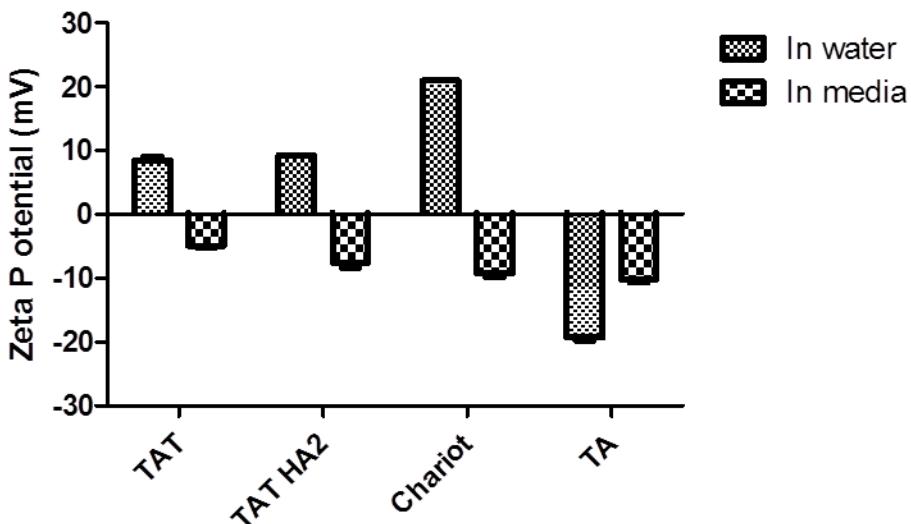
Figure 28: ICP-MS Cellular Uptake of GNRs AR 3 with Endocytosis Inhibitors

Malvern Zetasizer was also used to look at the hydrodynamic diameter (nm) of the GNRs in media to examine agglomeration using dynamic light scattering. Since the aspect ratios for all the GNR samples are the same, hydrodynamic diameters were compared to approximate the size of the adsorptive layer. Table 6 shows that tannic acid GNRs experienced significant agglomeration in media compared to other GNRs. It could be due to tannic acid's strong affinity for proteins. Tannic acid is known to form complexes with proteins through many different methods, and is even used to sediment out proteins from wines (172).

To complement dynamic light scattering agglomeration results, a stability ratio was also calculated using data from UV-Visible Spectrophotometery. This stability measurement compares the area under the longitudinal SPR peak for GNRs in water and in media. A stability ratio of 1 indicates no agglomeration whereas smaller ratios indicate increasing agglomeration. Table 1 shows that TA GNRs are slightly agglomerated whereas the other GNRs are completely stable. This correlates with the finding that TA has the largest agglomerate size as measured with dynamic light scattering.

Table 6: Light Scattering and Agglomeration of GNRs AR 3 in Biological Media			
GNR Functionalization	Hydrodynamic Diameter (nm) in Media	Standard Deviation	Stability Ratio in Media
TAT	19.47	0.412	0.986
TAT HA2	13.87	0.344	1.06
Chariot	15.62	0.397	0.990
TA	175.2	1.44	0.833

4.3.4 TEM Fixation Data. Intracellular localization of the GNRs was determined by visualization using TEM. Images were taken for GNRs functionalized with TAT, TAT HA2, Chariot, tannic acid, and PEG-COOH. Figure 29 shows the whole cell with the nucleus and cell wall labeled for tannic acid (a) and TAT HA2 (b). These show that the GNRs are localized in agglomerates within the cell. It is not clear if they are in intracellular vesicles or free in the cytoplasm, although it is clear they are not in or near the nucleus. Additional images including the entire cell as well as an up close view of the nanoparticles in the cell are included in the Appendix.
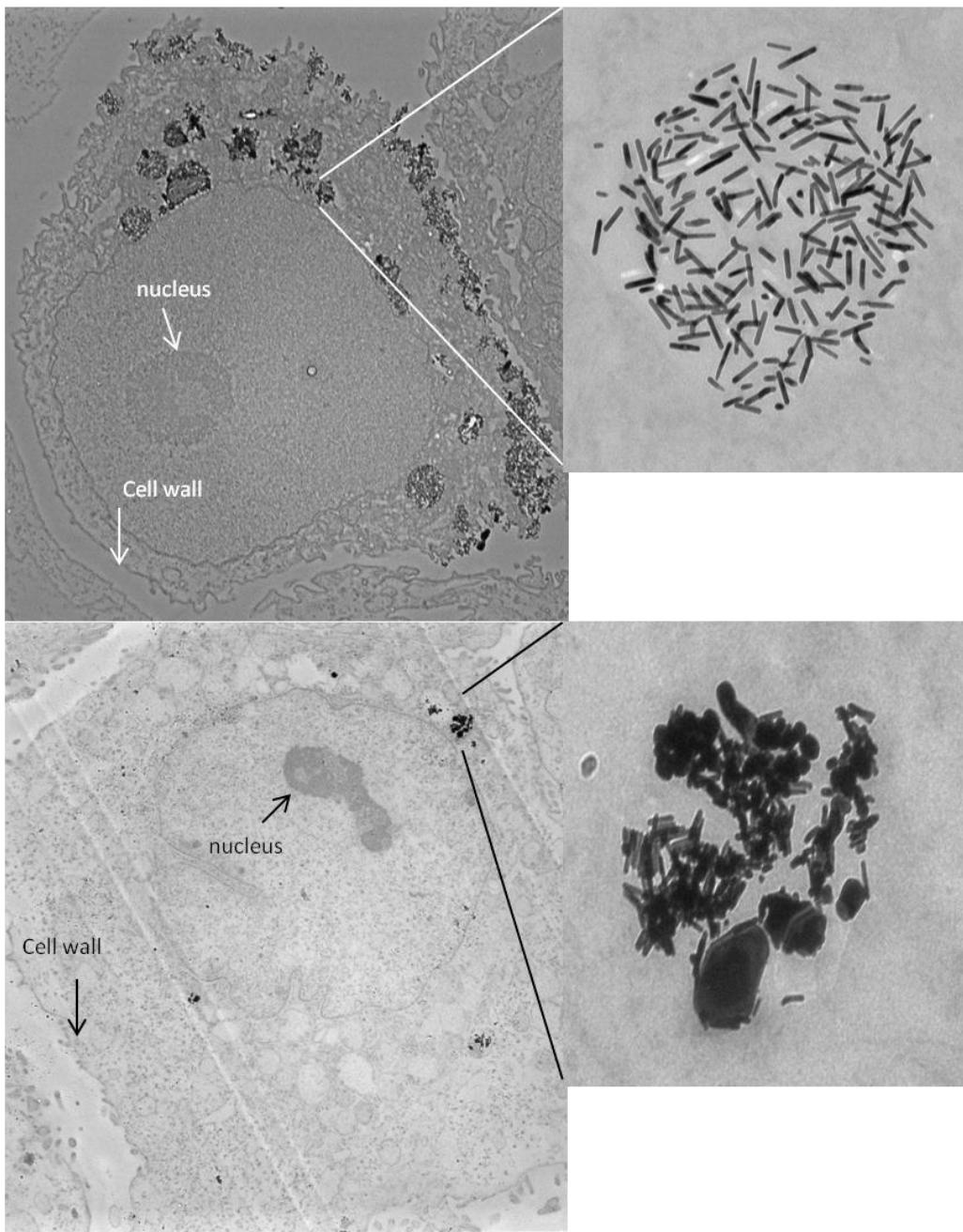
Figure 29: TEM of Functionalized GNRs in HaCaT Cells
A: Tannic Acid AR 6, B: TAT HA2 AR 6

48

The following images in Figure 30 are GNR particles in fixed cells using TEM. The orientation of the particles in the cells can be assessed using these images. These images show tight agglomerates for the positively charged GNRs whereas tannic acid has a looser packing. The orientation of tannic acid is unique in that there are more individual particles seen as opposed to large clumps of GNRs.
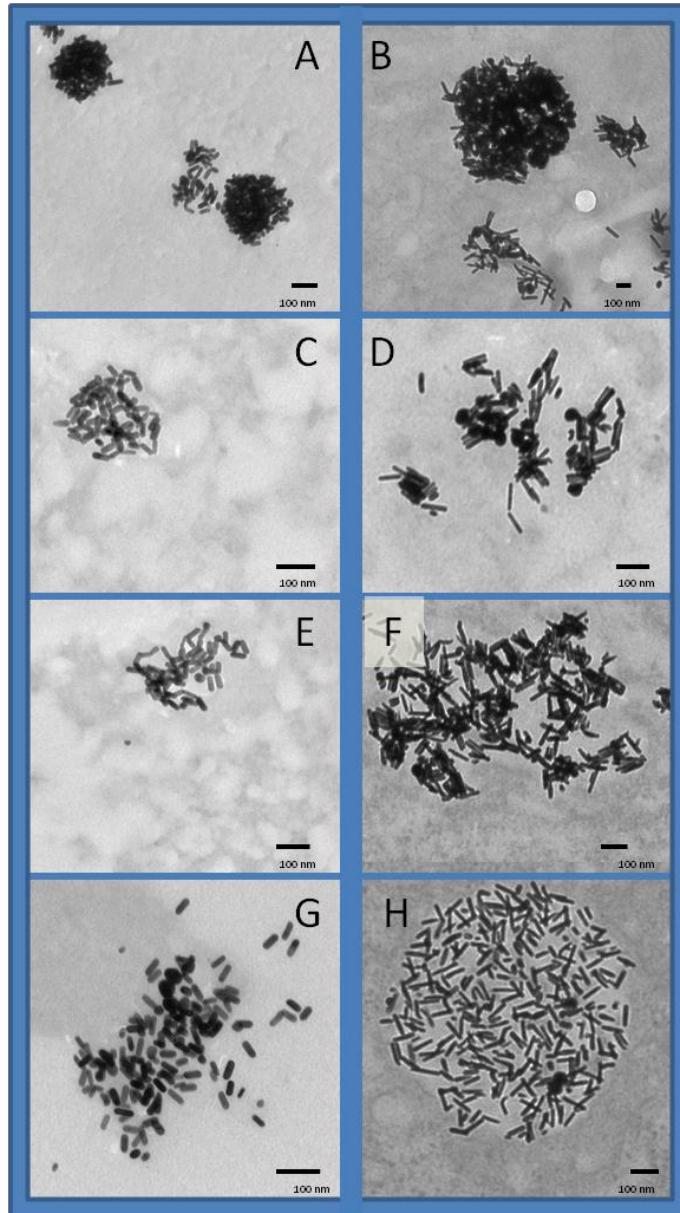
Figure 30: TEM of GNR Agglomerates in HaCaT Cells
A: Chariot AR 3, B: Chariot AR 6, C: TAT AR 3, D: TAT AR 6, E: TAT HA2 AR 3,
F: TAT HA2 AR 6, G: Tannic Acid AR 3, H: Tannic Acid AR 6

4.3.5 Colocalization Studies. TEM fixation studies are a good indicator of intracellular localization. However, it has been debated whether these images can definitively show whether the particles are localized in endosomes. Colocalization studies using confocal microscopy can

show exactly where GNRs are located compared to endosomes because the endosomes and particles can be fluorescently tagged. Figure 31 shows confocal images of GNRs in cells after a 3 hour time point. The nuclei are stained blue with DAPI, the endosomes are stained red with TRITC, and the particles are functionalized with naturally fluorescent Doxorubicin and are green in the images. It can be seen in A-C that there are many large yellow spots indicating colocalization of GNRs and endosomes. However, in image D there are few yellow spots indicating that GNRs are not localized in endosomes.
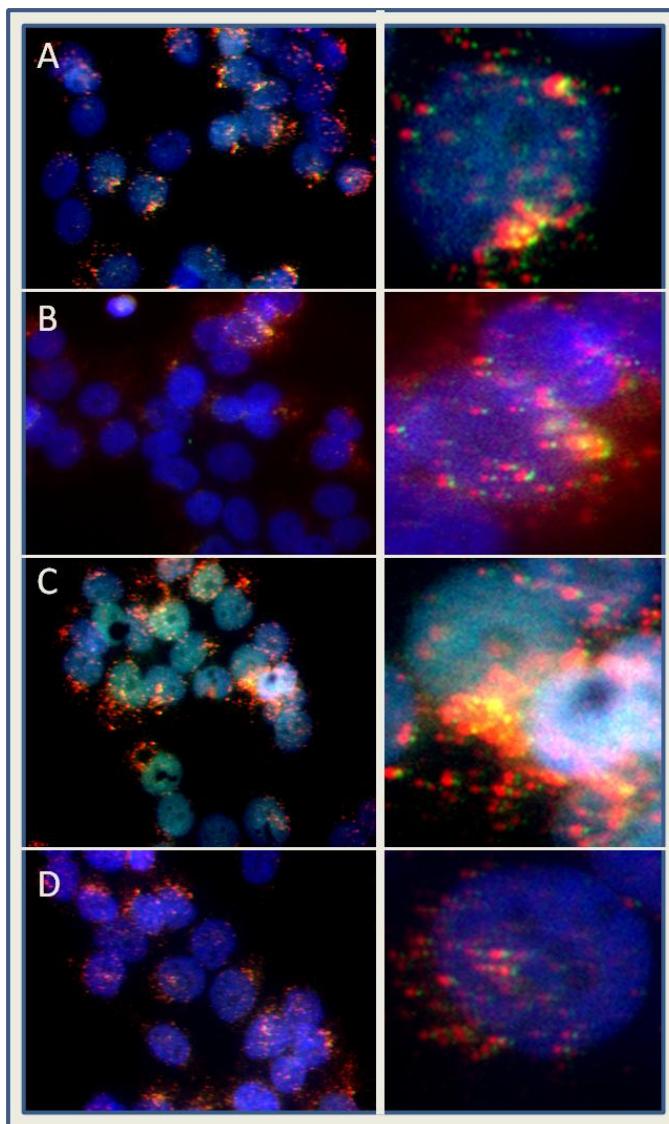
Figure 31: Colocalization Images of DOX-GNRs and Endosomes
A: Chariot, B: TAT, C: TAT HA2, D: Tannic Acid

4.4   Discussion

Investigation of GNRs functionalized with TAT, TAT HA2, Chariot, and Tannic Acid showed that the particles are non-toxic up to 50 µg/mL, when the particles show a slight toxicity (Figure 24,25). Thus, for the further experiments a concentration of 15 µg/mL was used. These results also show that the materials are valid for biological and biomedical applications if used at appropriate concentrations. Additionally, the results show that there is no difference in toxicities between ARs 3 and 6 or between surface functionalizations of TAT, TAT HA2, Chariot, or tannic acid.

In order to look at the cellular uptake of the GNR samples quantitatively, ICP-MS was used. ICP-MS is a type of very sensitive mass spectrometry that can detect a range of metals and non-metals below one part per trillion. It was found that for both AR 3 and AR 6, the order of uptake from highest to lowest was Chariot, TAT/TAT HA2, and tannic acid (Figure 26). This is also the decreasing order of their surface charges as shown by their zeta potentials listed in Table 5. Therefore, the higher the surface charge of the nanoparticle the more cellular uptake. This could be due to the fact that positively charged particles have better interactions with the negatively charged cellular membrane. Additionally it was shown that AR 6 GNRs have higher uptake than AR 3 GNRs of the same surface charge (Figure 26). When looking at the dimensions of the GNRs shown in Table 4 it can be seen that AR 6 has longer length than AR 3 but a smaller width than AR 3. Therefore, uptake of GNRs could be dependent mostly on the width.

According to the results of the endocytosis inhibitor studies, multiple types of endocytosis are used by each of the GNR surface chemistries except tannic acid. 4ºC inhibited any form of energy dependent uptake, Genistein inhibited caveolae mediated endocytosis, EIPA inhibited macropinocytosis, and Chlorpromazine inhibited clathrin mediated endocytosis. The results are shown in Table 7.

Table 7: Percent Inhibition of Endocytosis Inhibitors		
Surface Chemistry	Inhibitor	% Inhibited
TAT	4ºC	89.18
	Genistein	45.88
	EIPA	86.96
	Chlorpromazine	92.76
TAT HA2	4ºC	81.25
	Genistein	31.93
	EIPA	81.89
	Chlorpromazine	90.23
Chariot	4ºC	95.90
	Genistein	69.34
	EIPA	89.43
	Chlorpromazine	69.31
Tannic Acid	4ºC	0.87
	Genistein	-57.62
	EIPA	3.08
	Chlorpromazine	-6.85

Incubation at 4ºC severely inhibited uptake of all the surface chemistries except for tannic acid. This result suggests that all the surface chemistries are taken up by some form of endocytosis whereas tannic acid enters the cell independent of endocytosis. For all GNRs functionalized with TAT and TAT HA2 the highest percents of inhibition came from EIPA and Chlorpromazine meaning that macropinocytosis and clathrin mediated endocytosis were the main mechanisms of uptake being used. This makes sense since macropinocytosis is often the dominant mechanism for the uptake of large particles (73), such as the GNRs used in this study.

Additionally, adsorption of serum proteins as a result of exposure to biological media with serum has been shown to result in receptor mediated endocytosis, which is a type of clathrin mediated endocytosis (68). Chariot GNRs are severely inhibited with all inhibitors, meaning that it uses all the endocytosis mechanisms heavily. This could explain why uptake of Chariot is so high because uptake can occur through so many different cellular methods. It appears that surface chemistry does have an effect on the mechanism of uptake of GNRs AR 3.

Agglomeration is a common issue with the use of GNRs and is a topic which is not very well understood. While the GNR solutions were not agglomerated in water as shown by UV-Vis data, they are likely to agglomerate when exposed to media with serum (169). Since all the biological studies are performed with GNRs in media with serum it is important to examine this behavior. Agglomeration studies were performed with GNRs in media with serum to see if there was an effect on agglomeration based on surface chemistry, and also if the agglomeration patterns were linked to any other bio-effects studied. Zeta potential measurements indicated that adsorption of proteins was occurring after exposure to media with serum. Dynamic light scattering and a ratio calculated from UV-Vis studies demonstrated that tannic acid GNRs were the only surface chemistry which experienced some agglomeration. All other surface chemistries were completely stable in media. This could be due to tannic acid's high affinity for proteins which might be causing the agglomeration (172).

By examining the TEM images for the GNRs functionalized with TAT, TAT HA2, Chariot^{TM}, and tannic acid it can be seen where the particles are localizing in the cell. For all the samples, the GNRs are located in mostly agglomerates. The GNRs are not significantly agglomerated in media, and so this agglomeration occurs during or after cellular uptake. It is not clear whether the agglomerates are located in intracellular vesicles such as endosomes or whether they are present in the cytoplasm. There do not appear to be any GNRs localized in the nucleus.

From viewing the GNR agglomerates in cells with TEM, it can be seen that tannic acid (Figure 32A) has a unique orientation compared to the other particle surface chemistries (e.g. TAT HA2 Figure 32B). There are more individual particles rather than tight agglomerates. This orientation was examined in a quantitative manner using Image J. The image was converted to a binary image as shown in Figure 32 and the particle area fraction of the GNRs was calculated.
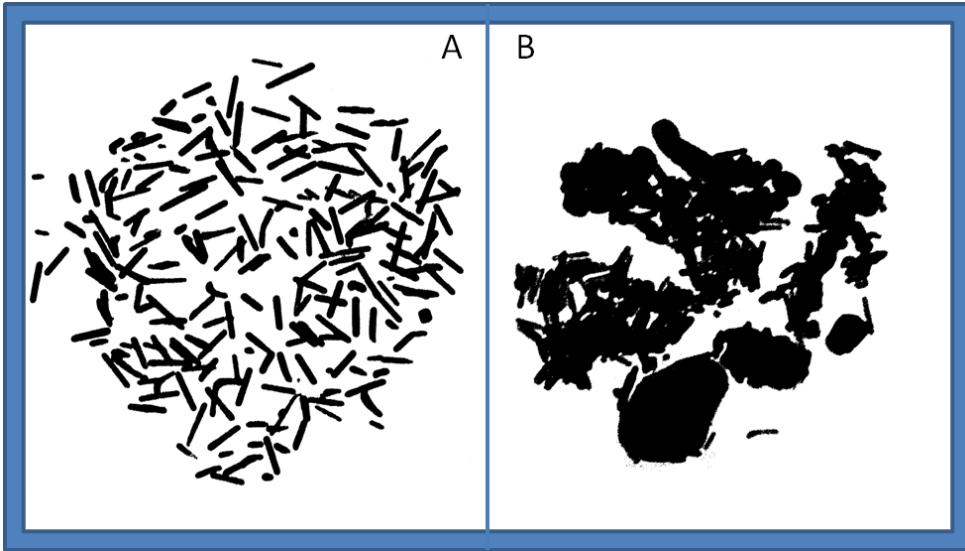
Figure 32: Image J Analysis of GNR Orientation in HaCaT Cells
A: Tannic Acid, AR 6, particle area fraction: 25.3   B: TAT HA2 AR 6, particle area fraction: 51.5

This unique orientation of tannic acid GNRs could be useful for delivery applications. Additionally tighter agglomerates might be better for imaging applications as they would produce stronger scattering. Knowledge of the orientation of agglomerates in cells could be useful for design of future applications.

Further evidence for the intracellular localization of the GNRs was shown in the confocal images in Figure 31. For these confocal experiments, Doxorubicin was functionalized to the GNRs as a model biomolecule for delivery. In the images the red spots are endosomes, the blue are nuclei, and the green are the GNRs. It can be seen that the Doxorubicin functionalization was successful as seen by the presence of green dots in the cells. This means that the GNRs used in this study can be further functionalized with a biomolecule of interest and achieve delivery into the cells. The yellow spots represent co-localization, and appear whenever a green GNR is in the same position as a red endosome. Since the images are on only one z plane, co-localization with endosomes can be seen with certainty.

Confocal microscopy shows both green and red spots. These are either GNRs that are free from endosomes or that have already migrated into lysosomes. There are large yellow spots indicating colocalization in all the pictures, except for the tannic acid GNRs. This confirms the endocytosis inhibitor data which showed that tannic acid is not taken up by endocytosis. This result has not been shown before and makes tannic acid extremely useful for delivery applications.

4.5 Conclusion

It was found that the GNRs used in this study were biocompatible and therefore could be used in biological applications. There was not a difference in toxicity between AR 3 and AR 6 or between the surface functionalizations of TAT, TAT HA2, Tannic Acid, or Chariot.

Cellular uptake increased with increasing positive surface charge of the GNRs. Additionally, a smaller width of GNRs resulted in higher uptake when looking at GNRs of AR 3

and AR 6. GNRs functionalized with TAT, TAT HA2, and Chariot were taken up by a variety of types of endocytosis with macropinocytosis being the dominant method. Tannic acid GNRs were shown to be uptaken into the cell independent of endocytosis.

The GNRs used in this study appear to be adsorbing proteins from biological media with serum, affecting their surface chemistry. No agglomeration occurs after exposure of the GNRs to biological media in serum except for tannic acid GNRs. This could be due to tannic acid's high affinity for proteins.

It was shown that GNRs localize inside the cell in agglomerates outside of the nucleus. A model biomolecule was successfully functionalized to the GNRs used in the study indicating the use of these GNRs as delivery agents. From the results of this study, tannic acid would be the best candidate for delivery applications. Tannic acid has been shown to be uptaken into the cell independent of endocytosis which would allow it to reach other intracellular targets of interest if it were additionally functionalized with another targeting moiety. It also has a unique orientation inside the cell which could be useful for delivery as well. Tannic acid is also very inexpensive compared to the other functionalizations used in this study.

These results indicate that functionalization of GNRs can be used to achieve desired intracellular localization. Tannic Acid GNRs specifically have high potential to be used for delivery applications in the future due to their non-endosomal uptake.

5.0 SUMMARY AND CONCLUSIONS

The seed mediated growth procedure for GNRs was successfully used to synthesize GNRs AR 3 and AR 6. The depletion induced separation procedure was used to purify the GNR samples resulting in high yield of GNRs. These GNRs were successfully functionalized with TAT, TAT HA2, Chariot, and Tannic Acid using an addition procedure. The change of zeta potential confirmed this functionalization. TAT and TAT HA2 were hypothesized to be bound covalently to the gold through their cystein groups whereas Chariot and Tannic Acid were hypothesized to be bound to the gold by electrostatic interactions. The GNRs' size and shape was characterized using TEM and UV-Vis. TEM measurements correlated well with calculations for GNR dimensions derived from UV-Vis absorption data.

The functionalized GNRs of both AR 3 and AR 6 showed negligible toxicity at concentrations up to 50 µg/mL as shown by the MTS assay, indicating their ability to be used in biological applications. Measurements of zeta potential of GNRs in biological media show that all samples adsorb proteins from the serum, causing their zeta potentials to shift to a similar negative value. Dynamic Light Scattering and a calculated UV-Vis stability ratio showed that all the functionalized GNRs are stable in biological media except for tannic acid GNRs, which form agglomerates. Cellular uptake in HaCaT cells was dependent on both AR and surface chemistry. AR 6 had higher uptake than AR 3 for each of the surface functionalizations. When comparing surface chemistries without changing aspect ratio, the higher positively charged GNRs had higher cellular uptake. This trend is probably due to the increased interactions of positive particles with the negatively charged cellular membrane. TEM provided qualitative data of uptake into cells. GNRs were seen to localize in intracellular agglomerates though it was unclear if they were in endosomes, lysosomes, or free in the cytoplasm.

Endocytosis inhibitors were used to look at the mechanism of uptake of AR 3 GNRs functionalized with TAT, TAT HA2, Tannic Acid and Chariot. A 4ºC incubation was used

which would inhibit any energy dependent uptake mechanism, and thus inhibits all forms of endocytosis. EIPA was used to inhibit macropinocytosis, Genistein was used to inhibit caveaolae mediated endocytosis, and Chlorpromazine was used to inhibit clathrin mediated endocytosis. It was found that TAT, TAT HA2, and Chariot were uptaken by a variety of endocytosis methods typically dominated by macropinocytosis. Macropinocytosis has been previously shown as the main mechanism for uptake of large nanoparticles. Tannic Acid, however, was not inhibited by any of the endocytosis inhibitors. This indicates that tannic acid is uptaken by a non-endosomal method, making it ideal for delivery applications.

To examine GNRs for delivery applications as well as further examine intracellular localization, immunofluorescent studies were conducted using confocal microscopy. Functionalized GNRs were further functionalized with Doxorubicin (DOX), an anti cancer drug and nautrally fluorescent substance, using an addition procedure. GNRs were exposed to HaCaT cells in which endosomes were fluorescently stained with EEA1 antibody. Firstly, it was seen that GNRs were successfully functionalized with DOX due to fluorescent particles visible in the FITC region. Additionally, it was seen that many GNRs were localized in endosomes in TAT, TAT HA2, and Chariot GNRs. However, tannic acid GNRs appeared to be free from endosomes. This correlates with the endocytosis inhibitor data and further shows tannic acid is not uptaken by endocytosis and is localized outside of endosomes. This is an extremely useful result and shows that tannic acid GNRs would be very useful in delivery, bio-imaging, and subcellular targeting applications.

6.0 REFERENCES

1. Becker, R., Liedberg, B., Kaal, P. 2010, CTAB Promoted Synthesis of Au Nanorods – Temperature Effects and Stability Considerations. Journal of Colloid and Interface Science 343: 25-20.

2. Motoyama, Y., Applebaum, R.P., Parker, R. 2011, The National Nanotechnology Initiative: Federal Support for Science and Technology, or Hidden Industrial Policy? Technology in Society 33: 109-118.

3. Balbus, J., Denison, R., Florini, K., Walsh, S. 2005, Getting Nanotechnology Right the First Time. Issues in Science and Technology 65-71.

4. El-Sayed, I., Huang, X., El-Sayed, MA. 2005, Selective laser photo-thermal therapy of epithelial carcinoma using anti-EFGR conjugated Gold Nanoparticles. Cancer Letters 239: 129-135.

5. Stern, J., Stanfield, J., Kabbani, W., Hsieh, JT, Cadeddu, J. 2008, Selective Prostate Cancer Thermal Ablation with Laser Activated Gold Nanoshells. The Journal of Urology 179: 748-753.

6. Chen, C., Lin, Y.P., Wang, C.W., Tzeng, H.C., Wu, C.H., Chen, Y.C., Chen, C.P., Chen, L.C., Wu, Y.C. 2006, DNA-Gold Nanorod Conjugates for Remote Control of Localized Gene Expression by near Infrared Irradiation. Journal of American Chemical Society 128: 3709-3715.

7. Huang, X., Neretina, S., El-Sayed, M. 2009, Gold Nanorods: From Synthesis and Properties to Biological and Biomedical Applications. Advanced Materials 21: 4880-4910.

8. Jain, P.K., Lee, K.S., El-Sayed, I.H., El-Sayed, M.A. 2006, Calculated Absorption and Scattering Properties of Gold Nanoparticles of Different Size, Shape, and Composition: Applications in Biological Imaging and Biomedicine. Journal of Physical Chemistry B 110: 7238-7248.

9. Link, S. El-Sayed, M.A. 2000, Shape and Size Dependence of Radiative, Nonradiative, and Photothermal Properties of Gold Nanocrystals. International Reviews in Physical Chemistry 19: 409-453.

10. Link, S., El-Sayed, M.A. 2003, Optical Properties and Ultrafast Dynamics of Metallic Nanocrystals. Annual Reviews in Physical Chemistry 54: 331-3

11. Jain, P.K., Huang, X., El-Sayed, M.A. 2008, Noble Metals on the Nanoscale: Optical and Photothermal Properties and Some Applications in Imaging, Sensing, Biology, and Medicine. Accounts of Chemical Research 41: 1578-1586.

12. Haes, A.J., Stuart, D.A., Nie, S., Van Duyne, R.P. 2004, Using Solution-Phase Nanoparticles, Surface-Confined Nanoparticle Arrays and Single Nanoparticles as Biological Sensing Platforms. Journal of Fluorescence 14: 355-367.

13. Sun, Y., Mayers, B., Xia, Y. 2002, Template-Engaged Replacement Reaction: A One-Step Approach to the Large-Scale Synthesis of Metal Nanostructures with Hollow Interiors. Nano Letters 2: 481-485.

14. Gans, R. 1915, Forms of Ultramicroscopic Particles of Silver. Annals of Physics 47: 270-284.

15. Purcell, E.M., Pennypacker, C.R. 1973, Scattering and Absorption of Light by Nonspherical Dielectric Grains. Astrophysics Journal 186: 705-714.

16. Lee, K.S., El-Sayed, M.A. 2005, Dependence of the Enhanced Optical Scattering Efficiency Relative to that of Absorption for Gold Metal Nanorods on Aspect Ratio, Size, End-Cap Shape, and Medium Refractive Index. Journal of Physical Chemistry B 109: 20331-20338.

17. Loo, C., Lin, A., Hirsch, L., Lee, M., Barton, J., Halas, N., West, J., Drezek, R. (2004), Nanoshell-Enabled Photonics-Based Imaging and Therapy of Cancer. *Technology in Cancer Research and Treatment 3:* 33-40.

18. Huang, X., Jain, P.K., El-Sayed, I.H., El-Sayed, M.A. 2008, Plasmonic Photothermal Therapy Using Gold Nanoparticles. Lasers Medical Science 23: 217-228.

19. Perez-Juste, J., Pastoriza-Santox, I., Liz-Marzan, L.M., Mulvaney, P. 2005, Gold Nanorods: Synthesis, Characterization and Applications. Coordination Chemistry Reviews 249: 1870-1901.

20. Jain, P.K., Huang, W., El-Sayed, M.A. 2007, On the Universal Scaling Behavior of the Distance Decay of Plasmon Coupling in Metal Nanoparticle Pairs: A Plasmon Ruler Equation. Nanoletters 7: 2080-2088.

21. Su, K.H., Wei, Q.H., Zhang, X., Mock, J.J., Smith, D.R., Schultz, S. 2003, Interparticle Coupling Effects on Plasmon Resonances of Nanogold Particles. Nanoletters 3: 1087-1090.

22. Sonnichsen, C., Reinhard, B.M., Liphardt, J., Alivisatos, A.P. 2005, A Molecular Ruler Based on Plasmon Coupling of Single Gold and Silver Nanoparticles. Nature Biotechnology 23: 741-745.

23. Rechberger, W., Hohenau, A., Leitner, A., Krenn, J.R., Lamprecht, B., Aussenegg, F.R. 2003, Optical Properties of Two Interacting Gold Nanoparticles. Optics Communications, 220: 137-141.

24. Foss, C.A., Hornyak, G.L., Stockert, J.A., Martin, C.R. 1992, Optical Properties of Composite Membranes Containing Arrays of Nanoscopic Gold Cylinders. Journal of Physical Chemistry 96: 7497-7499.

25. Martin, C.R. 1994, Nanomaterials: A Membrane-Based Synthetic Approach. Science 266: 1961-1966

26. Yu, Y., Chang, S.S., Lee, C.L., Chris Wang, C.R. 1997, Gold Nanorods: Electrochemical Synthesis and Optical Properties. Journal of Physical Chemistry B 101: 6661-6664.

27. Chang, S.S., Shih, C.W., Chen, C.D., Lai, W.C., Chris Wang, C.R. 2003, The Shape Transition of Gold Nanorods. Langmuir 15: 701-709.

28. Wiesner, J., Wokaun, A. 1989, Anisometric Gold Colloids. Preparation, Characterization, and Optical Properties. Chemical Physics Letters 157: 569-575.

29. Jana, N.R., Gearheart, L., Murphy, C.J. 2001, Seed-Mediated Growth Approach for Shape-Controlled Synthesis of Spheroidal and Rod-like Gold Nanoparticles Using a Surfactant Template. Advanced Materials 13: 1389-1393.

30. Nikoobakht, B., El-Sayed, M.A. 2003, Preparation and Growth Mechanism of Gold Nanorods (NRs) Using Seed-Mediated Growth Method. Chemistry of Materials 15: 1957-1962.

31. Li, M., Wei, L., Zhang, X., Yu, X. 2008, High Temperature Seedless Synthesis of Au NRs Using BDAC/CTAB Co-Surfactant. Chinese Journal of Chemical Physics 21: 476-480.

32. Kim, F., Song, J.H., Yang, P. 2002, Photochemical Synthesis of Gold Nanorods. Journal of the American Chemical Society 124: 14316-14317.

33. Esumi, K., Hara, J., Aihara, N., Usui, K., Torigroe, K. 1998, Preparation of Anisotropic Gold Particles Using a Gemini Surfactant Template. Journal of Colloid and Interface Science 208: 578-581.

34. Leontidis, E., Kleitou, K., Kyprianidou-Leodidou T., Bekiari, V., Lianos, P. 2002, Gold Colloids from Cationic Surface Solutions: Mechanisms That Control Particle Morphology. Langmuir 18: 3659-3668.

35. Park, H.J., Ah, C.J., Kim, W.J., Choi, I.S., Lee, K.P., Yun, W.S. 2006, Temperature-induced Control of Aspect Ratio of Gold Nanorods. Journal of Vacuum Science Technology 24: 1323-1324.

36. Wang, C., Wang, T., Ma, Z., Su, Z. 2005, pH-tuned Synthesis of Gold Nanostructures from Gold Nanorods with Different Aspect Ratios. Nanotechnology 16: 2555-2560.

37. Park, W.M., Huh, Y.S., Hong, W.H. 2009, Aspect-Ratio-Controlled Synthesis of High-Aspect-Ratio Gold Nanorods in High-Yield. Current Applied Physics 9: 140-143.

38. Busbee, B.D., Obare, S.O., Murphy, C.J. 2003, An Improved Synthesis of High-Aspect Ratio Gold Nanorods. Advanced Materials 15: 414-416.

39. Gao, J., Bender, C.M., Murphy, C.J. 2003, Dependence of the Gold Nanorod Aspect Ratio on the Nature of the Directing Surfactant in Aqueous Solution. Langmuir 19: 9065-9070.

40. Chithrani D, Ghazani A., Chan W. 2006, Determining the Size and Shape Dependence of Gold Nanoparticle Uptake into Mammalian Cells. Nano Letters 6: 662-667.

41. Smith, D.K., Korgel, B.A. 2008, The Importance of the CTAB Surfactant on the Colloidal Seed-Mediated Synthesis of Gold Nanorods. Langmuir 24: 644-649.

42. Murphy, C.J., Thompson, L.B., Alkilany, A. M., Sisco, P.N., Boulos, S.P., Sivapalan, S.T., Yang, J.A., Chemak, D.J., Huang, J. 2010, *The Many Faces of Gold Nanorods*. The Journal of Physical Chemistry Letters, 1, 2867-2875.

43. Jana, N. R., Gearheart, L., Murphy, C. J. 2001, Wet chemical synthesis of high aspect ratio cylindrical gold nanorods. Journal of Physical Chemistry B 105: 4065–4067.

44. Kim, F., Song, J.H., Yang, P. 2002, Photochemical Synthesis of Gold Nanorods. Journal of American Chemical Society 124: 14316-14317.

45. Khanal, B.P., Zubarev, E.R. 2008, Purification of High Aspect Ratio Gold Nanorods: Complete Removal of Platelets. Journal of the American Chemical Society 130: 12634-12635.

46. Sharma, V., Park, K., Srinivasarao, M. 2009, Shape Separation of Gold Nanorods Using Centrifugation. PNAS 106: 4981-4985.

47. Liu, F.K., Ko, F.H., Huang, P.W., Wu, C.H., Chu, T.C. 2005, Studying the size/shape separation and optical properties of silver nanoparticles by capillary electrophoresis. Journal of Chromatography A 1062: 139–145.

48. Wei, G.T., Liu, F.K., Wang, C.R.C. 1999, Shape Separation of Nanometer Gold Particles by Size Exclusion Chromatography. Analytical Chemistry 71: 2085-2091.

49. Park, K., Koerner, H., Vaia, R. 2010, Depletion-Induced Shape and Size Selection of Gold Nanoparticles. Nanoletters 10: 1433-1439.

50. Niidom, T., Yamagata, Y., Okamoto, Y., Akiyama, Y., Takahashi, H., Kawano, T., Katayama, Y., Niidome, Y. 2006, PEG-modified gold nanorods with a stealth character for in vivo applications. Journal of Controlled Release 114: 343-347.

51. Alkilany, AM., Nagaria, PK., Hexel, CR., Shaw, TJ., Murphy, CJ., Wyatt, MD. 2009, Cellular Uptake and Cytotoxicity of Gold Nanorods: Molecular Origin or Cytotoxicity and Surface Effects. Small 5: 701-708.

52. Chen, C.C., Lin, Y.P., Wang, C.W., Tzeng, H.C., Wu, C.H., Chen, Y.C., Chen, C.P., Chen, L.C., Wu, Y.C. 2006, DNA-Gold Nanorod Conjugates for Remote Control of Localized Gene Expression by near Infrared Irradiation. Journal of the American Chemical Society 128: 3709–3715.

53. Liu, Y. Shipton, MK., Ryan, J., Kaufman, ED., Franzen, S., Feldheim, DL. 2007, Synthesis, Stability, and Cellular Internalization of Gold Nanoparticles Containing Mixed Peptide-Poly(ethylene glycol) Monolayers. Analytical Chemistry 79: 2221-2229.

54. Orendorff, C.J., Alam, T.M., Sasaki, D.Y., Bunker, B.C., Boigt, J.A. 2009, Phospholipid-Gold Nanorod Composites. ACS Nano 3: 971-983.

55. Hubert, F., Testard, F., Spalla, O. 2008, Cetyltrimethylammonium Bromide Silver Bromide Complex As the Capping Agent of Gold Nanorods. Langmuir 24: 9219-9222.

56. Gittins, D.I., Caruso, F. 2001, Tailoring the Polyelectrolyte Coating of Metal Nanoparticles. Journal of Physical Chemistry B 105: 6846-6852.

57. Qiu, Y., Liu, Y., Wang, L., Xu, L., Bai, R., Ji, Y., Wu, X., Zhao, Y., Li, Y. Chen, C. 2010, Surface Chemistry and aspect ratio mediated cellular uptake of Au nanorods. Biomaterials 31: 7606-7619.

58. Alkilany, A. M., Frey, R. L., Ferry, J. L., Murphy, C. J. 2008, Gold Nanorods As Nanoadmicelles: 1-Naphthol Partitioning into a Nanorod-Bound Surfactant Bilayer. Langmuir 24: 10235–10239.

59. Obare, S. O., Jana, N. R., Murphy, C. J. 2001, Preparation of Polystyrene- And Silica-Coated Gold Nanorods and Their Use As Templates for the Synthesis of Hollow Nanotubes. Nanoletters 1: 601–603.

60. Sun, Z., Yang, Z., Zhou, J., Yeung, M. H., Ni,W.,Wu, H.,Wang, J. 2009, A General Approach to the Synthesis of Gold-Metal Sulfide Core-Shell and Heterostructures. Angewandte Chemie International Edition 48: 2881–2885.

61. Alper, J., Crespo, M., Hamad-Schifferli, K. 2009, Release Mechanism of Octadecyl Rhodamine B Chloride from Au Nanorods by Ultrafast Laser Pulses. J. Phys. Chem. C 113: 5967-5973.

62. Malugin, A., Ghanderhari, H. 2010, Cellular uptake and toxicity of gold nanoparticles in prostate cancer cells: a comparative study of rods and spheres. Journal of Applied Toxicology 30: 212-217.

63. Ghandehari, H., Arnida, M. 2010, Cellular Uptake and Toxicity of Gold Nanoparticles in Prostate Cancer Cells: A Comparitive Study of Rods and Spheres. Journal of Applied Toxicology 30: 212-217.

64. Levy, R., Shaheen, U., Cesbron, Y., See, V. 2010, Gold nanoparticles delivery in mammalian live cells: a critical review. Nano Reviews 1: 1-30.

65. Chithrani, B.D., Ghazani, A.A., Chan, W.C.W. 2006, Determining the Size and Shape Dependence of Gold Nanoparticle Uptake into Mammalian Cells. Nanoletters 6: 662-668.

66. Chou, L., Ming, K., Chan, W. 2011, Strategies for the Intracellular Delivery of Nanoparticles. Chem. Soc. Rev. 40: 233-245.

67. Hamblin, M.R., Miller, J.L, Rizvi, L., Loew, H.G., Hasan, T. 2003, Pegylation of charged polymer-photosensitiser conjugates: effects on photodynamic efficacy 89: 937-943.

68. Zhao, F., Zhao, Y., Liu, Y., Chang, X., Chen, C., Zhao, Y. 2011, Cellular Uptake, Intracellular Trafficking, and Cytotoxicity of Nanomaterials. Small 7:1322-1337.

69. Lao, F., Chen, L., Li, W., Ge, C., Qu, Y., Sun, Q., Zhao, Y., Han, D., Chen, C. 2009, Fullerene Nanoparticles Selectively Enter Oxidation-Damaged Cerebral Microvessel Endothelial Cells and Inhibit JNK-Related Apoptosis. ACS Nano 3: 3358-3368.

70. Cho, K., Wang, X., Nie, S. 2008, Therapeutic Nanoparticles for Drug Delivery in Cancer. Clinical Cancer Research 14: 1310-1316.

71. Jones, A.T. 2007, Macropinocytosis: Searching for an Endocytic Identity and Role in the Uptake of Cell Penetrating Peptides. Journal of Cellular and Molecular Medicine 11: 670-684.

72. Rejman, J., Oberle, V., Zuhorn, I.S., Hoekstra, D. 2004, Size-Dependent Internalization of Particles via the Pathways of Clathrin- and Caveolae-Mediated Endocytosis. Biochemical Journal 377: 159–169.

73. Vercauteren, D., Vandenbroucke, R.E., Jones, A.T., Rejman, J., Demeester, J., De Smedt, S.C., Sanders, N.N., Braeckmans, K. 2010, The Use of Inhibitors to Study Endocytic Pathways of Gene Carriers: Optimization and Pitfalls. Molecular Therapy 18:561-569.

74. Gratton, S.E.A., Ropp, P.A., Pohlhaus, P.D., Luft, J.C., Madden, V.J., Napier, M.E., DeSimone, J.M. 2008, The Effect of Particle Design on Cellular Internalization Pathways. Proceedings of the National Academy of Sciences 105: 11613-11618.

75. Lewinski, N., Colvin, V., Drezek, R.D. 2008, Cytotoxicity of Nanoparticles. Small 4: 26-49.

76. Chou, L., Ming, K., Chan, W. 2011, Strategies for the Intracellular Delivery of Nanoparticles. Chemical Society Reviews 40: 233-245.

77. Lentacker, I., Geers, B., Demeester, J., De Smedt, C.D., Sanders, N.N. 2010, Design and Evaluation of Doxorubicin-containing Microbubbles for Ultrasound-triggered Doxorubicin Delivery: Cytotoxicity and Mechanisms Involved. Molecular Therapy 18: 101-108.

78. Otani, K., Yamahara, K., Ohnishi, S., Obata, H., Kitamura, S., Nagaya, N. 2009, Nonviral Delivery of SiRNA into Mesenchymal Stem Cells by a Combination of Ultrasound and Microbubbles. Journal of Controlled Release 133: 146-153.

79. Mehier-Humbert, S., Bettinger, T., Yan, F., Guy, R.H. 2005, *Ultrasound-Mediated Gene Delivery: Kinetics of Plasmid Internalization and Gene Expression*. Journal of Controlled Release, 104: 203-211.

80. Greber, U.F., Way, M. 2006, A Superhighway to Virus Infection. Cell 124: 741-754.

81. Al-Jamal, W.T., Al-Jamal, K.T., Bomans, B.H., Frederik, P.M., Kostarelos, K. 2008, *Functionalized-Quantum-Dot-Liposome Hybrids as Multidomal Nanoparticles for Cancer.* Small, 4(9), 1406-1415.

82. Babic, M., Horak, D., Trchova, M., Jendelova, P., Glogarova, K., Lesny, P., Herynek, V., Hajek, M., Sykova, E. 2008, Poly(L-lysine)-Modified Iron Oxide Nanoparticles for Stem Cell Labeling. Bioconjugate Chemistry 19: 740-750.

83. Herrero, M.A., Toma, F.M., Al-Jamal, K.T., Kostarelos, K., Bianco, A., Da Ros, T., Bano, F., Casalis, L., Scoles, G., Prato, M. 2009, Synthesis and Characterization of a Carbon Nanotube-Dendron Series for Efficient siRNA Delivery. Journal of the American Chemical Society 131: 9843-9848.

84. Rhim, W.K., Kim, J.S., Nam, J.M. 2008, Lipid-Gold Nanoparticle Hybrid-Based Gene Delivery. Small 4: 1651-1655.

85. Chithrani, D.B., Dunne, M., Stewart, J., Allen, C., Jaffray, D.A. 2010, Cellular Uptake and Transport of Gold Nanoparticles Incorporated in a Liposomal Carrier. Nanomedicine 6: 161-169.

86. Barry, E.L, Gesek, F.A., Friedman, P.A. 1993, Introduction of Antisense Oligonucleotides into Cells by Permeabilization with Streptolysin O. Biotechniques 15: 1016-1018.

87. Hilgenbrink, A.R., Low, P.S. 2005, Folate Receptor-Mediated Drug Targeting: From Therapeutics to Diagnostics. Journal of Pharmaceutical Sciences 94: 2135-2146.

88. Nakase, I., Kobayashi, S., Futaki, S. 2010, Endosome-Disruptive Peptides for Improving Cytosolic Delivery of Bioactive Molecules. Peptide Science 94: 763-770.

89. Nel, A.E., Madler, L., Velegol, D., Xia, T., Hoek, E.M.V, Somasundaran, P., Klaessig, F., Castranova, V., Thompson, M. 2009, Understanding Biophysicochemical Interactions at the Nano-Bio Interface. Nature Materials 8: 543-557.

90. Lakadamyali, M., Rust, M.J., Zhuang, X. 2004, Endocytosis of Influenza Viruses. Microbes and Infection 6: 929-936.

91. Han, X., Bushweller, J.H., Cafiso, D.S., Tamm, L.K. 2001, Membrane Structure and Fusion-Triggering Conformational Change of the Fusion Domain From Influenza Hemagglutinin. Nature Structural and Molecular Biology 8: 715-720.

92. Esbj rner, E. ., gl c ka, ., Lincoln, P., Gr s lund, A., Nord n, B. 2 00 , Membrane Binding of pH-Sensitive Influenza Fusion Peptides. Positioning, Configuration, and Induced Leakage in a Lipid Vesicle Model. Biochemistry 46: 13490-13504.

93. Kakimoto, S., Hamada, T., Komatsu, Y., Takagi, M., Tanabe, T., Azuma, H., Shinkai, S., Nagasaki, T. 2009, The Conjugation of Diptheria Toxin T Domain to Poly(ethylenimine) Based Vectors for Enhanced Endosomal Escape During Gene Transfection. Biomaterials 30: 402-208.

94. Subbarao, N.K., Parente, R.A., Szoka, F.C., Nadasdi, L., Pongracz, K. 1987, The pH-Dependent Bilayer Destabilization by an Amphipathic Peptide. Biochemistry 26: 2964-2972.

95. Kobayashi, S., Nakase, I., Kawabata, N., Yu, H-H., Pujals, S., Imanishi, M., Girlat, E., Futaki, S. 2009, Cytosolic Targeting of Macromolecules Using a pH-Dependent Fusogenic Peptide in Combination with Cationic Liposomes. Bioconjugate Chemistry 20: 953-959.

96. Mandal, D., Maran, A., Yaszemski, M.J., Bolander, M.E., & Sarkar, G. 2009, Cellular Uptake of Gold Nanoparticles Directly Cross-linked with Carrier Petides by Osteosarcoma Cells. Journal of Material Science 20: 347-350.

97. Fuente, J.M., & Berry, C.C. 2005, Tat Peptide as an Efficient Molecule To Translocate Gold Nanoparticles into the Cell Nucleus. Bioconjugate Chemistry 16: 1176-1180.

98. Khalil, I.A., Kogure, K., Akita, H., & Harashima, H. 2006, Uptake Pathways and Subsequent Intracellular Trafficking in Nonviral Gene Delivery. Pharmacological Reviews 58: 32-43.

99. Kumar, S., Harrison, N., Richards-Kortum, R. & Sokolov, K. 2007, Plasmonic Nanosensors for Imaging Intracellular Biomarkers in Live Cells. NANO Letters 7: 1338-1343.

100. Sokolov, K., Follen, M., Aaron, J., Pavlova, I., Malpica, A., Lotan, R., Richards-Kortum, R. 2003, Real-Time Vital Optical Imaging of Precancer Using Anti-Epidermal Growth Factor Receptor Antibodies Conjugated to Gold Nanoparticles. Cancer Research 63: 1999-2004.

101. Dixit, V., Van den Bossche, J., Sherman, D.M., Thompson, D.H., Andres, R.P. 2006, Synthesis and Grafting of Thioctic Acid-PEG-Folate Conjugates onto Au Nanoparticles for Selective Targeting of Folate Receptor-Positive Tumor Cells. Bioconjugate Chemistry 17: 603-609.

102. Prabaharan, M., Grailer, J.J., Pilla, S., Steeber, D.A., Gong, S. 2009, Gold Nanoparticles with a Monolayer of Doxorubicin-Conjugated Amphiphilic Block Copolymer for Tumor-Targeted Drug Delivery. Biomaterials 30: 6065-6075.

103. Patra, C.R., Bhattacharya, R., Mukherjee, P. 2010, Fabrication and Functional Characterization of Gold Nanoconjugates for Potential Application in Ovarian Cancer. Journal of Materials Chemistry 20: 547-554.

104. Chen, Y.H., Tsai, C.Y., Huang, P.Y., Chang, M.Y., Cheng, P.C., Chou, C.H., Chen, D.H., Wang, C.R., Shia, A.L., Wu, C.L. 2007, Methotrexate Conjugated to Gold Nanoparticles Inhibits Tumor Growth in a Syngeneic Lung Tumor Model. Molecular Pharmacology 4: 713-722.

105. Paciotti, G.F., Myer, L., Weinreich, D., Goia, D., Pavel, N., McLaughlin, R.E., Tamarkin, L. 2004, Colloidal Gold: A Novel Nanoparticle Vector for Tumor Directed Drug Delivery. Drug Delivery 11: 169-183.

106. Paciotti, G.F., Kingston, D.G.I., Tamarkin, L. 2006, Colloidal Gold Nanoparticles: A Novel Nanoparticle Platform for Developing Multifunctional Tumor-Targeted Drug Delivery Vectors. Drug Delivery Reviews 67: 47-54.

107. McIntosh, C.M., Esposito, E.A., Boal, A.K., Simard, J.M., Martin, C.T., Rotello, V.M. 2001, Inhibition of DNA Transcription Using Cationic Mixed Monolayer Protected Gold Clusters. Journal of the American Chemical Society 123: 7626-7629.

108. Rana, S., Baja, A., Mout, R., Rotell, V.M. 2011, Monlayer Coated Gold Nanoparticles for Delivery Applications. Advanced Drug Delivery Reviews 64: 200-216.

109. Derfus, A.M., Chen, A.A., Min, D., Ruoslahti, E., & Bhatia, S.N. 2007, Targeted Quantum Dot Conjugates for siRNA Delivery. Bionconjugate Chemistry 18: 1391-1396.

110. Murthy, N., Xu, M., Schuck, S., Kunisawas, J., Shastri, N., Frechet, J.M.J. 2003, A Macromolecular Delivery Vehicle for Protein-Based Vaccines: Acid-Degradable Protein-Loaded Microgels. Proceedings of the National Academy of Sciences 100: 4995-5000.

111. Ghosh, P., Yang, X.C., Arvizo, R., Zhu, Z.J., Agasti, S.S., Mo, Z.H., Rotello, V.M. 2010, Intracellular Delivery of a Membrane-Impermeable Enzyme in Active Form Using Functionalized Gold Nanoparticles. Journal of the American Chemical Society 132: 2642-2645.

112. Joshi, H.M., Bhumkar, D.R., Joshi, K., Pokharkar, V., Sastry, M. 2006, Gold Nanoparticles as Carriers for Efficience Transmucosal Insulin Delivery. Langmuir 22: 300-305.

113. Visaria, R.K., Griffin, R.J., Williams, B.W., Ebbini, E.S., Paciotti, G.F., Song, C.W., Bischof, J.C. 2006, Enhancement of Tumor Thermal Therapy Using Gold Nanoparticle-Assisted Tumor Necrosis Factor-Alpha Delivery. Molecular Cancer Therapy 5: 1014-1020.

114. Huang, X., Megn, X., Tang, F., Li, L., Chen, D., Liu, H., Zhang, Y., & Ren, J. 2008, Mesoporous Magnetic Hollow Nanoparticles—Protein Carriers for Lysosome Escaping and Cytosolic Delivery. IOP Science 19: 1-8.

115. Gibson, J.D., Khanal, B.P., Zubarev, E.R. 2007, Paclitaxel-Functionalized Gold Nanoparticles. Journal of the American Chemical Society 129: 11653-11661.

116. Hwu, J.R., Lin, Y.S., Josephrajan, T., Hsu, M.H., Cheng, F.Y., Yeh, C.S., Su, W.C., Shieh, D.B. 2009, Targeted Paclitaxel by Conjugation to Iron Oxide and Gold Nanoparticles. Journal of the American Chemical Society 131: 66-68.

117. Anderson, M.E. 1998, Glutathione: An Overview of Biosynthesis and Modulation. Chemico-Biological Interactions 111: 1-14.

118. Agasti, S.S., Chompoosor, A., You, C.C., Ghosh, P., Kim, C.K., Rotello, V.M. 2009, Photoregulated Release of Caged Anticancer Drugs from Gold Nanoparticles. Journal of the American Chemical Society 131: 5728-5729.

119. Kim, C.K., Ghosh, P., Pagliuca, C., Zhu, Z.J., Menichetti, S., Rotello, V.M. 2009, Entrapment of Hydrophobic Drugs in Nanoparticle Monolayers with Efficient Release into Cancer Cells. Journal of the American Chemical Society 131: 1360-1361.

120. Mocellin, S., Bronte, V., Nitti, D. 2007, Nitric Oxide, A Double Edged Sword in Cancer Biology: Searching for Therapeutic Opportunities. Medicinal Research Reviews 27: 317-352.

121. Wadia, J.S., Stan, R.V., Dowdy, S.F. 2004, Transducible TAT-HA Fusogenic Peptide Enhances Escape of TAT-fusion Proteins After Lipid Raft Macropinocytosis. Nature Medicine 10: 310-315.

122. Han, X., Bushweller, J.H., Cafiso, D.S., Tamm, L.K. 2001, Membrane Structure and Fusion-Triggering and Conformational Change of the Fusion Domain from Influenza Hemagglutinin. Nature Structural Biology 8: 715-720.

123. Koshman, Y.E., Waters, S.B., Walker, L.A., Los, T., Tombe, P., Goldspink, P.H., Russell, B. 2008, Delivery and Visualization of Proteins Conjugated to Quantum Dots in Cardiac Myocytes. Journal of Molecular Cell Cardiology 45: 853-856.

124. Rozenzhak, S.M., Kadakia, M.P., Caserta, T.M., Westbrook, T.R., Stone, M.O., Naik, R.R. 2005, Cellular Internalization and Targeting of Semiconductor Quantum Dots. The Royal Society of Chemistry 2217-2219.

125. "Chariot." *Active Motif.* December 13, 2012. <http://www.activemotif.com/documents/5.pdf>.

126. David A Bender. "tannic acid." *A Dictionary of Food and Nutrition*. 2005. *Encyclopedia.com.* 23 Jul. 2012 <http://www.encyclopedia.com>.

127. Bradly M. Stacy. "Controlled Synthesis of Gold Nanorods with Varying Aspect Ratios and Their Biological Applications." *OhioLink*. 2012. *Ohiolink.edu*. 23 July 2012. <http://etd.ohiolink.edu/view.cgi?acc_num=dayton1335361890>.

128. Kohli, R. 2009, The Nature and Characterization of Nanoparticles. MRS Proceedings 1184-1195.

129. Singh, N. 2009, Conference Scene-Nanotoxicology: Health and Environmental Impacts. Nanomedicine 4: 385-390.

130. Hussain, S.M., Braydich-Stolle, L.K., Schrand, A.M., Murdock, R.C., Yu, K.O., Mattie, D.M., Schlager, J.J., Terrones, M. (2009). Toxicity Evaluation for Safe Use of Nanomaterials: Recent Achievements and Technical Challenges. *Advanced Materials,* 21, 1549-1559.

131. Grossman, J.H., McNeil, S.E. (2011). Preclinical Efficacy and Toxicity Testing of Engineered Nanomaterials. *Nanomedicine*, 2, 71-79.

132. Moudgil, B. "Developing Experimental Approaches for the Evaluation of Toxicological Interactions of Nanoscale Materials." Univeristy of Florida Particle Engineering Research Center. 31 July 2012. <http://www.dtic.mil/cgi-bin/GetTRDoc?Location=U2&doc=GetTRDoc.pdf&AD=ADA440025>

133. Nikoobakht B (2001) Synthesis, characterization and self-assembly of gold nanorods an surface-enhanced Raman studies. PhD thesis (Georgia Institute of Technology, Atlanta, GA).

134. Juste J.P., L.M. Liz-Marzan, S. Carnie, D.Y.C. Chan, P. Mulvaney. (2004*). Electric-Field-Directed Growth of Gold Nanorods in Aqueous Surfactant Solutions*. Advanced Functional Materials 14, 571-579.

135. Brian M. Tissue. "Ultraviolet and Visible Absorption Spectroscopy (UV-Vis)." Virginia Tech Chemistry Department. 13 June 2012. <http://www.files.chem.vt.edu/chem-ed/spec/uv-vis/uv-vis.html>.

136. "The Transmission Electron Microscope." Nobelprize.org. 11 December 2012. <http://www.nobelprize.org/educational/physics/microscopes/tem/index.html>.

137. "Zeta Potential Measurement Using Laser Doppler Electrophoresis (LDE)." *Malvern.* 14 June 2012.

138. "Toxicity" Medicine.net. 11 December 2012. <http://www.medterms.com/script/main/art.asp?articlekey=34093>.

139. "In Vitro" Medicine.net 11 December 2012 <http://www.medterms.com/script/main/art.asp?articlekey=4033>.

140. Ekwall, B., Barile, F.A., Castano, A., et al. 1998, MEIC evaluation of acute systemic toxicity. Part VI. The prediction of human toxicity by rodent LD50 values and results from 61 in vitro methods. *Altern. Lab. Anim.* 26: 617-658.

141. Hurtt, M.E., Cappon, G.D. & Browning, A. 2003, Proposal for a tiered approach to developmental toxicity testing for veterinary pharmaceutical products for food-producing animals. *Food Chem. Toxicol.* 41: 611-619.

142. Gold, L.S. & Slone, T.H. 1993, Prediction of carcinogenicity from two versus four sex-species groups in the carcinogenic potency database. *J. Toxicol. Environ. Health.* 39: 143-157.

143. Doe, J.E., Boobis, A.R., Blacker, A., Dellarco, V., Doerrer, N.G., Franklin, et al. 2006, A Tiered Approach to Systemic Toxicity Testing for Agricultural Chemical Safety Assessment. *Crit. Rev. Toxicol.* 36: 37-68.

144. Cooper, R.L., Lamb, J.C., Barlow, S.M., Bentley, K., Brady, A.M., Doerrer, N.G., et al. 2006, A Tiered Approach to Life Stages Testing for Agricultural Chemical Safety Assessment. *Crit. Rev. Toxicol.* 36: 69-98.

145. "Council Directive." EUR-Lex. 10 December 2012. < http://eur-lex.europa.eu/LexUriServ/LexUriServ.do?uri=CELEX:31986L0609:EN:NOT>.

146. Repetto, G., del Peso, A., Zurita, J.L. 2008, Neutral Red Uptake Assay for the Estimation of Cell Viability/Cytotoxicity. Nature Protocols 3: 1125-1131.

147. Fotakis, G., Timbrell, J.A. (2006). *In vitro Cytotoxicity Assays: Comparison of LDH, Neutral Red, MTT, and Protein Assay in Heptaoma Cell Lines Following Exposure to Cadmium Chloride.* Toxicology Letters, 160:2, 171-177.

148. "DCFDA Cellular R   S Detection Assay   it." 2011. Abcam. 20 July 2012. < http://www.abcam.com/ps/products/113/ab113851/documents/ab113851%20protocol%20final%20v2%20(website).pdf>.

149. Zhao, M., Kircher, M.F., Josephson, L., Weissleder, R. 2002, Differential Conjugation of Tat Peptide to Superparamagnetic Nanoparticles and Its Effect on Cellular Uptake. Bioconjugate Chemistry 13: 840-844.

150. Josephon, L., Tung, C.H., Moore, A., Weissleder, R. 1999, High-Efficiency Intracellular Magnetic Labeling with Novel Superparamagnetic-Tat Peptide Conjugates. Bioconjugate Chemistry 10: 186-191.

151. Suk, J.S., Suh, J., Choy, K., Lai, S.K., Fu, J., Hanes, J. 2006, Gene Delivery to Differentiated Neurotypic Cells with RGD and HIV TAT Peptide Functionalized Polymeric Nanoparticles. Biomaterials 27: 5143-5150.

152. Apaja, P.M., Tussa, J.T., Pietila, E.M., Rajaniemi, H.J., Petaja-Repo, U.E. 2006, Luteinizing Hormone Receptor Ectodomain Splice Variant Misroutes the Full-Length Receptor into a Subcompartment of the Endoplasmic Reticulum. Molecular Biology of the Cell 17: 2243-2255.

153. Van der Wijk, T., Tomassen, S.F., Houtsmuller, A.B., de Jonge, H.R., Tilly, B.C. 2003, Increased Vesicle Recycling in Response to Osmotic Cell Swelling. Cause and Consequence of Hypotonicity-provoked ATP Release. Journal of Biological Chemistry 278: 40020-40025.

154. Tsai, C.Y., Lee, D.S., Tsai, Y.H., Chan, B., Luh, T.Y., Chen, P.J., Chen, P.H. 2004, Shrinking Gold Nanoparticles: Dramatic Effect of A Cryogenic Process on Tannic Acid/Sodium Citrate-Generated Gold Nanoparticles. Materials Letters 58: 2023-2026.

155. Lin, D., Xing, B. 2008, Tannic Acid Adsorption and Its Role for Stabilizing Carbon Nanotube Suspensions. Environment Science and Technology 42: 5917-5923.

156. Wang, L., Liu, Y., Li, W. Jiang, X., Yinglu, J., Wu, X., Ligeng, X., Qiu, Y., Zhao, K., Wei, T. Li, Y., Zhao, Y., Chen, C. 2010, Selective Targeting of Gold Nanorods at the Mitochondria of Cancer Cells: Implications for Cancer Therapy. Nano Letters 11: 772-780.

157. Wang, L.H., Rothberg, K.G., Anderson, R.G. 1993, Mis-Assembly of Clathrin Lattices on Endosomes Reveals a Regulatory Switch for Coated Pit Formation. Journal of Cell Biology 123: 1107-1117.

158. Nakase, I., Niwa, M., Takeuchi, T., Sonomura, K., Kawabata, N., Koike, Y., Takehashi, M., Tanaka, S., Ueda, K., Simpson, J.C., Jones, A.T., Sugiura, Y., Futaki, S. 2004, Cellular Uptake of Arginine-Rich Peptides: Roles for Macropinocytosis and Actin Rearrangement. Molecular Therapy 10: 1011-1022.

159. Phillis, J.W., Ren, J., 'Re gan, M.H. 2000, Inhibition of Na(+)/H(+) Exchange by 5-(N-ethyl-N-isopropyl)-amiloride Reduces Free Fatty Acid Efflux from the Ischemic Reperfused Rat Cerebral Cortex. Brain Research 884: 155-162.

160. Khan, J.A., Pillai, B., Das, T.K., Singh, Y., Maiti, S. 2007, Molecular Effects of Uptake of Gold Nanoparticles in HeLa Cells. ChemBioChem 8: 12370-1240.

161. Dausend, J., Musyanovych, A., Dass, M., Walther, P., Schrezenmeier, H., Landfester, K., Mailander, V. 2008, Uptake Mechanism of Oppositely Charged Fluorescent Nanoparticles in HeLa Cells. Macromolecular Bioscience 8: 1135-1143.

162. Zhao, F., Zhao, Y., Liu, Y., Chang, X., Chen, C., Zhao, Y. 2011, Cellular Uptake, Intracellular Trafficking, and Cytotoxicity of Nanomaterials. Small 7: 1322-1337.

163. Brandenberger, C., Muhlfeld, C., Ali, Z., Lenz, A-G., Schmid, O., Parak, W.J., Gehr, P., Rothen-Rutishauser, B. 2010, Quantitative Evaluation of Cellular Uptake and Trafficking of Plain and Polyethylene Glycol-Coated Gold Nanoparticles. Small 6: 1669-1678.

164. Rejman, J., Oberle, V., Zuhorn, I.S., Hoekstra, D. 2004, Size-Dependent Internalization of Particles via the Pathways of clathrin- and Caveolae-Mediated Endocytosis. Biochemical Journal 377: 159-169.

165. Gratton, S.E.A., Ropp, P.A., Pohlhaus, P.D., Luft, J.C., Madden, V.J., Napier, M.E., DeSimone, J.M. 2008, The Effect of Particle Design on Cellular Internalization Pathways. Proceedings of the National Academy of Sciences 105: 11613-11618.

166. Min, Y., Akbulut, M., Kristiansen, K., Golan, Y., Israelachvili, J. 2008, The Role of Interparticle and External Forces in Nanoparticle Assembly. Nature Materials 7: 527-538.

167. Wang, Z., Tiruppathi, C., Minshall, R.D., Malik, A.B. 2009, Size and Dynamics of Caveolae Studied Using Nanoparticles in Living Endothelial Cells. ACS Nano 3: 4110-4116.

168. Albanese, A., Chan,W.C. 2011, Effect of Gold Nanoparticle Aggregation on Cell Uptake and Toxicity. ACS Nano 5: 5478-5479.

169. Mukhopadhyay, A., Grabinski, C., Nabiul Afrooz, A.R.M., Saleh, N.B., Hussain, S. 2012, Effect of Gold Nanosphere Surface Chemistry on Protein Adsorption and Cell Uptake In Vitro. App Biochem Biotechnol 167: 327-337.

170. Nakanishi, J., Nakayama, H., Shimizu, T., Ishida, H., Kikuchi, Y., Yamaguchi, K., Horiike, Y. 2009, Light-Regulated Activation of Cellular Signaling by Gold Nanoparticles That Capture and Release Amines. J. Am. Chem. Soc. 131: 3822-3823.

171. Kah, J.C.Y., Chen, J., Zubieta, A., Hamad-Schifferli, K. 2012, Exploiting the Protein Corona around Gold Nanorods for Loading and Triggered Release. ACS Nano 6: 6730-6740.

172. Chung, K.T., Wong, T.Y., Wei, C.I., Huan, Y.W., Lin, Y. 1998, Tannins and Human Health: A Review. Critical Reviews in Food Science and Nutrition 38: 421-464.

APPENDIX

TEM Images of GNRs in HaCaT Cells
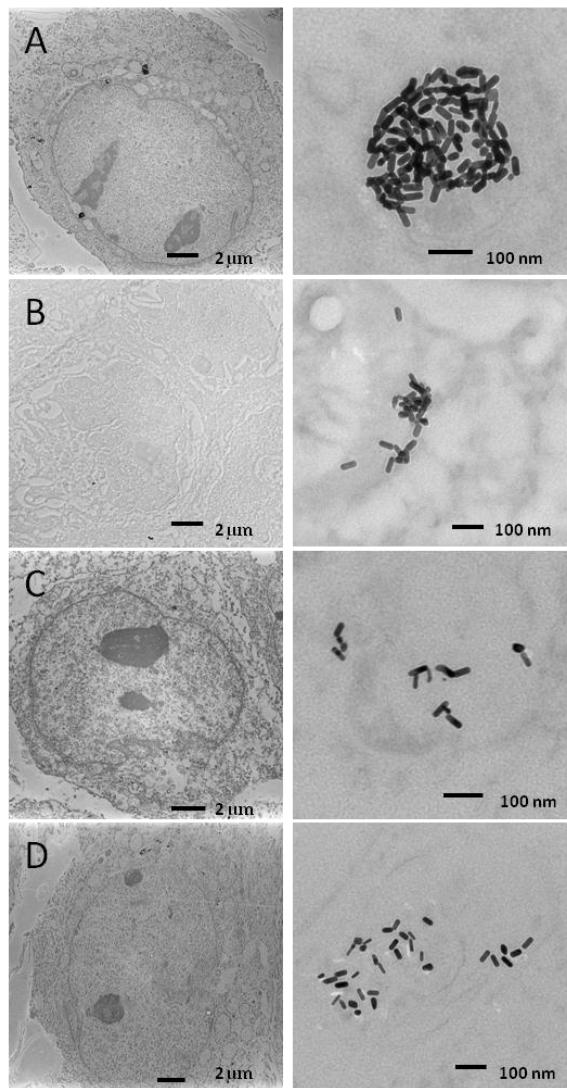
Figure A-1:   Cellular Uptake of GNRs AR 3 in HaCaT Cells Imaged by TEM.
A: Chariot GNRs, B: TAT GNRs, C: TAT HA2 GNRs, D: Tannic Acid GNRs
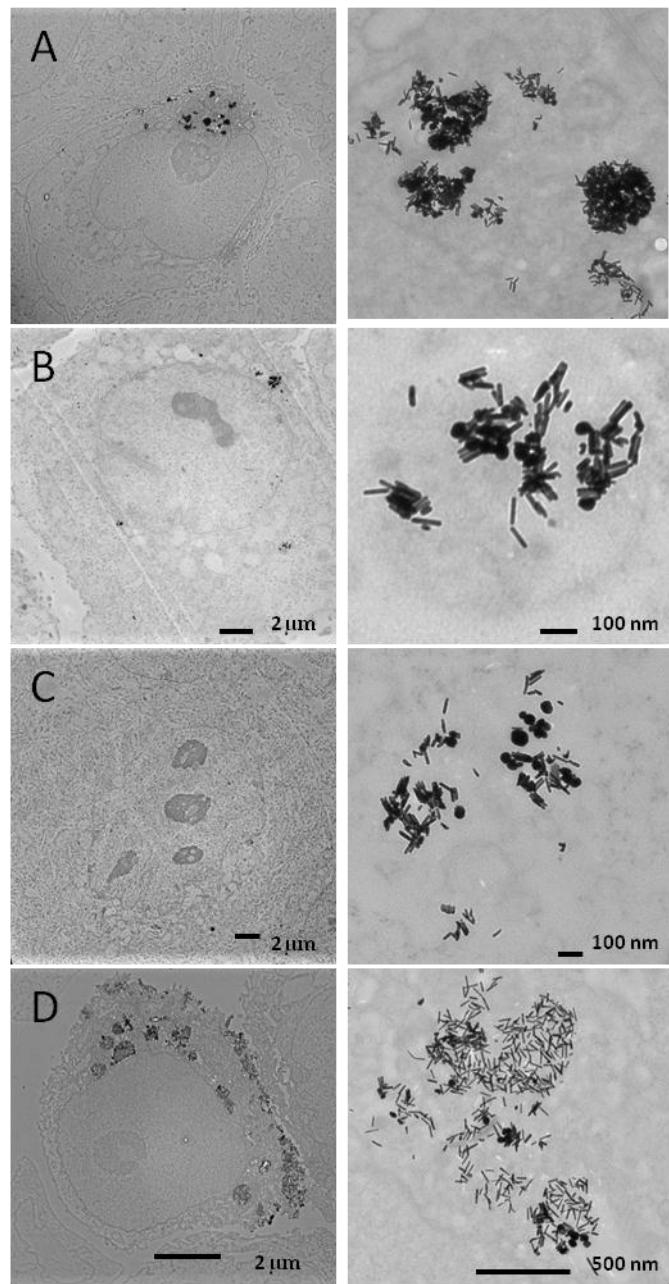
Figure A-2:   Cellular uptake of GNRs AR 6 in HaCaT cells imaged by TEM.
A: Chariot GNRs, B: TAT GNRs, C: TAT HA2 GNRs, D: Tannic Acid GNRs

Functionalization Calculations

In order to calculate how much to add of a certain functionalization (PEG, TAT, TAT HA2, Chariot or Tannic Acid) calculations based on UV-Vis can be used to determine the concentration of the GNR solution, surface area of the GNRs, and thus the amount of 0.001 M functionalizing agent to be added. First the molar concentration is determined using the absorbance of the SPR peak from the UV-Vis plot as well as the extinction coefficient listed in Table 2. This molar concentration is converted to mass concentration as seen below.

$$\textbf{\textit{Molar Concentration}} \left[\frac{\textbf{\textit{mol}}}{\textbf{\textit{L}}}\right] = \frac{Absorption\ (A)}{extinction\ coefficient} \tag{17}$$

$$\frac{GNRs}{L} = Molar\ Concentration \left[\frac{mol}{L}\right] * 6.022\ x\ 10^{-23} \frac{particles}{mole} \tag{18}$$

$$\frac{Volume\ of\ GNRs(cm^3)}{L} = \frac{GNRs}{L} * Diameter\ (nm) * \frac{cm}{1x\ 10^7\ nm} * 10^{-14} \left(\frac{cm^2}{GNR}\right) \tag{19}$$

$$\textbf{\textit{Concentration}} \left(\frac{\boldsymbol{\mu g}}{\textbf{\textit{mL}}}\right) = \frac{Volume\ of\ GNRs(cm^3)}{L} * \rho_{gold} \left(\frac{g}{cm^3}\right) * \frac{1x10^6\ \mu g}{g} * \frac{L}{1x10^3\ mL} \tag{20}$$

The amount of functionalizing agent, such as PEG, to be added to a GNR solution can be calculated based on the amount of solution, concentration of GNRs, and surface area of the particle. The equations used for this calculation are show below:

$$Surface\ Area\ of\ GNR\ (nm^2) = 2\pi RL + 2\pi R^2 \tag{21}$$

$$\frac{Number\ PEG}{1\ GNR} = 4 * Surface\ Area\ of\ GNR \tag{22}$$

$$Number\ of\ PEG\ needed\ = \frac{Number\ PEG}{1\ GNR} * \frac{GNRs}{L} * mL\ of\ GNR\ solution * \frac{L}{1000\ mL} \tag{23}$$

$$\begin{aligned}\textbf{\textit{Amount of}}\ .\,\textbf{\textit{001 M PEG solution needed}}\ (\textbf{5\% \textit{excess}})(\textbf{\textit{mL}})\\ = Number\ of\ PEG\ Needed * \frac{1\ mole}{6.022\ x\ 10^{23}\ number\ PEG} * \frac{1}{.001\frac{mol}{L}} * \frac{1000\ ml}{L} * 1.05\end{aligned} \tag{24}$$

These calculations show how much volume to add of a 0.001 M solution to functionalize any aspect ratio or concentration of GNRs.

Baseline UV-Vis Graphs

In order to create a baseline for the UV-Vis absorbance graphs, sterile water was run on UV-Vis since the GNRs were present in a solution of sterile water. This ensures that it is truly the GNRs which are absorbing light at each wavelength as opposed to water absorbing the light. Three different baseline graphs are shown which were run on different days for different GNR solutions (Figure 35). They appear to be in very good agreement, indicating the baseline readings would create accurate UV-Vis graphs for the GNRs.
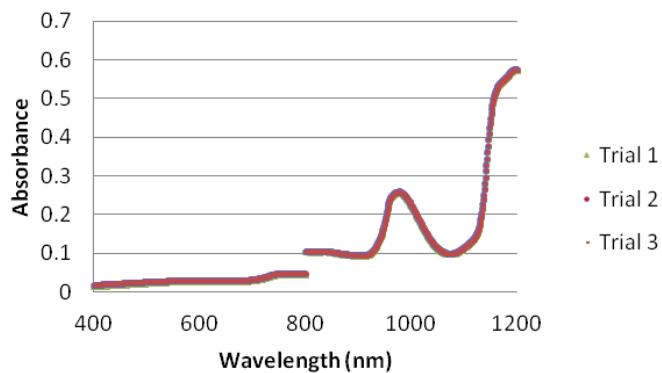
Figure A-3: UV-Vis Absorption of Sterile Water Used as a Baseline

LIST OF ACRONYMS

AR	Aspect Ratio
BDAC	Benzyldimethylhexadecylammonium chloride
BSA	Bovine Serum Albumin
CDE	Clathrin-dependent Endocytosis
CIE	Clathrin-independent Endocytosis
CLSM	Confocal Laser Scanning Microscope
CPP	Cell Penetrating Peptide
CTAB	Cetyltrimethylammonium bromide
DOX	Doxorubicin
EIPA	5-(N-Ethyl-N-isopropyl)amiloride
EMR.	Electromagnetic Radiation
EPR	Enhanced Permeability and Retention
GNR	Gold Nanorod
GSH	Glutathione
HA	Hemaglutinin
HIV	Human Immunodeficiency Virus
HSI	Hyperspectral Imaging
ICP-MS	Inductively Coupled Plasma Mass Spectrometry
LDE	Laser Doppler Electrophoresis
LDH	Lactate Dehydrogenase
LSP	Longitudinal Surface Plasmon
LSPR	Localized Surface Plasmon Resonance
MMH	Mesoporous Magnetic Hollow Nanoparticle
NIR	Near Infrared
NLS	Nuclear Localization Signal
NNI	National Nanotechnology Initiatve
PAA	Polyacrylic Acid
PAH	Poly(allylamine) hydrochloride
PBS	Phosphate Buffered Saline
PDDAC	Poly(diallyldimethyl ammonium chloride)
PEG	Polyethylene Glycol
PEI	Polyethyleneimine
PSS	Polystyrene Sulfonate
RME	Receptor Mediated Endocytosis
ROS	Reactive Oxygen Species
SPR	Surface Plasmon Resonance
TAT	Transactivator of Transcription
TEM	Transmission Electron Microscope
UV-Vis	Ultra-visible Spectroscopy